**SUPPLEMENTAL INFORMATION FOR**

# Edge-centric connectome-genetic markers of bridging factor to comorbidity between depression and anxiety

**Running title:** Bridging factor of depression-anxiety comorbidity


**Author List**

Zhiyi Chen[1,2,3*†], Yancheng Tang[4†], Xuerong Liu[1], Wei Li[1†], Yuanyuan Hu[5,6†], Bowen Hu[7†], Ting Xu[2,8,9], Rong Zhang[2], Lei Xia[1], Jing-Xuan Zhang[1], Zhibing Xiao[7], Ji Chen[10], Zhengzhi Feng[1], Yuan Zhou[5,6*], Qinghua He[2], Jiang Qiu[2], Xu Lei[2], Hong Chen[2], Shaozheng Qin[7*], Tingyong Feng[2*]

**Affiliations**

[1] Experimental Research Center for Medical and Psychological Science, School of Psychology, Third Military Medical University, Chongqing, 400038, China

[2] School of Psychology, Southwest University, Chongqing, 400415, China

[3] Key Laboratory of Cognition and Personality, Ministry of Education, 400415, China

[4] Key Laboratory of Brain-Machine Intelligence for Information Behavior (Ministry of Education and Shanghai), School of Business and Management, Shanghai International Studies University, Shanghai, 200083 China

[5] CAS Key Laboratory of Behavioral Science, Institute of Psychology, Chinese Academy of Sciences, Beijing, 100101, China

[6] Department of Psychology, University of Chinese Academy of Sciences, Beijing, 100049, China

[7] State Key Laboratory of Cognitive Neuroscience and Learning & IDG/McGovern Institute for Brain Research, Beijing Normal University, Beijing, 100032, China

[8] The Center of Psychosomatic Medicine, Sichuan Provincial Center for Mental Health, Sichuan Provincial People's Hospital, Chengdu, 611731, China

[9] The Clinical Hospital of Chengdu Brain Science Institute, MOE Key Laboratory for Neuroinformation, University of Electronic Science and Technology of China, Chengdu, 611731, China

[10] Center for Brain Health and Brain Technology, Global Institute of Future Technology, Institute of Psychology and Behavioral Science, Shanghai Jiao Tong University, 200240, China

[†]These authors contributed equally: Zhiyi Chen, Yancheng Tang, Wei Li, Yuanyuan Hu, and Bowen Hu

[*]Correspondence at: Zhiyi Chen (chenzhiyi@tmmu.edu.cn), Yuan Zhou (zhouyuan@psych.ac.cn), Shaozheng Qin (szqin@bnu.edu.cn), and Tingyong Feng (fengty0@swu.edu.cn)

**CONTENT**

**SUPPLEMENTAL METHODS**

## 1. Participants

To strengthen the sample representativeness, we recruited this non-WEIRD (Western, Educated, Industrialized, Rich and Democratic) nationwide sample covering the almost all the regions of China (total *n* = 2, 022, aged from 19-27, M ± S.D., 20.04 ± 2.00 years old) from independent collectors during Nov, 2019 - Feb, 2022 **(Tab. S1)**. The data collection has been completed by this consortium (Gut-Gene-Brain-Behavior Data Project of Chinese Personality, GGBBP), with five independent research teams (i.e., Principal Investigators, H.Q.H., Q.J., L.X., C.H., F.T.Y.) for relatively independent data collections. In this vein, despite the same scanner center, the whole sample could be partitioned into these relatively independent subsamples that the present study used **(Tab. S2)**. The geospatial distributions of the present sample has been shown to cover almost all the regions of the China, which were derived from 945 counties/administrative regions across 327 cities. Furthermore, a total of 30 ethnicities were included in the present sample, especially in these ethnic minorities (< 1% of the whole population in the China) **(Tab. S3)**. Rather biases to include participants with socioeconomic advantages, this sample also included ones with low- and middle- incomes by categorizing them from annual data of the National Bureau of Statistics of the China. Finally, we took the potential confounding of COVID-19 into accounts by excluding participants who were infected by SARS-Cov-2 in these neuroimaging-related analyses. Details for the symptoms scores in this sample have been sorted in the **Tab. S4**.

| | **Females** | **Males** |
|---|---|---|
| **Sociodemographic characteristics** | | |
| *N* | 1326 | 696 |
| Age, *years, M (SD)* | 20.20 (2.04) | 19.88 (1.96) |
| Ethnicity, *the number of categories* | 29 | 25 |
| Handedness, *left (right)* | 107 (1219) | 90 (606) |
| Family incomes per year, *grades, M (SD)* | 2.04 (1.42) | 2.06 (1.39) |
| **Scanning-related psychological status** | | |
| Mood States, *scores, M (SD)* | 96.96 (15.59) | 97.71 (16.20) |
| Mind wondering during scanning, *scores, M (SD)* | | |
| Discontinuity of Mind | 9.65 (2.08) | 9.20 (2.27) |
| Theory of Mind | 8.91 (2.34) | 8.96 (2.53) |
| Self | 11.35 (1.65) | 11.07 (1.83) |
| Planning | 10.10 (2.59) | 9.80 (2.61) |
| Sleepiness | 10.29 (2.53) | 10.09 (2.68) |
| Comfort | 8.87 (2.27) | 8.39 (2.48) |
| Somatic awareness | 9.65 (2.38) | 10.03 (2.43) |

| | | |
|---|---|---|
| Health concern | 10.91 (1.73) | 10.71 (1.79) |
| Visual Thought | 10.29 (2.42) | 10.07 (2.37) |
| Verbal Thought | 8.66 (2.44) | 8.22 (2.48) |

**Tab S1. Sociodemographic characteristics of this nationwide sample (*n* = 2,022).** The mood states for all the participants were estimated by abbreviated Profile of Mood States Scale (PMOS) for describing the current mood status when they reached lab, with total 40 items covering stress, anger, fatigue, depression, energy, panic and self-esteem. Furthermore, the post-scanning examinations to the scanning mind-wondering had been done by the updated the Amsterdam Resting-State Questionnaire (ARSQ) 2.0 covering 10 factors mentioned within the table, which was an index to quantify resting-state minds during scanning. The grades of family incomes (per year) were categorized into five ones by criterion that made by National Bureau of Statistics of China: 1 = < ¥ 25,000, 2 = ¥ 25,000 - 100,000, 3 = ¥ 100,000 - 240,000, 4 = ¥ 240,000 - 400,000, 5 = > ¥ 400,000.

| **Ethnicity** | ***N*** | **Proportion** |
|---|---|---|
| Han | 1685 | 83.3% |
| Bai | 11 | 0.5% |
| Buyi | 25 | 1.2% |
| Zang | 11 | 0.5% |
| Chaoxian | 3 | 0.1% |
| Chuanqing | 4 | 0.2% |
| Dai | 1 | <0.1% |
| Dongxiang | 1 | <0.1% |
| Dong | 16 | 0.8% |
| Dulong | 1 | <0.1% |
| Yi | 3 | 0.1% |
| Ha-ni | 5 | 0.2% |
| Kazakhstan | 5 | 0.2% |
| Hui | 39 | 1.9% |
| Li | 4 | 0.2% |
| Susu | 2 | <0.1% |
| Manchu | 16 | 0.8% |
| Mongolian | 12 | 0.6% |
| Miao | 33 | 1.6% |
| Na-xi | 1 | <0.1% |
| Nv | 1 | <0.1% |
| Qiang | 3 | 0.1% |
| Chi | 2 | <0.1% |
| Tujia | 61 | 3.0% |
| Tu | 6 | 0.3% |
| Uygurs | 25 | 1.2% |
| Yao | 3 | 0.1% |
| Yii | 21 | 1.0% |
| Yugu | 1 | <0.1% |

| | | |
|---|---|---|
| Zhuang | 21 | 1.0% |

**Tab S2. Ethnicity of participants in the present sample (*n* = 2,022).** The “Han” is the ethnic majority in the China, while others (ethnic minorities) are less than 1% of the whole populations.

| | Main sample | Validation sample | Generalization sample | Generalization sample (ethnic minorities) | Generalization sample (ethnic majority) | Generalization sample (post-COVID19) |
|---|---|---|---|---|---|---|
| **Sociodemographic characteristics** | | | | | | |
| *N* | 241 | 240 | 244 | 133 | 237 | 219 |
| Sex, *females* | 142 | 159 | 129 | 86 | 179 | 146 |
| Age, *years, M (SD)* | 19.20 (1.94) | 18.56 (0.82) | 21.92 (2.07) | 19.95 (1.71) | 19.09 (0.89) | 19.17 (1.01) |
| Ethnicity, *the number of categories* | 1 (Han) | 13 | 19 | 23 (excluded Han) | 1 (Han) | 18 |
| Handedness, *left (right)* | 28 (213) | 14 (226) | 23 (221) | 23 (110) | 25 (212) | 30 (189) |
| Family incomes per year, *grades, M (SD)* | 1.98 (1.40) | 2.45 (1.57) | 2.14 (1.42) | 1.58 (1.11) | 2.09 (0.89) | 1.79 (1.27) |
| **Scanning-related psychological status** | | | | | | |
| Mood States, *scores, M (SD)* | 97.55 (16.27) | 99.10 (15.69) | 94.81 (15.40) | 97.41 (14.40) | 98.70 (15.87) | 99.23 (16.50) |
| Mind wondering during scanning, *scores, M (SD)* | | | | | | |
| Discontinuity of Mind | 9.35 (2.05) | 9.44 (2.18) | 9.56 (2.11) | 9.48 (2.01) | 9.66 (2.19) | 9.39 (2.07) |
| Theory of Mind | 8.51 (2.40) | 8.67 (2.42) | 9.00 (2.48) | 9.48 (2.21) | 8.80 (2.32) | 8.92 (2.39) |
| Self | 11.07 (1.73) | 11.12 (1.81) | 11.25 (1.72) | 11.52 (1.50) | 11.29 (1.69) | 11.23 (1.67) |
| Planning | 9.77 (2.52) | 9.72 (2.78) | 9.83 (2.68) | 10.18 (2.42) | 10.02 (2.49) | 9.87 (2.71) |
| Sleepiness | 10.26 (2.51) | 10.37 (2.65) | 10.32 (2.62) | 9.69 (2.52) | 10.59 (2.22) | 10.18 (2.63) |
| Comfort | 8.66 (2.32) | 8.70 (2.38) | 8.57 (2.49) | 8.66 (2.14) | 8.53 (2.30) | 8.67 (2.38) |
| Somatic awareness | 9.51 (2.26) | 9.33 (2.45) | 9.91 (2.51) | 9.97 (2.23) | 9.68 (2.42) | 10.02 (2.30) |

| | | | | | | |
|---|---|---|---|---|---|---|
| Health concern | 10.87 (1.71) | 10.78 (1.69) | 10.86 (1.81) | 10.87 (1.74) | 10.50 (1.76) | 10.73 (1.78) |
| Visual Thought | 10.01 (2.31) | 10.04 (2.54) | 10.25 (2.28) | 10.61 (2.28) | 10.27 (2.35) | 10.29 (2.32) |
| Verbal Thought | 8.18 (2.26) | 8.27 (2.54) | 8.52 (2.39) | 8.86 (2.57) | 8.61 (2.35) | 8.73 (2.47) |

**Tab S3. Sociodemographic characteristics of each subsample.** The mood states for all the participants were estimated by abbreviated Profile of Mood States Scale (PMOS) for describing the current mood status when they reached lab, with total 40 items covering stress, anger, fatigue, depression, energy, panic and self-esteem. Furthermore, the post-scanning examinations to the scanning mind-wondering had been done by the updated the Amsterdam Resting-State Questionnaire (ARSQ) 2.0 covering 10 factors mentioned within the table, which was an index to quantify resting-state minds during scanning. The grades of family incomes (per year) were categorized into five ones by criterion that made by National Bureau of Statistics of China: 1 = < ¥ 25,000, 2 = ¥ 25,000 - 100,000, 3 = ¥ 100,000 - 240,000, 4 = ¥ 240,000 - 400,000, 5 = > ¥ 400,000. In the China, the “Han” was the ethnic majority, with over 95% populations.

| | Mean (Std. D) | Min/Max | Interquartile range (IQR) | Proportion of exceeding threshold, % | Proportion of both exceeding threshold, % |
|---|---|---|---|---|---|
| **SDS** | 56.18 (10.97) | 31.25/100 | 47.50-63.75 | 74.20 (1499/2020) | 81.32 (1219/1499) |
| **TAI** | 43.36 (7.70) | 22.00/72.0 | 38.00-48.00 | 68.30 (1380/2020) | |

**Tab S4. Summary to symptom scores for Zung self-reported depression scale (SDS) and trait part of state-trait anxiety inventory (STAI).** Threshold to rate high depression (anxiety) was set by referring to Dunstan & Scott, 2019 (Dennis *et al*, 2013).

## 2. Behavioral data clean and imputation

We utilized on the R packages of "DataExplorer" to automatically detect the outliers and missing data from our dataset relating to measurements to the depression and anxiety (see Supplement 2). No prominent outliers were captured, whereas it found complete random missing (CRM) values in a portion of variables (A1-A10: ARSQ1-10, Amsterdam Resting-State Questionnaire), with all less than 5% from the total counts. Thus, we further used the R packages of "MICE" to inspect and impute these missing values by using predictive matching method (PMM). Based on the Monte Carlo simulations, the the third pool was selected as the final dataset given the visual inspections from density plots **(Fig. S1-2)**.

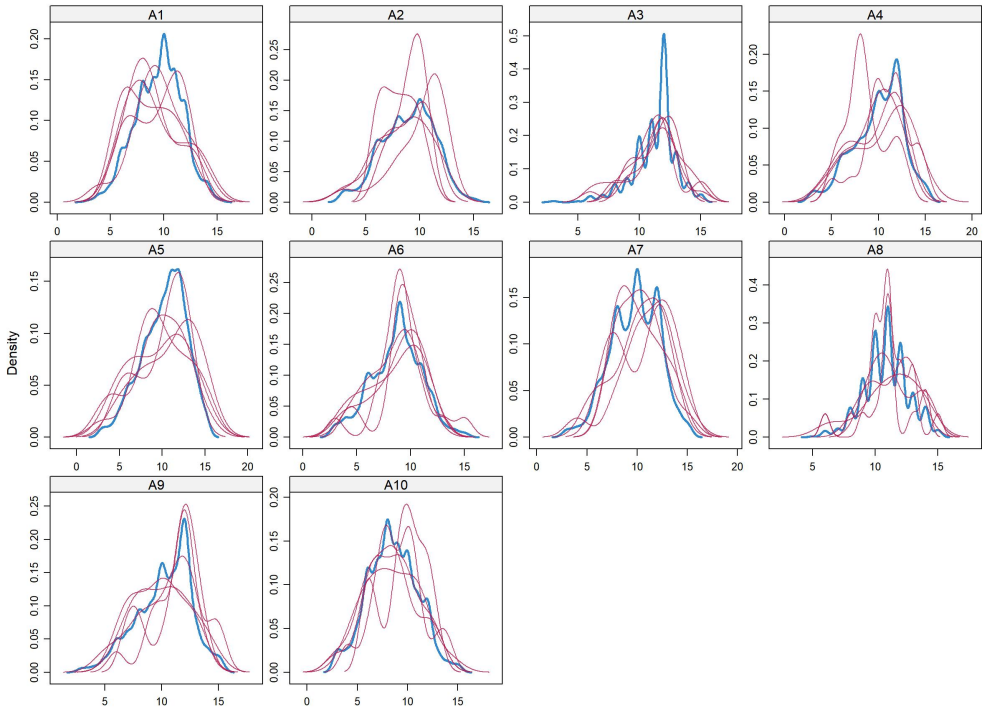


**Fig S1. Density plots of five imputation data pools.** We showcased top 10 items with missing values after imputing simulated values, with each magenta line for one density of imputed dataset. A total of five simulated datasets are provided. Blue line indicates the density of original dataset (before imputation). Source data are provided as a Source Data file.

To measure the symptoms in the pre- clinical cohorts, we capitalized on the Zung's self-report depression scale (SDS) and status-trait anxiety inventory (STAI), respectively. The SDS was one of the most widely-used tool to measure one's depressive symptoms or activities, with prominently good psychometric merits in general population[1,2]. This scale contained 20 items describing the depressive symptoms in daily life, with higher scores for severer symptom by 5-point Likert-formed style[3]. In addition, the trait domain of this Spielberger's STAI (STAI-T) had been used to measure one's anxious symptoms in the present study, given the superior reliability[4]. This STAI-T also included 20 items to depict anxiety-related affects and feelings, which was widely deployed for network analysis[5-7]. Given no non-clinical measurements to bipolar disorder, the present study included symptoms relating to depression and anxiety mentioned above only. All the participants were required to rate all the items of these scales, one-by-one. We detected and further simulated these missing data by using Monte-Carlo predictive matching method (PMM) from multiple imputation.

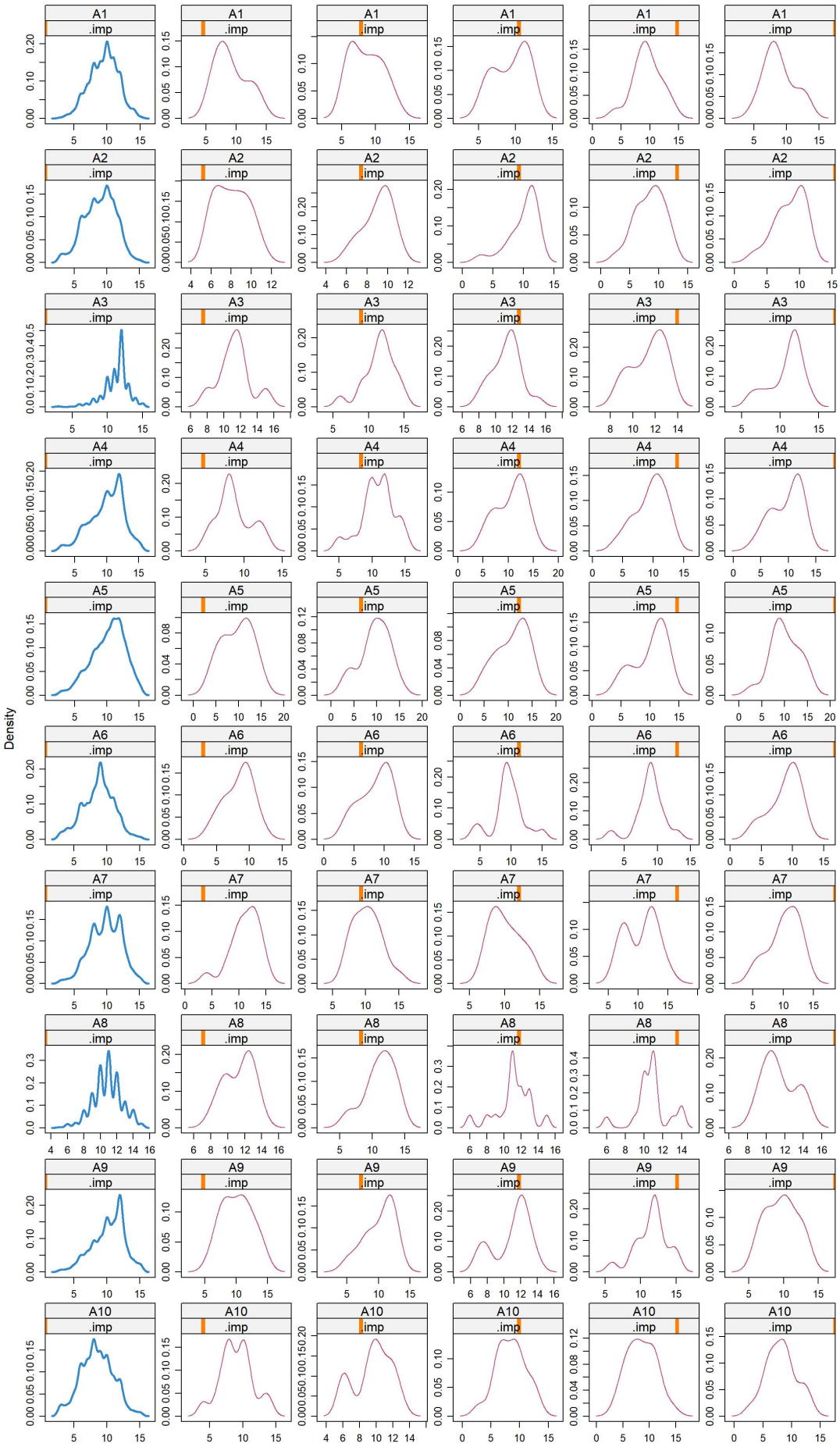
A1
A2
A3
A4
A5
A6
A7
A8
A9
A10
.imp
Density

**Fig S2. Density plots of imputation for each data pool.** We showcased top 10 items with missing values after imputing simulated values, with each magenta line for one density of imputed dataset. total of five simulated datasets are provided, with each one was colored by magenta line. At the left, the blue line indicated density of original dataset (before imputation). Source data are provided as a Source Data file.

**3. Neuroimaging data collection and preprocessing**

All the neuroimaging data have been acquired by the same scanner (Siemens Prisma, 3T, SIMENS MAGNETOM, Erlangen, Germany), but were implemented by relatively independent collectors *(see above)*. To reduce head-motion, we made use of foam padding. Participants were instructed to keep eyes open, and to take a rest without thinking during 480-seconds scanning.

Scanning parameters for the resting-state functional MRI have been detailed underneath: Time Repetitive (TR) = 2000 ms, Time Echo (TE) = 30 ms, slices = 62, Field of View (FoV) = 224 mm, base resolution = 112, Flip angle (FA) = 90°, Dist.factor = 15 %, Phase enc.dir = P>>A, Accel.factor slice = 2, Echo spacing = 0.54 ms. Corresponding field mappings were scanned with the following parameters: TR/TE1/TE2 = 620 ms/4.92 ms/7.38 ms, Voxel size = 2.0 × 2.0 × 2.0 mm, Slices = 62, FoV = 224 mm, Base resolution = 112, Dist.factor = 15 %, FA = 60°.

The algorithm to estimate head-motion signal frame-by-frame that was used frequently for proceeding to thorough scrubbing, was called “Power frame-to-frame displacement (Power’s FD correction)” . All of the images were corrected by the frame-to-frame head-motion displacement (FD) strategy to rigorously control motion-related effects. Specifically, we first calculated the FD value for every volume/frame (time point) point) of each participant. The FD was broadly considered to be a robust measure for instantaneous head motion, and can be estimated as a scalar quantity for six-dimensional rigid body parameters by an empirical equation, $\mathrm{FD}_i = |\Delta d_{\mathrm{ix}}|+|\Delta d_{\mathrm{ix}}|+|\Delta d_{\mathrm{iz}}|+|\Delta d_{\mathrm{iy}}|+|\Delta \alpha_{\mathrm{i}}|+|\Delta \beta_{\mathrm{i}}|+|\Delta \gamma_{\mathrm{i}}|$, where $\Delta_{\mathrm{ix}} = d_{(\mathrm{i}-1)\mathrm{x}} - d_{\mathrm{ix}}$ and similarly for the other rigid body parameters ($[d_{\mathrm{iy}}, d_{\mathrm{iz}}, \alpha_{\mathrm{i}}, \beta_{\mathrm{i}}, \gamma_{\mathrm{i}}]$) . Then, these frames (volumes), whose the FD value was greater than 0.2 mm (as well as 1 back and 2 forward neighbors of them) were excluded from the participant's time series in the analysis. To align point-to-point co-fluctuations in edge-centric connectome constructions, we included participants who were fully free from head-motion corrections.

Preprocessing of these neuroimaging data was in line with mainstreaming pipelines (e.g., HCP), and mainly included nine steps:

(1) Slice timing correction (piecewise cubic spline temporal interpolation);

(2) Motion correction (rigid-body, to the median volume of the resting-state of each run, and then between-runs/sessions);

(3) Quality control for motion correction;

(4) Linear and non-linear spatial normalization of the EPI template into these T2* functional images;

(5) Quality control for 4;

(6) Correction of slow time drifts (high-pass filtering with discrete cosines, cut-off frequency 0.01Hz);

(7) Correction of physiological noise (20 components, selection threshold 0.15);
(8) Resampling of the functional data in the MNI space with 3mm isotropic resolution);
(9) No spatial smoothing.

**4. Network-wise associations between depressive and anxious symptoms**

To test whether the network-wise correlations of depressive and anxious symptoms beyond univariate analysis, we capitalized on the multivariate Mantel's test, with statistical significance at $p < .05$. This test had been implemented by R packages of "LinkET", in conjunction of "vegan" and "tidyverse". All the parameters were in line with defaults ones that these packages provided. Results showed the statistically significant correlations between networks of depressive and anxious symptoms ($r = .40$, $p < .001$, $n = 2{,}022$), enabling to infer the network-wise association between them.

**5. Estimates of bridging centrality from network model**

To capture bridging symptoms in the depression-anxiety comorbidity, we carried on the EBICglasso (graphic least absolute shrinkage and selection operator with Extended Bayesian Information Criterion) Gaussian graph-theoretical model for establishing symptom-centered network to estimate bridging centrality. Here, each item was modeled as "node", and these "edges" were estimated by the conditional correlations of pairs of these node for forming the "graphic network". As guided by didactic framework, the EBICglasso algorithm was used for regularization of this network to control the false-positive errors, thus generating the final symptom-centered network. Furthermore, we estimated topological centrality of this network by using 5 topologically nodal and 5 topologically bridging centrality, with high values of centrality for detecting hubs, including Strength, Betweenness, Closeness, Expected Influence (EI) for nodal ones and including bridge strength, bridge betweeness, bridge closeness as well bridge 1-step/2-step EI for bridging ones. Bridge strength indicates a node's total connectivity with other disorders; Bridge betweenness assesses the number of times a node lies on the shortest path between any two nodes from two distinict disorders; Bridge closeness reflects the average distance from a node to all nodes outside of its own disorder; The 1-step Bridge expected influence, much like bridge strength, indicates a node's sum connectivity with other disorders. However, in the case of bridge expected influence, we do not take the absolute value of edges before summing them; The 2-step Bridge expected influence indicates a node's strength by summing values of edge with both direct and indirect connections to other disorder. In total, these metrics reflect the multifarious measurements on many aspects of bridging centrality. Details of how to calculate these topological metrics can be found elsewhere[9,10]. Estimates of this network have been carried by R packages of "bootnet", "qgraph" and "networktools".

**6. Normalized Shannon's entropy**

We deployed the normalized Shannon's entropy (SE) to quantify the extent of which symptoms possessed high bridging centrality across differently topological properties. The mathematical description of the SE has been detailed underneath, where $p$ indicated probability of a given hub across all the 5 bridging centrality.

$$H(X) = -\sum_{i=1}^{m} p_i \log_2 (p_i)$$

Specifically, extracting these nodes with top 50% higher centrality (herein called “hubs”) in each topological property were iterated, thus generating 20 (hubs) x 5 (topological metrics of bridging centrality) matrix. Further, this matrix was vectored to describe which topological properties were captured to determine “hubs” for a given node. Finally, the SE was estimated for all the given nodes, indicating how often this node was rated “hub” across these 5 topological properties. For comparability, we linearly normalized these raw SE into interval of [0, 1]. In total, the nodes with higher SE were more likely to be hubs across multifarious topological properties (i.e. bridging centrality).

**7. Statistical powers of network analysis**

We used Monte Carlo simulation method that proposed recently to conduct the sample size estimations for this network analysis[8]. As guided by this method, we firstly optimized the outcome (sensitivity = 0.6) and statistical power (specificity = 0.8). Then, the Monte Carlo simulations (*n* = 5,000) had been done to calculate these parameters across putative sample sizes, with curve-fitting methods to estimate these statistics. Finally, by using the Bootstrapping method (*n* = 10,000), the uncertainty bounds had been estimated around these curves for determining sample size. These analyses were validated as well. These sample size analyses have been carried out by using R packages of “powerly”. We found that 1,622 participants were required to ensure such statistical powers in the present study **(Fig. S3-6)**.

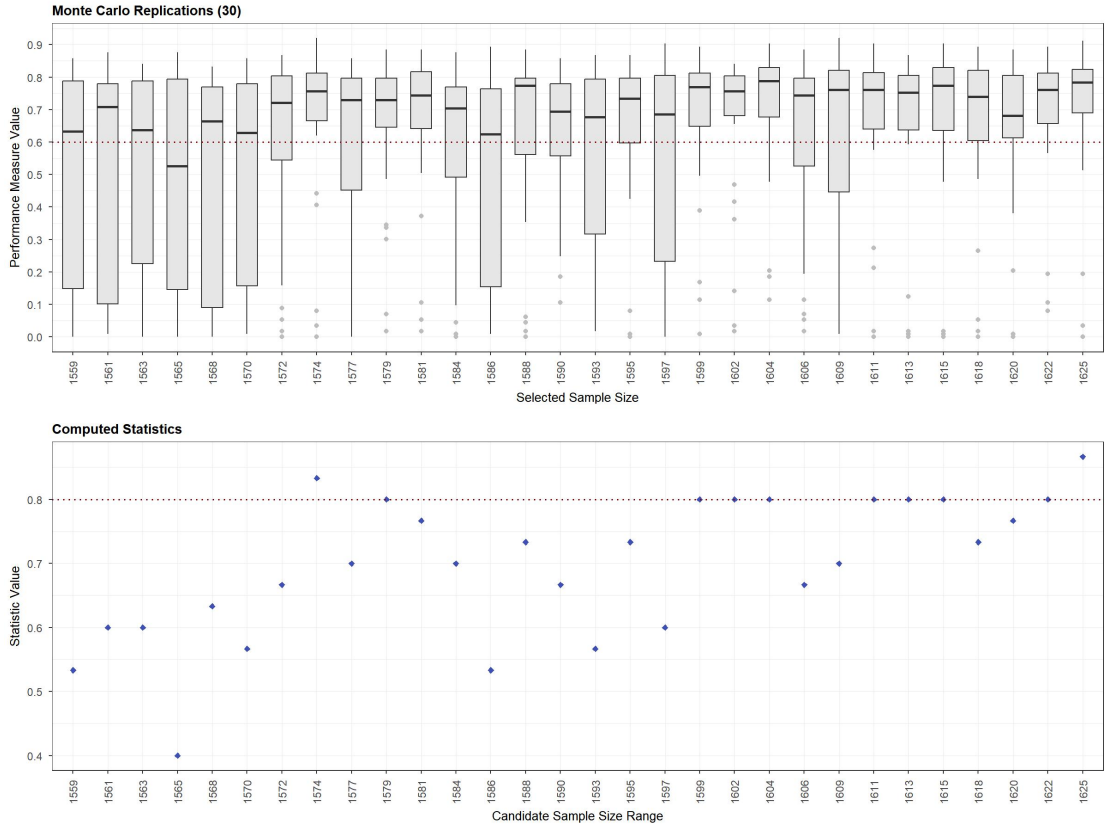

**Fig S3. Monte Carlo simulations to performance (outcome, upper) and statistical power (bottom).** At the top panel, each column showed the model performances of a given sample size across 30 Monte Carlo replications. The dashed red line indicated an acceptable criterion to determine optimal model performance. At the bottom panel, each blue point indicated the statistical value from network model by given sample sizes. The dashed red line indicated an acceptable criterion to determine optimal model performance. No inferential statistics are conducted here. Source data are provided as a Source Data file.

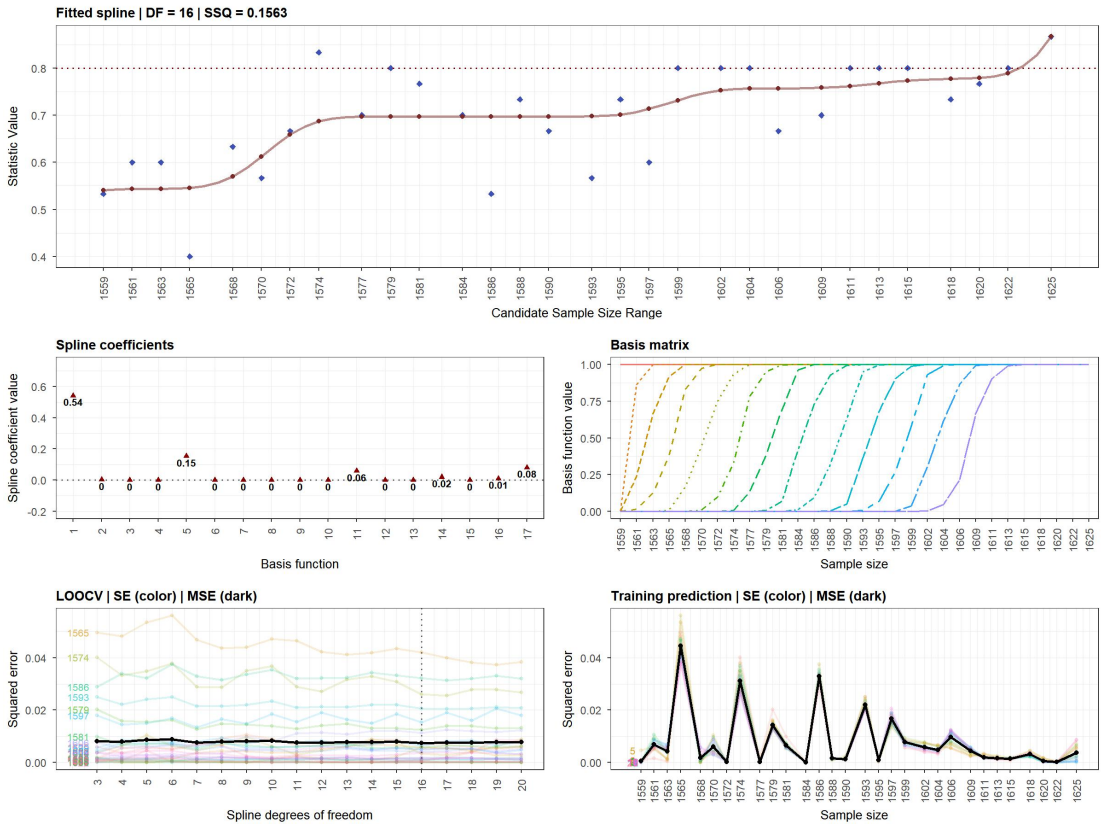


**Fig S4. Curve-fitting statistics varied from different sample sizes.** At the top panel, each blue point indicated the statistical value from network model by given sample sizes. The dashed red line indicated an acceptable criterion to determine optimal model performance. This translucent red line indicated a optimal curve-fitting. In the left-middle panel, the spline coefficients (marked by the red triangle) are presented by varying from 10 different basis functions. In the right-middle panel, each line represented a basis function to show the changes of values across sample size. Colors were just used to differentiate basis functions each other. In the left-bottom panel, the squared errors are estimated across different spline degrees of freedom. Colors for lines were just used to differentiate sample sizes each other. For the right panel, colors for lines were used to differentiate spline degrees of freedom each other. No inferential statistics are conducted here. Source data are provided as a Source Data file.

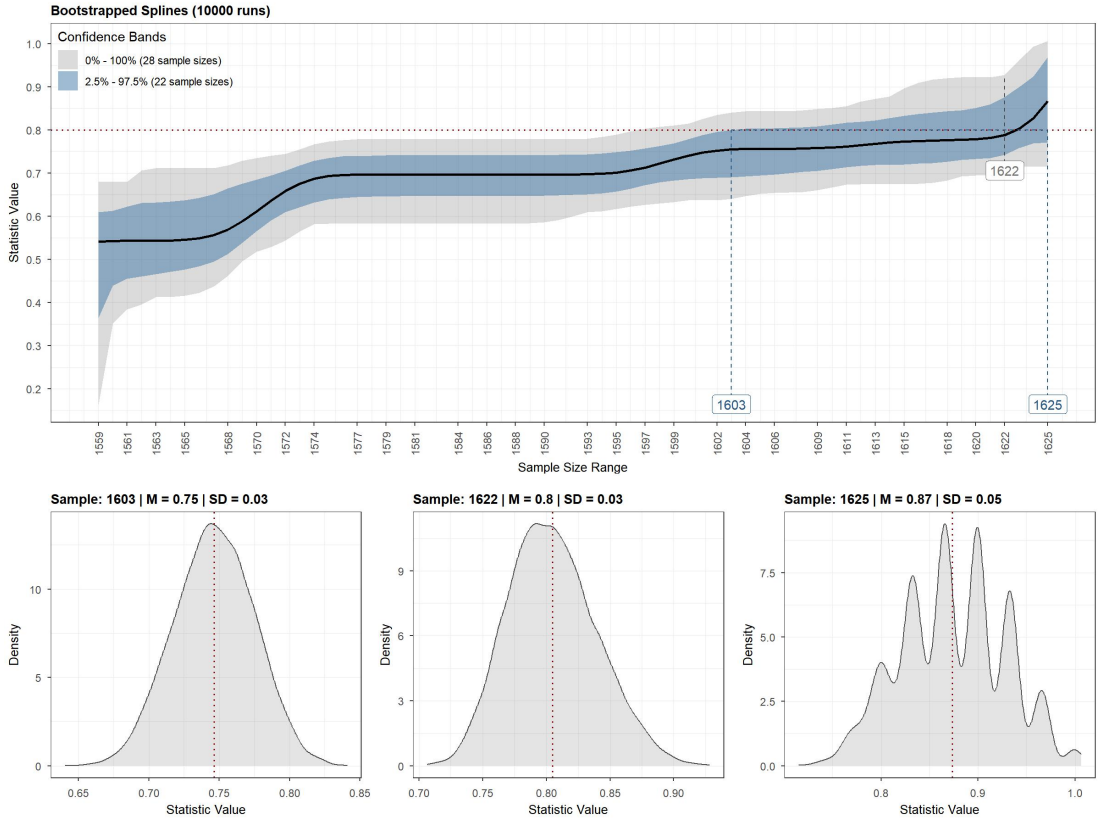


**Fig S5. Estimates of confidence of sample sizes to fulfill required statistics.** At the top panel, the blue (gray) shadow pictured the 95% (100%) confidence bands of statistics from network model across 10000 Bootstrapping pseudo-samples. The dashed red line indicated an acceptable criterion to determine optimal model performance. In the bottom panel, the red dashed line indicated the optimal density of statistics from network model to given sample sizes. No inferential statistics are conducted here. Source data are provided as a Source Data file.

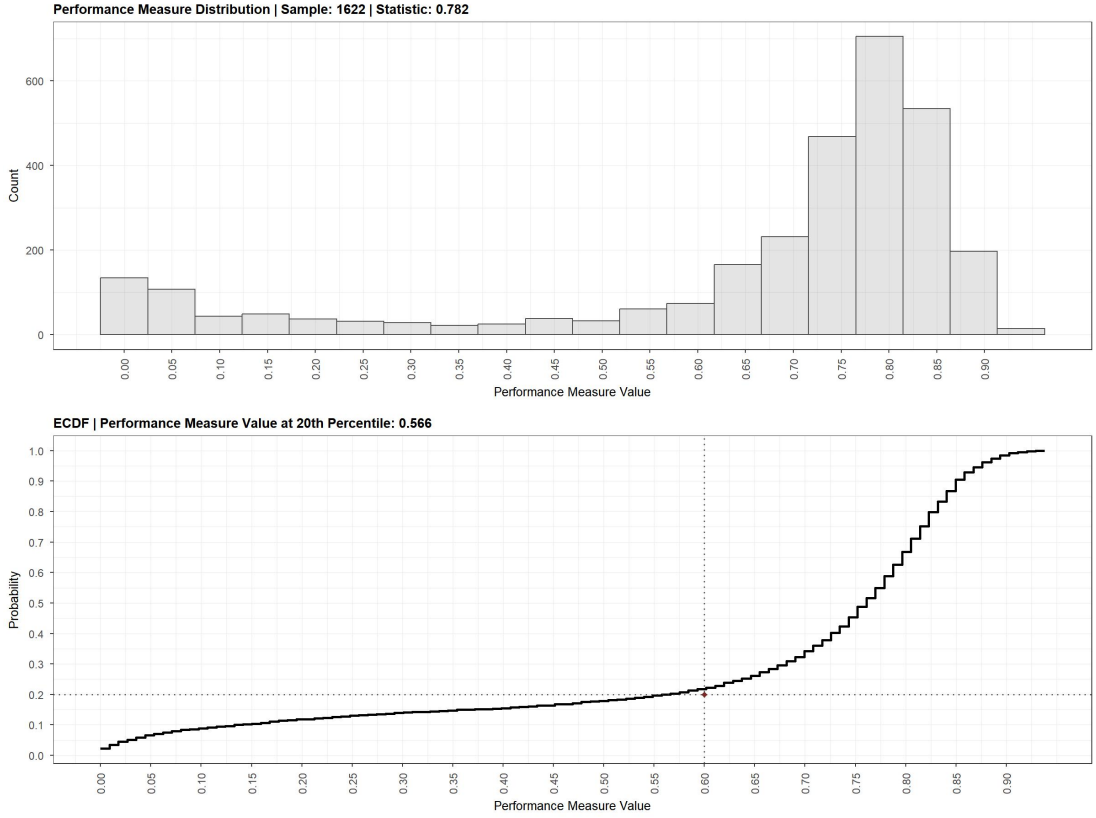


**Fig S6. Results of sample size estimates to outcome and statistical powers.** At the bottom panel, this black solid curve indicated probability of model performances by Empirical Cumulative Distribution Function (ECDF). This red point depicted the cutoff of this curve. No inferential statistics are conducted here. Source data are provided as a Source Data file.

### 8. Stability estimates to network analysis

We used the Bootstrapping method to estimate the stability of this network analysis, that was to evaluate whether these network-analytic outcome could be replicated when the participants of this sample were randomly dropped out. In this vein, the stability coefficient (CS) depicting the correlations of network-wise statistics between original sample and pseudo-samples that produced by randomly dropped out participants. As default parameters, a correlation of at least 0.7 (default) between statistics based on the original network and statistics computed with less cases was used as constrictions.

### 9. Parallel analysis, permutation test, general linear regression model and measure invariance

As in line with the *p* factor, we constructed a factor structure with a common factor, and further showed well goodness-of-fits (RMSEA = 0.065, 90% CI: 0.056 - 0.071; SRMR = 0.033, TLI = 0.901, CFI = 0.936, BIC = 81.521). Moreover, multi-factor structures were examined as well **(see Tab. S5)**. Moreover, we used the parallel analysis in the exploratory factor analysis (EFA) to examine whether other multi-factor structures were overfitting. Parallel analysis is a technique used to decide how many factors to retain in the EFA. It works by comparing eigenvalues from the actual data to those from random data of the same size. After performing EFA on the original dataset to extract initial eigenvalues, random datasets are created and analyzed similarly to calculate

average eigenvalues for each factor. Actual data eigenvalues that are larger than the corresponding averages from the random data suggest meaningful underlying factors. Factors are retained if their eigenvalues exceed the average random eigenvalues, distinguishing them from noise. This method helps prevent retaining too many or too few factors for causing overfitting or underfitting, providing a more empirical approach to determine factor structure [9,10]. By doing so, we found that the number of factors that decomposed from these 12 bridging symptoms should not exceed to two. Thus, we only examined one-factor and bifactor structure in this dataset. Although the multi-factor structures were found better goodness-of-fits, these structures were determined to at high risks of overfitting, and were thus regarded for poor performance in the model fitting.

| Structure | RMSEA | RMSEA 90% CI | SRMR | TLI | CFI | BIC |
|---|---|---|---|---|---|---|
| bifactor | 0.100 | 0.095-0.106 | 0.066 | 0.764 | 0.807 | 744.530 |
| 3-factor | 0.034 | 0.027-0.041 | 0.016 | 0.972 | 0.986 | -139.640 |
| 4-factor | 0.029 | 0.021-0.038 | 0.012 | 0.980 | 0.993 | -117.887 |
| 5-factor | 0.022 | 0.01-0.033 | 0.008 | 0.989 | 0.997 | -90.645 |
| 6-factor | 0.000 | 0-0.022 | 0.004 | 1.002 | 1.000 | -60.924 |
| 7-factor | 0.000 | 0-0.028 | 0.002 | 1.006 | 1.000 | -21.371 |

**Tab S5. Goodness-of-fit to multi-factor structures.** RMSEA = root-mean-square error of approximation; SRMR = Standardized Root Mean Square Residual; TLI = Tucker-Lewis Index; CFI = Comparative Fit Index; BIC = Bayesian Information Criterion. Model performances to the multi-factors were italicized as they exposed to the risk of overfitting.

To estimate whether the single factor structure could be best-fitting one in characterizing general structure of these 12 bridging symptoms, we capitalized on the permutation test at $n$ = 1,000. Specifically, we identified that these 12 bridging symptoms were derived from both depression and anxiety, with 5 of 12 to anxiety (i.e., item 5, 12, 14, 16, 18) and with 7 of 12 to depression (i.e., item 1, 11, 13, 16-19). Thus, in the first step, we randomly shuffled the item number from all the item in depression and anxiety, respectively. In the second step, the items that were renumbered had been selected out by matching the original ones (that we found above, e.g., item 5, 12, 14 ,16 in the anxiety and item 1, 11, 13 in the depression), thus generating a pseudo-bridging symptom set with 12 items. In the third step, this procedure had been iterated for 1,000 times to obtain the null distribution of these bridging symptoms. In the last step, the statistical significance was calculated by comparing Explained Variance Ratio (EVR, %) from the original one to this null distribution.

Beyond the conceptual framework, to justify whether this conceptualized "*cb* factor" is statistically distinct to the general psychopathological factor (i.e., *p* factor), we build upon the general linear regression model by using the "glm" function at the R, with the DV for the total scores of all the depression and anxiety symptoms (representing severity in the comorbidity) and with IV for the individual bridging symptom (s), *cb* factor scores, or *p* factor scores, respectively. Given the colinearity issue, no statistical inferences were used to in the model comparisons. Model performances were evaluated by AIC (Akaike Information Criterion) and BIC (Bayesian

Information Criterion), R2 and RMSE (Root Mean Squared Error). Results showed that the *cb* factor explained well to the total scores of all the symptoms compared to the *p* factor **(see Tab. S6)**.

| Model (IV) | AIC | BIC | R2 | RMSE | P value for β (uncorrected) |
|---|---|---|---|---|---|
| TAI5 | 13868.03 | 13884.86 | 0.067 | 7.459 | < .001 |
| TAI12 | 13960.81 | 13977.65 | 0.023 | 7.632 | < .001 |
| TAI14 | 13859.78 | 13876.61 | 0.071 | 7.443 | < .001 |
| TAI16 | 13813.57 | 13830.40 | 0.092 | 7.359 | < .001 |
| TAI18 | 13824.21 | 13841.04 | 0.086 | 7.378 | < .001 |
| SDS1 | 13907.55 | 13924.39 | 0.048 | 7.532 | < .001 |
| SDS11 | 13935.55 | 13952.39 | 0.035 | 7.584 | < .001 |
| SDS13 | 13880.37 | 13897.20 | 0.061 | 7.481 | < .001 |
| SDS16 | 13843.20 | 13860.03 | 0.078 | 7.413 | < .001 |
| SDS17 | 13734.40 | 13751.24 | 0.126 | 7.216 | < .001 |
| SDS18 | 13760.26 | 13777.10 | 0.115 | 7.262 | < .001 |
| SDS19 | 13976.14 | 13992.98 | 0.015 | 7.661 | < .001 |
| **The *cb* factor** | **13355.59** | **13372.43** | **0.275** | **6.571** | **< .001** |
| The *p* factor | 14006.72 | 14023.56 | 0.001 | 7.719 | 0.345 |

**Tab S6. Model performance for comparisons between regressors (individual symptoms, the cb factor scores and the p factor scores ).** The best-fitting model has been marked by bold font. The general linear regression model was used here, with the two-sided *z* test to examine whether the $\beta$ could reach statistical significance ($p < .05$, uncorrected).

To ensure the measure invariance across populations, we have capitalized on the Jeffreys-Zellner-Siow Bayesian factor (BF) statistics with aprior Cauchy distribution for estimating between-group variants of the *cb* factor scores on sex (male vs. female), ethnicity (majority vs. minority) and pandemic periods (pre-pandemic vs. post-pandemic). Here, the strong posterior evidences to support between-group variance were mathematically quantified as $BF_{10} > 3$. Results showed the weak Bayesian evidences to support significant between-group variants for *cb* factor scores, including sex ($BF_{10} = 2.7$), ethnicity ($BF_{10} = 0.2$) and pandemic periods ($BF_{10} = 0.1$), respectively, which demonstrated no prominent across-population variations in this conceptualized metric. Full results have been tabulated into the **Tab S7**.

| Population variables | $BF_{10}$ | 95% Credible Interval | Median | Error, % |
|---|---|---|---|---|
| Sex | 2.680 | 0.039 - 0.222 | 0.131 | 0.008 |
| Ethnicity | 0.163 | -0.049-0.183 | 0.067 | 0.163 |
| Pandemic periods | 0.094 | -0.095-0.178 | 0.041 | 0.207 |

**Tab S7. Bayesian factor evidence strengths of population-based variances for the *cb* factor.** $BF_{10}$ indicated the strength of Bayesian evidence supporting alternative hypothesis than null hypothesis.

**10. Edge-centric functional connectome (eFC) construction**

Rather nodal functional connectivity, we established the eFC to characterize the "edge-to-edge" communication patterns by using brain resting-state functional connectivity MRI (rs-fcMRI). The Schaefer-100 atlas was used to parcel cortical areas into 100 regions, and time series of each region were extracted to be z-scored firstly. Then, we obtained "edge time series" by estimating the dot products of these time series, one-by-one, that was to calculate instantaneous co-fluctuations, with positively high values for the instantaneously synchronization (and vice verse). Thus, we gained 4,950 ($100\times99/2$) "edge time series" for all the "node pairs" of these parceled regions. Finally, as same as nodal functional connectome, the edge-to-edge connectome was built upon for containing 12,248,775 ($4{,}950 \times 4{,}949/2$) unique eFCs by correlating each pair of these 4,950 "edge time series" for each participant, with each edge-to-edge correlation coefficient for defining one eFC strength. The high eFC strength indicated similarity of nodal communication patterns[11]. For examining whether the high centrality of these edge-centric nodes that we found in the visual inspections reached statistical significance, we used the Permutation test at $n$ = 1,000. We outputted the degree centrality of this graph as "true value", and randomly shuffled edges in this graph for 1,000 times to generate 1,000 pseudo-graphs. Furthermore, the degree centrality for all these pseudo-graphs had been all estimated to generate the null distribution. Finally, the statistical significance was estimated by comparing this "true value" in this null distribution.

**11. Edge-centric connectome-based predictive model (eCPM)**

Once these eFCs had been calculated, the edge-centric connectome-based predictive model (eCPM) was built to predict the *cb* factor scores to untangle its brain signatures. In line with the original CPM, we firstly estimated the inter-subject conditional correlations of all the eFCs to the *cb* factor scores. Second, we retained eFCs that reached statistical significance ($p$ < .05, uncorrected), and generated the thresholding postive and positive mask, respectively. The positive (negative) mask included all the eFCs that were positively (negatively) correlated with the *cb* factor scores. These correlations were adjusted for these variables of no interests, including sex, age, scanning-related psychological status, socioeconomic status, and ethnicity. Furthermore, in each mask, the sum of all the eFC values has been caculated as individual neural feature for each participants, thus extracting the positive and negative eFC feature. Finally, we trained the machine-learning models with support vector algorithm to predict the *cb* factor scores by using the positive eFC feature, negative eFC feature or both in the main sample, but to test the performance of this trained model in these independent samples. Model performance was estimated by the mean square error and $R^2$ of predicted values to true ones. Here, the linear support vector regression (SVR) model was deployed, with no specific parameter modifications to strengthen methodological robustness. We used the linear kernel in this SVR model, which adopted default model parameters. These analyses were all carried out the "Statistics to Machine Learning toolbox" of MATLAB (MathWorks Inc.).

**12. Quantitative univariate twin study analysis**

We utilized on the Beijing Twin Study Dataset (2011-2017) containing 245 pairs of twins to probe into the phenotypic heritability of the eFC features (127 monozygotic twins and 118 pairs of

dizygotic twins, aged at 16-28, M = 21.0, S.D. = 2.57). All the collections and preprocessing of their neuroimaging data were in line with the main analysis. Details for this dataset can be found elsewhere[12,13]. We firstly established a univariate ACE (A, additive genetic effect; common factor, C; unique environment, E) model by using the OpenMx package (3.1.2) at R platform. Once we have built upon the full ACE model, these nested submodels dropping out at least one parameters (e.g., AE, CE, E) were compared to this full one for gaining the statistical significance of the additive genetic effects ($a^2$) in this given model. The $X^2$, along with Akaike information criterion (AIC) or Bayesian Information Criterion (BIC), were used to quantify the goodness-of-fitting, with the less AIC or BIC for better fitting performance. A statistical significant $X^2$ difference between full model and one nested submodel indicated that the nested model fitted worse than the full model, otherwise non-significant one could determine that this nested model with fewer parameters (compared to full models) was the best-fitting model, given the model parsimony.

**13. AHBA dataset and preprocessing**

AHBA dataset was built by AIBS (Allen Institute for Brain Science) (http://human.brain-map.org, RRID: SCR_007416) for providing whole-brain spatially heterogeneous gene expression level from six donors. These adult donors provided their postmortem brains (age = 42.50 ± 13.38, 1 females, two whole-brain samples and five left-hemisphere brain samples). All the donors are required to be no history of neuropsychiatric disorders or neurological conditions, such as brain injury, epilepsy and any substance abuses. These postmortem brains have been sampled within 30 hours from death (https://help.brain-map.org/download/attachments/2818165/). Each postmortem brain was firstly sliced into ~ 500 anatomical samples in each hemisphere. Then, the DNA microarray high-pass sequences technique was used to test the gene expression level for each sample. Afterwards, gene information for each sample was mapped into 3D MRI coordinate space (standard MNI space) by using precedent high-resolution T1 images. The whole dataset contained 3072 samples, and obtained qualified gene expression data from 58,692 probes. To obtain the group-averaged gene expression atlas, the normalization processes were implemented across samples and across donors. To conduct connectome-transcriptional analysis, we selected Schaefer-100 atlas with 100 regions for assignments.

As recommended pipeline[14], we preprocessed whole-brain transcriptional dataset by following this workflow (https://github.com/BMHLab/AHBAprocessing). Main steps for preparing this dataset included six section. (1) Gene information re-annotation. To obviate outdated gene annotation, the probe-to-gene mapping was implemented by using re-annotator toolbox for updating annotation information (probe *n* = 45,821 corresponding to 20,232 genes) (https://earray.chem.agilent.com/earray) in the hg38 sequencing database; (2) To remove background noise, the IBF (intensity-based filter) was used to filter probes that exceeded background (gene *n* = 10,190); (3) to tackle with multiple-probes for one gene, the gene annotation was determined by the highest correlation of RNA-seq to a given gene (probe selection); (4) for connectome-transcriptional analysis, each sample tissue was aligned into Schaefer-100 atlas in the MNI space, and the samples would be removed once the centroid Euclidean distance of sample to region in this atlas exceeded 2 mm; by using such criterion, 820 samples were retained to cover 100 regions in the atlas, with each sample for 10,027genes; (5) to

correct the inter-sample and inter-donor heterogeneity, scaled robust Sigmoid normalization has been used; for inter-sample variant, the first-step normalization was implemented across all the probes within sample; for each brain, the probes were normalized across all the sample; (6) for each region, gene expression levels are averaged across all the samples from six donors (gene selection). Following that, the final atlas-gene matrix was outputted to be pending for connectome-transcriptional alignment (100 x 10,027).

**14. Partial least squares (PLS) model**

Given the co-linearity structure for co-expressions of these gene in the AHBA, we build upon the partial least square (PLS) regression model to fitting the transcriptional expression levels from 10,027 genes to eFC-the-*cb*-factor representation similarity (RS). In this model, the first component could be captured by a linear combination of standardized predictors and responses, which was required to extract maximum variances ($u_1$, $v_1$). Thus, the correlation between $u_1$ and $v_1$ would be the maximum pair. Then, the observation matrix for each variate ($\mathbf{A}$, $\mathbf{B}$) could used to estimate the vector scores ($\hat{u_1}$, $\hat{v_1}$) for the first component. In this vein, the vector scores could be calculated by a Lagrange multiplier method.

$$\max\left(\hat{u_1}\cdot\hat{v_1}\right) = \rho^{(1)\mathrm{T}}\mathbf{A}^{\mathrm{T}}\mathbf{B}^{\gamma(1)}; \gamma^{(1)} = \frac{1}{\delta 1}\mathbf{B}^{\mathrm{T}}\mathbf{A}\rho^{(1)}$$

Following that, the regression model can be used for fitting response to $u_1$, one-by-one and verse vice. Then, the residual matrix can be obtained as $\mathbf{A1}$ and $\mathbf{B1}$. If the elements in both residual matrix approached zero, this component would be assumed to explained this model. If it is not this case, both residual matrix should be used to replace original correlation matrix for recalculating these statistics until the condition was fulfilled. In the resultant step, if the rank of observation matrix ($\mathrm{n} \times \mathrm{m}$) was smaller than minimum value at position of ($\mathrm{n}\text{-}1$, $\mathrm{m}$), all the qualified components would be considered to be extracted completely. In this case, the PLS can be used to fit $u \sim x$ to $y \sim u$. Statistical significance for each component has been estimated by the Permutation test. Further, the bootstrapping method with $n$ = 5,000 was deployed estimating weights and corresponding statistics ($Z$ values) for these genes. To balance both Type-I and Type-II errors, the statistical threshold was set to $Z > 3$ (PLS+) or $Z < -3$ (PLS-) to determine the significantly overexpressed or underexpressed genes. To prevent from over-fitting, we added the 10-fold cross-validation method in modelling this PLS regression. Results showed the acceptable mean-square error (MES) in all the submodels (averaged MSE = 1.43, IQR: 0.87-1.62), which demonstrated no significant over-fitting issue in establishing this PLS model.

**15. GAMBA decoding**

GAMBA platform was used to reveal the association between gene expression level and neuroimaging-derived phenotype by regression model. Main steps for decoding the gene list that we obtained in the current study has been provided in main texts. Here provided original descriptions for statistical details (http://dutchconnectomelab.nl/GAMBA/)[15]:

The association between the cortical gene expression profile and regional properties of different neuroimaging phenotypes is assessed using linear regression.

$$y_i = \beta_i \beta 1 X j + \varepsilon$$

where $Y_i$ indicates the normalized gene expression profile of gene i or the averaged profile of a gene set $i$, $X^j$ the normalized cortical profile of neuroimaging phenotype $j$, and cov the normalized covariate. Normalization is performed by substracting each value by the mean, followed by diving values by one standard deviation. The standardized regression coefficient $\beta_i$ and the corresponding p-value are obtained.

Furthermore, GAMBA tests whether the observed association is spatially specific and gene specific. The null-spin, null-random, null-coexpression, and null-brain models are used. Per gene and per brain imaging phenotype, GAMBA performs a z-test to examine whether the observed $\beta_1$ (i.e., the effect size) was higher than the average effect size observed in the null models.

$$z = (\beta_1 - u)/\sigma$$

where $\mu$, $\sigma$ indicate the mean and standard deviation of $\beta_1$ in different null conditions. A two-sided p-value was computed as follows:

$$p = 2\emptyset(-z)$$

where $\Phi$ is the standard normal cumulative distribution function. GAMBA implements Bonferroni and FDR correction with adjustable thresholds to correct for multiple comparisons in the analysis of each imaging modality. Results reaching significance are shown in darker colors, otherwise in lighter colors.

**16. Enrichment analysis**

We deployed the board-certified meta-analytical platform called "Metascape" (https://metascape.org/gp/index.html) with newest version (updated by ChatGPT resources) to delineate functional processes that were enriched from above gene sets (PLS1 and PLS2). The gene set was used as input for this platform, and was further annotated by multiple biological databases. Based on cumulative hypergeometric distribution, the statistical significance of such enrichment of biological process/pathways for this given gene set was estimated, with Benjamini-Hochberg FDR corrections. To promote understanding of such molecular understructures, the protein-to-protein interaction (PPI) enrichment was examined as well. By measuring physical interactions, the resultant PP network was established. Furthermore, we carried out the Molecular Complex Detection (MCODE) for capturing PP modules, with the same statistical inferences and corrections. To probe into the tissue-specific cell type-specific enrichment, we utilized on built-in databases (e.g., PaGenBase, Cell Type Signatures) of this platform for disentangling these associations as well.

The tissue-specific enrichment analysis had been further carried out by the additional Specific Expression Analysis (SEA, http://genetics.wustl.edu/jdlab/csea-tool-2/) tool[16]. This dataset possessed strengths to show the gene enrichment specificity by estimating the specificity index

probability (pSI). This metric described how this given gene set could enrich higher into specific tissues compared to other ones from different thresholds to include background enrichment terms (e.g., 0.0001, 0.001, 0.05)[17]. Furthermore, the neurodevelopmental enrichment across 6 brain systems (e.g., amygdala, cerebellum) from early fetal to young adulthood periods was examined in the SEA tool as well, with the *q* values < .05 at Benjamini-Hochberg FDR corrections.

**SUPPLEMENTAL RESULTS**

**1. Topological centrality of depression-anxiety comorbidity network**

We estimated mainstreaming topologically properties for the nodal and bridging centrality to this network, favoring to represent many aspects of this network architectures, including Strength, Betweenness, Closeness, Expected Influence (EI) for nodal ones and including bridge strength, bridge betweeness, bridge closeness as well bridge 1-step/2-step EI for bridging ones **(Tab. S8-9)**. Those nodes whom centrality was ranked at top 50% have been primarily selected as "putative hubs".

| Symptom | Strength | Betweenness | Closeness | Expected influence | Predictability |
|---|---|---|---|---|---|
| TAI1 | 0.937562981 | 13 | 0.001108502 | 0.937562981 | 0.432 |
| TAI2 | 0.986388843 | 16 | 0.001228951 | 0.763395403 | 0.308 |
| TAI3 | 1.044194229 | 21 | 0.001165895 | 0.801040687 | 0.377 |
| TAI4 | 0.679499946 | 0 | 0.001008205 | -0.420292525 | 0.165 |
| TAI5 | 1.201288484 | 59 | 0.001363786 | 1.101028476 | 0.403 |
| TAI6 | 0.68870526 | 0 | 0.000943941 | 0.678872028 | 0.37 |
| TAI7 | 1.151969109 | 45 | 0.001014756 | 1.151969109 | 0.469 |
| TAI8 | 0.984415426 | 7 | 0.001133833 | 0.856794005 | 0.372 |
| TAI9 | 0.998801014 | 11 | 0.001152646 | 0.859528342 | 0.393 |
| TAI10 | 1.144271233 | 29 | 0.001121412 | 1.120052512 | 0.493 |
| TAI11 | 0.974673878 | 25 | 0.001252823 | 0.950455157 | 0.383 |
| TAI12 | 1.171929297 | 78 | 0.00129668 | 0.94136073 | 0.367 |
| TAI13 | 0.893508516 | 52 | 0.001274969 | 0.893508516 | 0.321 |
| TAI14 | 0.755007378 | 75 | 0.001279505 | 0.755007378 | 0.285 |
| TAI15 | 0.893305758 | 2 | 0.00116903 | 0.879574214 | 0.328 |
| TAI16 | 1.092240938 | 46 | 0.001206457 | 1.092240938 | 0.443 |
| TAI17 | 0.990960768 | 22 | 0.001193346 | 0.87167716 | 0.403 |
| TAI18 | 1.304579951 | 52 | 0.001228719 | 1.114762302 | 0.463 |
| TAI19 | 0.829183126 | 41 | 0.001043406 | 0.773043447 | 0.341 |
| TAI20 | 0.675689463 | 8 | 0.001077644 | 0.608987745 | 0.233 |
| SDS1 | 1.14924404 | 23 | 0.001203528 | 1.14924404 | 0.408 |
| SDS2 | 0.426602591 | 0 | 0.000896685 | 0.349846857 | 0.125 |
| SDS3 | 0.961090036 | 15 | 0.001167294 | 0.917601309 | 0.301 |
| SDS4 | 0.557508491 | 2 | 0.000925933 | 0.557508491 | 0.143 |
| SDS5 | 0.084002454 | 0 | 0.00072832 | 0.058567933 | 0.007 |
| SDS6 | 0.478591707 | 0 | 0.001064618 | 0.395056985 | 0.111 |
| SDS7 | 0.472718239 | 1 | 0.000953768 | 0.223410417 | 0.054 |
| SDS8 | 0.463331457 | 6 | 0.000997463 | 0.339008866 | 0.058 |
| SDS9 | 0.785065083 | 18 | 0.001063482 | 0.648059628 | 0.133 |
| SDS10 | 0.929368717 | 73 | 0.001355738 | 0.869172919 | 0.316 |
| SDS11 | 1.18672751 | 97 | 0.001313202 | 1.18672751 | 0.438 |
| SDS12 | 0.993859957 | 40 | 0.001252217 | 0.993859957 | 0.405 |

| | | | | | |
|---|---|---|---|---|---|
| SDS13 | 1.165321475 | 40 | 0.001178713 | 1.138791854 | 0.292 |
| SDS14 | 1.094275069 | 36 | 0.001230613 | 1.061667416 | 0.468 |
| SDS15 | 0.997466119 | 32 | 0.001170268 | 0.723828257 | 0.199 |
| SDS16 | 0.898452993 | 36 | 0.001288421 | 0.898452993 | 0.353 |
| SDS17 | 1.089730839 | 77 | 0.001367477 | 0.979663296 | 0.462 |
| SDS18 | 1.331362953 | 79 | 0.001331696 | 1.184528572 | 0.542 |
| SDS19 | 0.912402939 | 66 | 0.001251597 | 0.880056529 | 0.141 |
| SDS20 | 0.861327842 | 13 | 0.001147165 | 0.767622216 | 0.254 |

**Tab S8. Topologically nodal centrality of nodes in this depression-anxiety comorbidity network.** SDS = The self-reported scale, TAI = trait anxiety inventory. The numbers of these abbreviations indicated corresponding items.

| Node | Bridge. Strength | Bridge. Betweenness | Bridge. Closeness | Bridge.1-step Expected influence | Bridge.2-step Expected influence |
|---|---|---|---|---|---|
| TAI1 | 0.157089968 | 6 | 0.038608913 | 0.157089968 | 0.425326014 |
| TAI2 | 0.16431403 | 2 | 0.040951227 | 0.16431403 | 0.408545344 |
| TAI3 | 0.24414109 | 23 | 0.038452068 | 0.165498837 | 0.392992505 |
| TAI4 | 0.175411327 | 0 | 0.026348318 | -0.081208883 | -0.20751795 |
| TAI5 | 0.566280634 | 45 | 0.05376303 | 0.566280634 | 1.060978698 |
| TAI6 | 0.036789981 | 0 | 0.036499329 | 0.036789981 | 0.16675198 |
| TAI7 | 0.186649998 | 28 | 0.039289275 | 0.186649998 | 0.373902807 |
| TAI8 | 0.195951057 | 2 | 0.039225743 | 0.195951057 | 0.509002147 |
| TAI9 | 0.081102823 | 0 | 0.037936361 | 0.048117424 | 0.231238084 |
| TAI10 | 0.209375364 | 17 | 0.039162575 | 0.209375364 | 0.54603245 |
| TAI11 | 0.16335734 | 22 | 0.045253391 | 0.16335734 | 0.502120472 |
| TAI12 | 0.30270261 | 46 | 0.042905157 | 0.182647428 | 0.421383768 |
| TAI13 | 0.159847193 | 39 | 0.043342882 | 0.159847193 | 0.416845639 |
| TAI14 | 0.336914115 | 33 | 0.045963881 | 0.336914115 | 0.53731982 |
| TAI15 | 0.130971435 | 2 | 0.03978008 | 0.123662038 | 0.371218545 |
| TAI16 | 0.244245356 | 34 | 0.041912188 | 0.244245356 | 0.556354594 |
| TAI17 | 0.122403844 | 13 | 0.04044384 | 0.090019976 | 0.293746749 |
| TAI18 | 0.387780442 | 31 | 0.04345569 | 0.387780442 | 0.810675254 |
| TAI19 | 0.131176121 | 15 | 0.038857225 | 0.075036443 | 0.285075146 |
| TAI20 | 0.149075302 | 11 | 0.040107753 | 0.149075302 | 0.339438893 |
| SDS1 | 0.395138867 | 15 | 0.041833977 | 0.395138867 | 0.777204967 |
| SDS2 | 0.166310191 | 0 | 0.033136251 | 0.166310191 | 0.342305593 |
| SDS3 | 0.12584244 | 8 | 0.040592362 | 0.082353713 | 0.402052101 |
| SDS4 | 0.119944752 | 0 | 0.031783685 | 0.119944752 | 0.285254541 |
| SDS5 | 0.017805476 | 0 | 0.027168046 | -0.007629045 | 0.009488998 |
| SDS6 | 0.035700211 | 0 | 0.038644693 | 0.023470945 | 0.086722898 |
| SDS7 | 0.094584903 | 0 | 0.031267939 | -0.014641822 | 0.011233959 |
| SDS8 | 0.175400956 | 4 | 0.036909053 | 0.051078365 | 0.162310932 |

| | | | | | |
|---|---|---|---|---|---|
| SDS9 | 0.055702396 | 7 | 0.035605787 | 0.034813613 | 0.173781844 |
| SDS10 | 0.23519793 | 30 | 0.046795541 | 0.203250603 | 0.456095019 |
| SDS11 | 0.153363091 | 46 | 0.047260697 | 0.153363091 | 0.423436329 |
| SDS12 | 0.138174006 | 25 | 0.047129897 | 0.138174006 | 0.439337157 |
| SDS13 | 0.367735008 | 29 | 0.040249113 | 0.367735008 | 0.706785427 |
| SDS14 | 0.235167216 | 18 | 0.045200087 | 0.235167216 | 0.619785451 |
| SDS15 | 0.263701975 | 20 | 0.038633767 | 0.144907492 | 0.439154151 |
| SDS16 | 0.47797695 | 28 | 0.052086187 | 0.47797695 | 0.795988196 |
| SDS17 | 0.257703431 | 47 | 0.05242785 | 0.257703431 | 0.675678775 |
| SDS18 | 0.304944865 | 38 | 0.049606365 | 0.304944865 | 0.762947606 |
| SDS19 | 0.375923974 | 54 | 0.046079727 | 0.343577564 | 0.651656996 |
| SDS20 | 0.14926139 | 10 | 0.041674577 | 0.083804235 | 0.220210018 |

**Tab S9. Topologically bridging centrality in this transdiganostic network.** SDS = The self-reported scale, TAI = trait anxiety inventory. The numbers of these abbreviations indicated corresponding items.

**2. Bridging symptoms of the depression-anxiety comorbidity network**

We determined the hubs of this network by using the normalized Shannon's entropy (SE), with high value for representing nodes that were ranked as "putative hubs" from multiple topological properties. We finally selected 12 nodes with > 0.8 SE values to be hubs of this network **(Tab. S10)**.

| Node | Shannon's entropy | Normalized Shannon's entropy |
|---|---|---|
| TAI5 | 3.321928095 | 1 |
| SDS18 | 3.321928095 | 1 |
| TAI18 | 3.121928095 | 0.984858662 |
| SDS11 | 2.846439345 | 0.948813115 |
| SDS17 | 2.846439345 | 0.948813115 |
| TAI14 | 2.521928095 | 0.898328913 |
| SDS1 | 2.521928095 | 0.898328913 |
| SDS19 | 2.521928095 | 0.898328913 |
| TAI12 | 2.160964047 | 0.835975008 |
| TAI16 | 2.160964047 | 0.835975008 |
| SDS13 | 2.160964047 | 0.835975008 |
| SDS16 | 2.160964047 | 0.835975008 |
| SDS14 | 1.770950594 | 0.762706907 |
| TAI7 | 1.356779649 | 0.678389825 |
| TAI10 | 1.356779649 | 0.678389825 |
| TAI13 | 1.356779649 | 0.678389825 |
| SDS10 | 1.356779649 | 0.678389825 |
| TAI11 | 0.921928095 | 0.581671866 |
| TAI1 | 0.468995594 | 0.468995594 |
| SDS12 | 0.468995594 | 0.468995594 |
| SDS15 | 0.468995594 | 0.468995594 |

| | | |
|---|---|---|
| TAI2 | 0 | - |
| TAI3 | 0 | - |
| TAI4 | 0 | - |
| TAI6 | 0 | - |
| TAI8 | 0 | - |
| TAI9 | 0 | - |
| TAI15 | 0 | - |
| TAI17 | 0 | - |
| TAI19 | 0 | - |
| TAI20 | 0 | - |
| SDS2 | 0 | - |
| SDS3 | 0 | - |
| SDS4 | 0 | - |
| SDS5 | 0 | - |
| SDS6 | 0 | - |
| SDS7 | 0 | - |
| SDS8 | 0 | - |
| SDS9 | 0 | - |
| SDS20 | 0 | - |

**Tab S10. The Shannon's entropy (SE) for each node across 10 topological properties.** SDS = The self-reported scale, TAI = trait anxiety inventory. The numbers of these abbreviations indicated corresponding items. All the nodes were reordered by descending scale based on SE values. "-" = "Not applicable".

### 3. Network Stability

The network stability (CS) was estimated by the correlations of these topological properties between original sample and pseudo-sample (s) that were randomly dropped. As indicated by didactic guidelines, the network could be determined stable if CS > 0.25 (preferably to > 0.5) [18,19]. Results showed that almost all the topological properties that the present used possessed high network stability. Some examples are given in the **Fig. S7-10**.

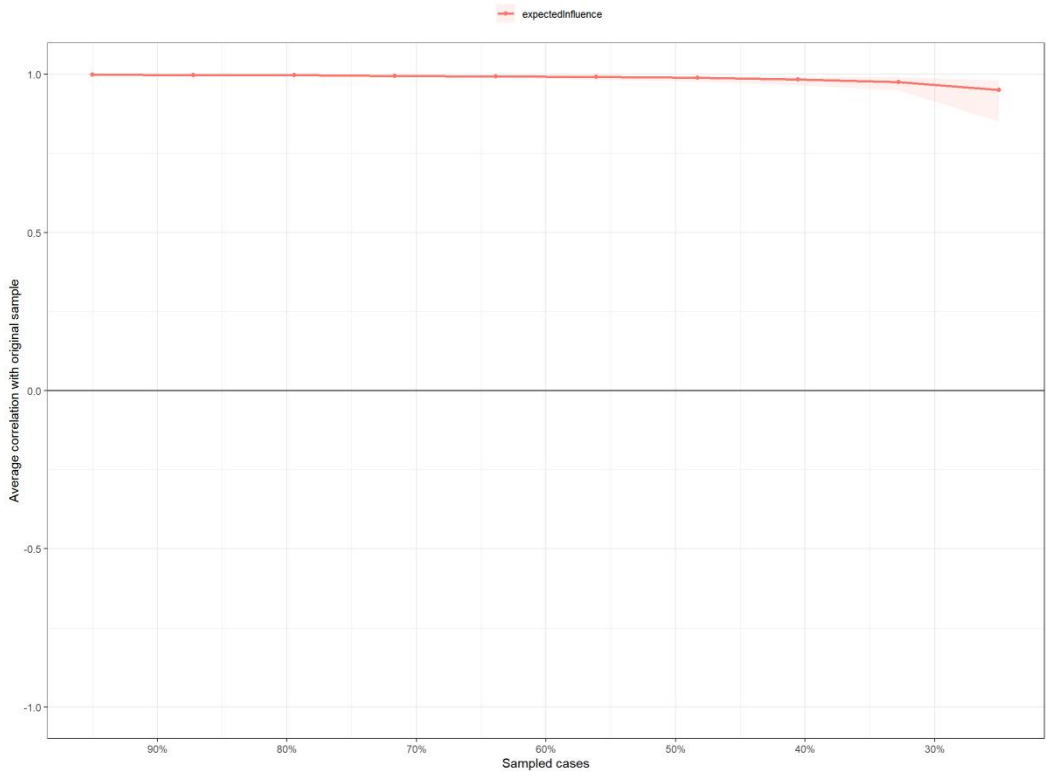


**Fig S7. Results of stability estimates for expected influence (EI).** The point in this plot indicated the averaged correlation coefficient of EI between original sample and pseudo-samples dropped cases, with 95% Confidence Interval (CI, colored by red shadow) from the Bootstrapping method (*n* = 5,000). No inferential statistics are conducted here. Source data are provided as a Source Data file.

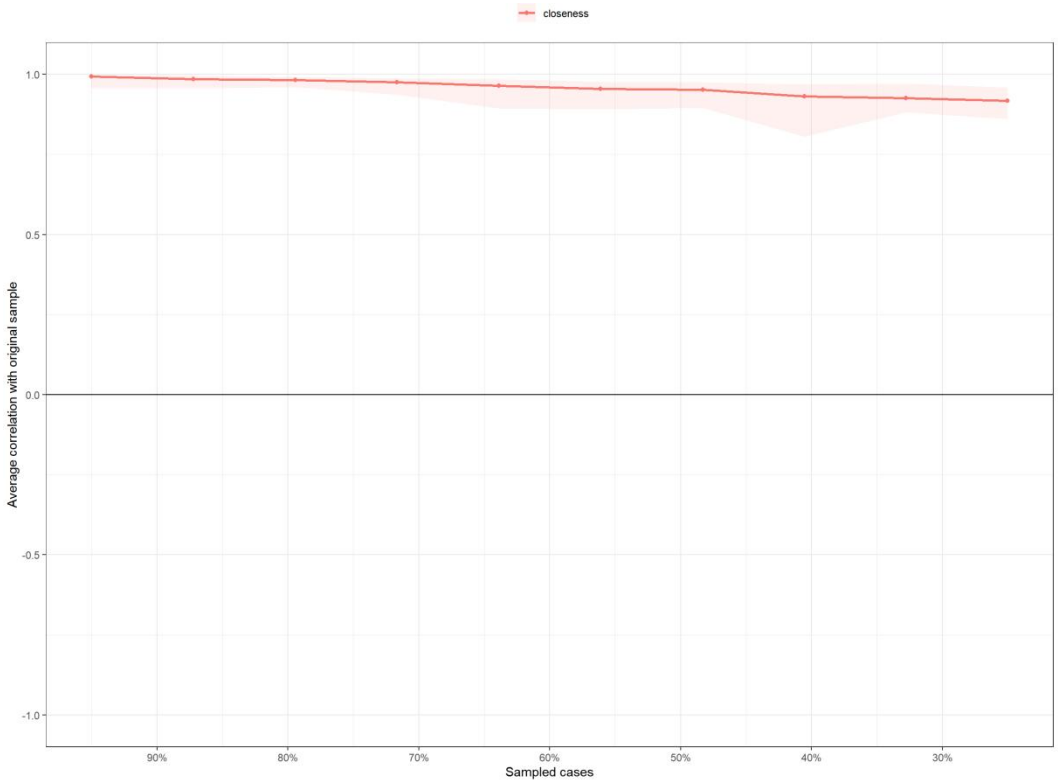


**Fig S8. Results of stability estimates for closeness.** The point in this plot indicated the averaged

correlation coefficient of EI between original sample and pseudo-samples dropped cases, with 95% Confidence Interval (CI, colored by red shadow) from the Bootstrapping method (*n* = 5,000). No inferential statistics are conducted here. Source data are provided as a Source Data file.

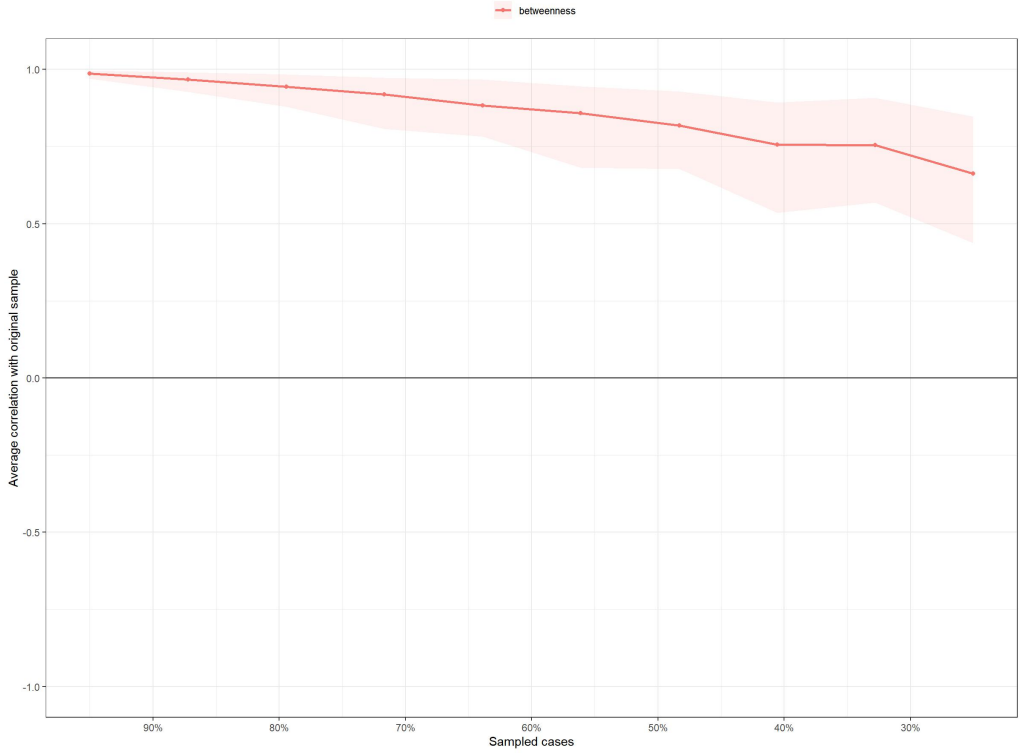


**Fig S9. Results of stability estimates for betweenness.** The point in this plot indicated the averaged correlation coefficient of EI between original sample and pseudo-samples dropped cases, with 95% Confidence Interval (CI, colored by red shadow) from the Bootstrapping method (*n* = 5,000). No inferential statistics are conducted here. Source data are provided as a Source Data file.

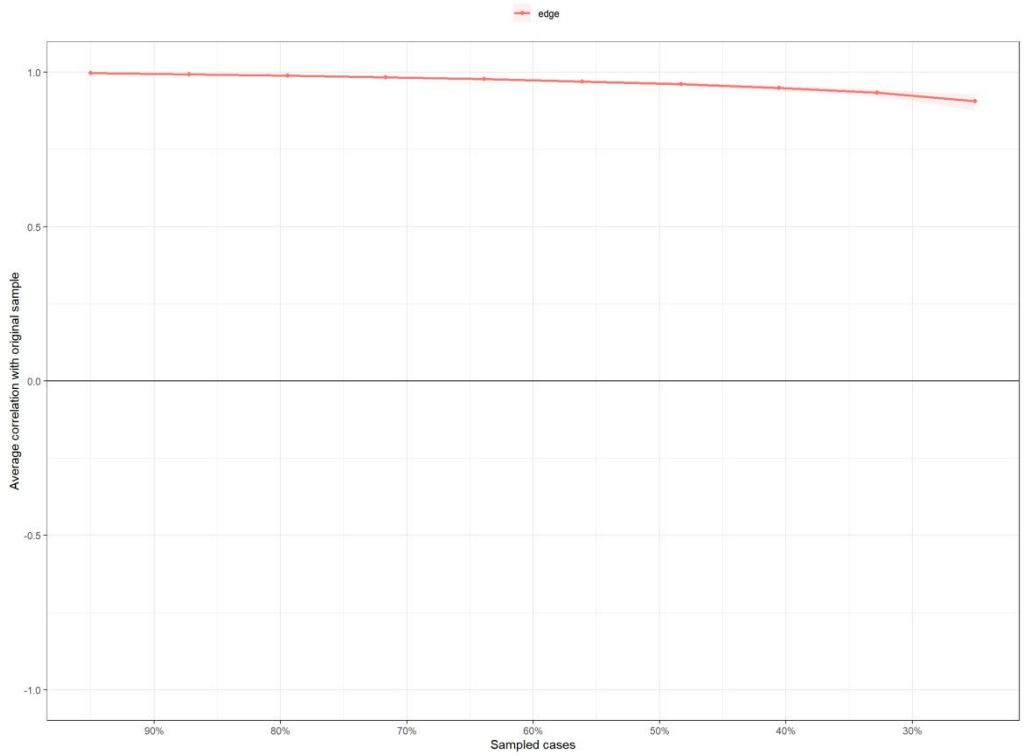


**Fig S10. Results of stability estimates for these edges.** The point in this plot indicated the averaged correlation coefficient of EI between original sample and pseudo-samples dropped cases, with 95% Confidence Interval (CI, colored by red shadow) from the Bootstrapping method (*n* = 5,000). No inferential statistics are conducted here. Source data are provided as a Source Data file.

**4. Linegraph of edge-centric functional connectome**

By using these node pairs as "edge node", the correlations between "edge time series" for all the pairs of these "edge nodes" have been calculated to define eFC, with maximum 12,248,775 eFC for each edge-centric connectome. To examine whether these eFCs represented brain intrinsic patterns, we estimated the topological properties of the representative connectome, and visualized it by using Fruchterman-Reingold algorithm. The layout and topological properties of this connectome was found to show the brain intrinsic architectures as previous studies[11,20-22], showing high degree in isual network (VIS), sensorimotor network (SMN) and attention networks (VAN/DAN). To estimate the statistical significance of degree centrality in these networks, we simulated 1,000 equivalent pseudo-connectomes by permuting edges from original connectome. By doing so, we constructed null distributions of degree centrality of these "edge nodes" in these network. Finally, the statistical significance to degree centrality of these "edge node" had been estimated by comparing true values in original connectome to ones in the null distribution, with Benjamini-Hochberg correction. Details of these topological properties have been sorted into the **Tab. S11**. These analyses have been implemented by the Gephi 0.9.2.

| | Averaged degree | Weighted averaged degree | Eigenvector averaged degree | Page Rank | Graphic diameter | Averaged path length | Averaged clustering |
|---|---|---|---|---|---|---|---|
| **Values** | 81.1 | 48.9 | 0.3 | 0.9 | 7.0 | 3.3 | 0.5 |

**Tab S11. Topological properties of linegraph of representative edge-centric connectome.**

**5. Contributive features of eFCs in the eCPM**

To capture contributive features in the eCPM, we integrated these eFCs in the thresholding masks for positive and negative feature into the Yeo-7 brain systems, respectively. Averaged r value of each system and the ratio of eFCs on the maximum possible connections of each system were estimated to quantify relative importance of these systems in this eCPM. Full results of both r values and ratios have been documented into the **Tab. S12-15** and **Fig. S11**. The permutation test at *n* = 5,000 was used to estimated the statistical significance of these metrics by building the random thresholding masks.

| | VAN | SMN | DAN | VAN | LIM | FPN | DMN |
|---|---|---|---|---|---|---|---|
| **R values** | 0.1897 | 0.1920 | 0.1867 | 0.1887 | 0.1918 | 0.1956 | 0.1894 |
| **Ratio, ‰** | 1.7 | 3.8 | 2.5 | 2.6 | 1.7 | 6.1 | 3.4 |

**Tab S12. Contributive positive eFC features of this eCPM in the left hemisphere.**

| | VAN | SMN | DAN | VAN | LIM | FPN | DMN |
|---|---|---|---|---|---|---|---|
| **R values** | 0.1906 | 0.1938 | 0.1948 | 0.1917 | 0.1903 | 0.1947 | 0.1905 |
| **Ratio, ‰** | 2.0 | 7.3 | 7.5 | 6.1 | 9.8 | 6.0 | 3.4 |

**Tab S13. Contributive positive eFC features of this eCPM in the right hemisphere.**

| | VAN | SMN | DAN | VAN | LIM | FPN | DMN |
|---|---|---|---|---|---|---|---|
| **R values** | -0.1919 | -0.1902 | -0.1888 | -0.1881 | -0.1924 | -0.1879 | -0.1926 |
| **Ratio, ‰** | 7.1 | 2.1 | 4.5 | 4.3 | 7.0 | 7.3 | 16 |

**Tab S14. Contributive negative eFC features of this eCPM in the left hemisphere.**

| | VAN | SMN | DAN | VAN | LIM | FPN | DMN |
|---|---|---|---|---|---|---|---|
| **R values** | -0.1900 | -0.1908 | -0.1932 | -0.1908 | -0.1891 | -0.1918 | -0.1909 |
| **Ratio, ‰** | 6.9 | 7.5 | 5.3 | 3.3 | 4.0 | 6.7 | 4.2 |

**Tab S15. Contributive negative eFC features of this eCPM in the right hemisphere.**

Rather the intra-connection, we estimated the normalized Shannon's entropy (SE) to estimate the extent which regional eFCs were involved into multiple between-system communications. Results of these SEs for all the regions have been tabulated into the **Tab. S16**.

| Nodes | Positive eFCs | Negative eFCs |
|---|---|---|
| 7Networks_LH_Vis_1 | 0.008278937 | 0.023526979 |

| | | |
|---|---|---|
| 7Networks_LH_Vis_2 | 0.019487785 | 0.022246584 |
| 7Networks_LH_Vis_3 | 0.02380469 | 0.017912525 |
| 7Networks_LH_Vis_4 | 0.018838337 | 0.02236405 |
| 7Networks_LH_Vis_5 | 0.02039961 | 0.017499251 |
| 7Networks_LH_Vis_6 | 0.0155083 | 0.025102951 |
| 7Networks_LH_Vis_7 | 0.018032115 | 0.018994557 |
| 7Networks_LH_Vis_8 | 0.021013274 | 0.015499801 |
| 7Networks_LH_Vis_9 | 0.021911527 | 0.018935179 |
| 7Networks_LH_SomMot_1 | 0.022128493 | 0.022562357 |
| 7Networks_LH_SomMot_2 | 0.022129083 | 0.024978453 |
| 7Networks_LH_SomMot_3 | 0.019675782 | 0.023960133 |
| 7Networks_LH_SomMot_4 | 0.01016405 | 0.022969775 |
| 7Networks_LH_SomMot_5 | 0.025035377 | 0.022527313 |
| 7Networks_LH_SomMot_6 | 0.013626217 | 0.027426521 |
| 7Networks_LH_DorsAttn_Post_1 | 0.016998582 | 0.014668867 |
| 7Networks_LH_DorsAttn_Post_2 | 0.021192783 | 0.019039743 |
| 7Networks_LH_DorsAttn_Post_3 | 0.017937633 | 0.024877649 |
| 7Networks_LH_DorsAttn_Post_4 | 0.018100963 | 0.016905552 |
| 7Networks_LH_DorsAttn_Post_5 | 0.021130776 | 0.024463099 |
| 7Networks_LH_DorsAttn_Post_6 | 0.021734886 | 0.021232519 |
| 7Networks_LH_DorsAttn_PrCv_1 | 0.017751238 | 0.020664434 |
| 7Networks_LH_DorsAttn_FEF_1 | 0.013458621 | 0.020979695 |
| 7Networks_LH_SalVentAttn_ParOper_1 | 0.021252696 | 0.027522416 |
| 7Networks_LH_SalVentAttn_FrOperIns_1 | 0.0229091 | 0.024456613 |
| 7Networks_LH_SalVentAttn_FrOperIns_2 | 0.016021388 | 0.022360573 |
| 7Networks_LH_SalVentAttn_PFCl_1 | 0.016323215 | 0.020147613 |
| 7Networks_LH_SalVentAttn_Med_1 | 0.02215668 | 0.025162543 |
| 7Networks_LH_SalVentAttn_Med_2 | 0.019793116 | 0.019579804 |
| 7Networks_LH_SalVentAttn_Med_3 | 0.022048044 | 0.024358117 |
| 7Networks_LH_Limbic_OFC_1 | 0.018198883 | 0.017027528 |
| 7Networks_LH_Limbic_TempPole_1 | 0.019218087 | 0.017626891 |
| 7Networks_LH_Limbic_TempPole_2 | 0.023669048 | 0.021099217 |
| 7Networks_LH_Cont_Par_1 | 0.019855301 | 0.018348581 |
| 7Networks_LH_Cont_PFCl_1 | 0.020259024 | 0.0189664 |
| 7Networks_LH_Cont_pCun_1 | 0.017013575 | 0.020902718 |
| 7Networks_LH_Cont_Cing_1 | 0.017065814 | 0.024823754 |
| 7Networks_LH_Default_Temp_1 | 0.019887545 | 0.017537814 |
| 7Networks_LH_Default_Temp_2 | 0.018944678 | 0.016227949 |
| 7Networks_LH_Default_Par_1 | 0.01736764 | 0.013727303 |
| 7Networks_LH_Default_Par_2 | 0.016242775 | 0.024454985 |
| 7Networks_LH_Default_PFC_1 | 0.015809831 | 0.023679125 |
| 7Networks_LH_Default_PFC_2 | 0.023257058 | 0.018450973 |
| 7Networks_LH_Default_PFC_3 | 0.026233517 | 0.018471415 |
| 7Networks_LH_Default_PFC_4 | 0.02358047 | 0.024935262 |

| | | |
|---|---|---|
| 7Networks_LH_Default_PFC_5 | 0.017079449 | 0.022399189 |
| 7Networks_LH_Default_PFC_6 | 0.0224692 | 0.026447381 |
| 7Networks_LH_Default_PFC_7 | 0.020496163 | 0.017414943 |
| 7Networks_LH_Default_pCunPCC_1 | 0.016413597 | 0.023934753 |
| 7Networks_LH_Default_pCunPCC_2 | 0.01779326 | 0.022313743 |
| 7Networks_RH_Vis_1 | 0.023964375 | 0.02761168 |
| 7Networks_RH_Vis_2 | 0.017198928 | 0.01935161 |
| 7Networks_RH_Vis_3 | 0.01873479 | 0.021181596 |
| 7Networks_RH_Vis_4 | 0.021579222 | 0.021586925 |
| 7Networks_RH_Vis_5 | 0.018019178 | 0.023120973 |
| 7Networks_RH_Vis_6 | 0.020415661 | 0.019975746 |
| 7Networks_RH_Vis_7 | 0.018246993 | 0.018351656 |
| 7Networks_RH_Vis_8 | 0.022423469 | 0.025990061 |
| 7Networks_RH_SomMot_1 | 0.016515224 | 0.018004288 |
| 7Networks_RH_SomMot_2 | 0.018335375 | 0.019761095 |
| 7Networks_RH_SomMot_3 | 0.014976475 | 0.019543248 |
| 7Networks_RH_SomMot_4 | 0.018845749 | 0.018513575 |
| 7Networks_RH_SomMot_5 | 0.021122496 | 0.025471746 |
| 7Networks_RH_SomMot_6 | 0.015840708 | 0.027941031 |
| 7Networks_RH_SomMot_7 | 0.017955936 | 0.01889151 |
| 7Networks_RH_SomMot_8 | 0.021908978 | 0.023768056 |
| 7Networks_RH_DorsAttn_Post_1 | 0.014141607 | 0.021139603 |
| 7Networks_RH_DorsAttn_Post_2 | 0.019699219 | 0.016567982 |
| 7Networks_RH_DorsAttn_Post_3 | 0.021130742 | 0.028532883 |
| 7Networks_RH_DorsAttn_Post_4 | 0.021400399 | 0.021045058 |
| 7Networks_RH_DorsAttn_Post_5 | 0.021622328 | 0.024123249 |
| 7Networks_RH_DorsAttn_PrCv_1 | 0.019413349 | 0.023735019 |
| 7Networks_RH_DorsAttn_FEF_1 | 0.016565146 | 0.028360028 |
| 7Networks_RH_SalVentAttn_TempOccPar_1 | 0.015780506 | 0.027328418 |
| 7Networks_RH_SalVentAttn_TempOccPar_2 | 0.02097935 | 0.019272967 |
| 7Networks_RH_SalVentAttn_FrOperIns_1 | 0.018368976 | 0.019756137 |
| 7Networks_RH_SalVentAttn_Med_1 | 0.021137547 | 0.024681622 |
| 7Networks_RH_SalVentAttn_Med_2 | 0.014936564 | 0.022604729 |
| 7Networks_RH_Limbic_OFC_1 | 0.019593935 | 0.01986848 |
| 7Networks_RH_Limbic_TempPole_1 | 0.015814518 | 0.022570099 |
| 7Networks_RH_Cont_Par_1 | 0.020800723 | 0.021162437 |
| 7Networks_RH_Cont_Par_2 | 0.019444301 | 0.019743863 |
| 7Networks_RH_Cont_PFCl_1 | 0.023200261 | 0.026805019 |
| 7Networks_RH_Cont_PFCl_2 | 0.018293919 | 0.022012015 |
| 7Networks_RH_Cont_PFCl_3 | 0.018916883 | 0.021465878 |
| 7Networks_RH_Cont_PFCl_4 | 0.017324789 | 0.026285869 |
| 7Networks_RH_Cont_Cing_1 | 0.014307327 | 0.017383884 |
| 7Networks_RH_Cont_PFCmp_1 | 0.016401365 | 0.019418006 |
| 7Networks_RH_Cont_pCun_1 | 0.013195505 | 0.015620564 |

| | | |
|---|---|---|
| 7Networks_RH_Default_Par_1 | 0.014130344 | 0.01638393 |
| 7Networks_RH_Default_Temp_1 | 0.018599677 | 0.01747309 |
| 7Networks_RH_Default_Temp_2 | 0.016450303 | 0.012786685 |
| 7Networks_RH_Default_Temp_3 | 0.018249402 | 0.024108366 |
| 7Networks_RH_Default_PFCv_1 | 0.020288539 | 0.013553518 |
| 7Networks_RH_Default_PFCv_2 | 0.017288716 | 0.025635102 |
| 7Networks_RH_Default_PFCdPFCm_1 | 0.018256936 | 0.018583207 |
| 7Networks_RH_Default_PFCdPFCm_2 | 0.015697744 | 0.023668185 |
| 7Networks_RH_Default_PFCdPFCm_3 | 0.018011648 | 0.014822151 |
| 7Networks_RH_Default_pCunPCC_1 | 0.013730984 | 0.021188886 |
| 7Networks_RH_Default_pCunPCC_2 | 0.018189496 | 0.027784596 |

**Tab S16. The Shannon's entropy for all the regions that derived from positive and negative eFCs.**

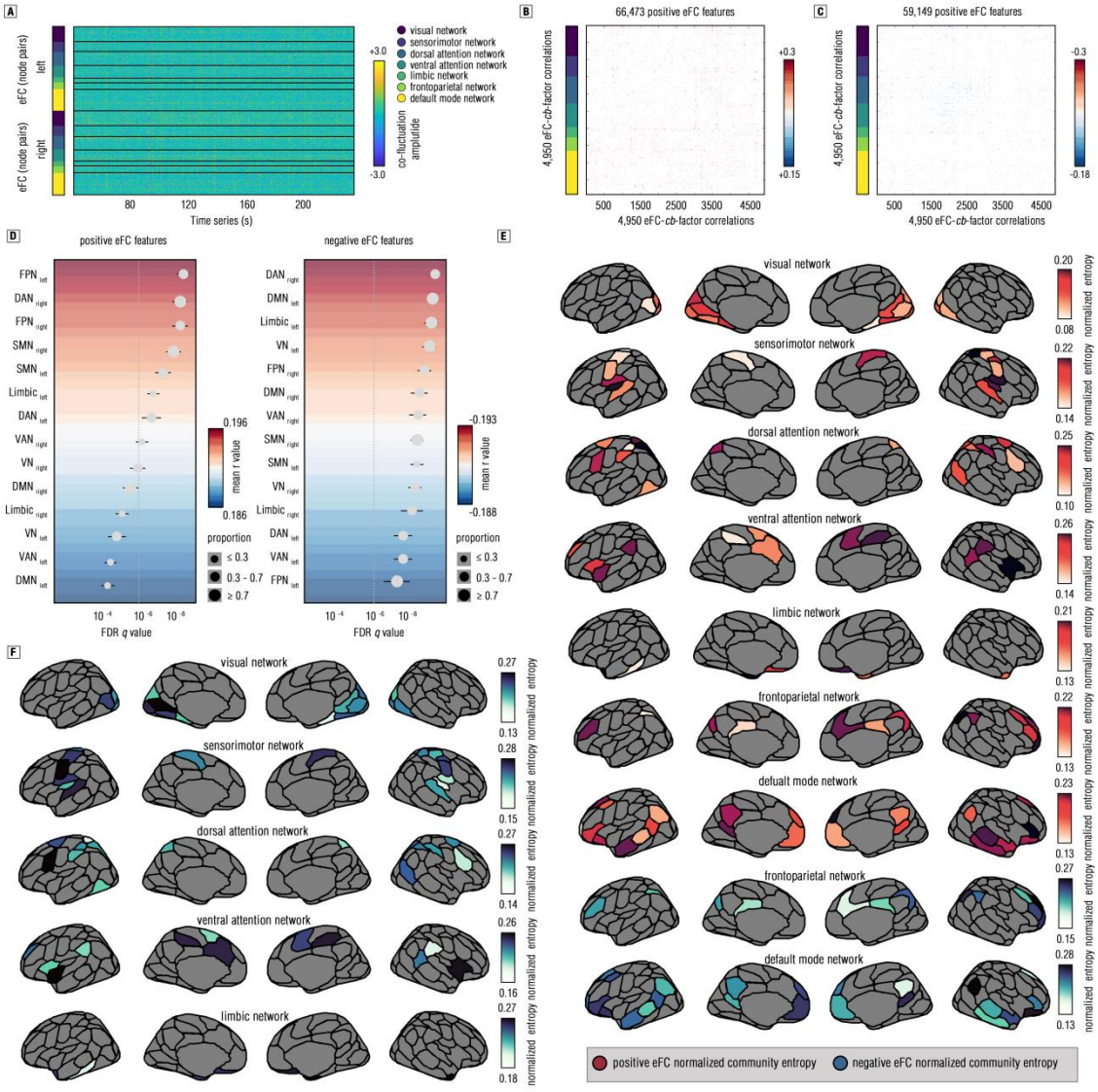


**Fig S11. Contributive eFC Features of trained eCPM. a**, It showed the "edge time series" for each edge-centric "node" by estimating co-fluctuations. The blocks in the left side of matrix indicated

corresponding brain system that parceled by Yeo-7 atlas. **b-c**, We have drawn matrix to show "contributive edges" in the eCPM, which were determined by the inter-subject positive (b) and negative (c) correlations between eFCs and the *cb* factor scores ($p < .05$, uncorrected). **d**, By estimating averaged correlation within each brain system, we showed the mean (95% confidence interval) correlation coefficient for each one (two-sided *r* tests, $q < .001$ Benjamini-Hochberg FDR correction), with descending order. The point size in these plots indicated the proportion of the number of included "contributive edges" on the possible maximum number within each brain system. **e-f**, We illustrated normalized entropy from "contributive edges" with positive correlations to the *cb* factor scores (e) and negative correlations to the *cb* factor scores (f) into Schaefer-100 atlas, and showed these results by using Yeo 7 brain system, respectively. Source data are provided as a Source Data file.

To verify the specificity of the predictive roles of eFC features in this trained eCPM, it has been tested for predicting single-disorder symptoms. Results showed that this trained eCPM did not surpass to predict single-disorder symptoms than the *cb* factor **(Fig. S12)**.

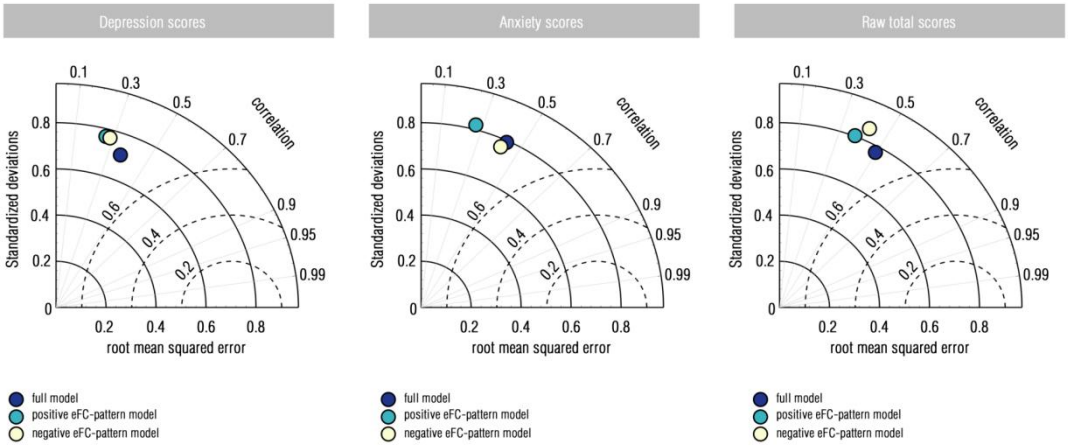


**Fig S12. Model performance for the trained eCPM on single-disorder symptoms.** By testing this trained eCPM for the single-disorder symptoms (raw total scores), we found the decreased predictability of this model for these single symptoms, irrespective of training from positive (positive eFC-pattern model), negative (negative eFC-pattern model) or the combined eFCs (full model). Source data are provided as a Source Data file.

### 6. Representation similarity of eFC to the *cb* factor

We capitalized on the representation similarity analysis to decode the multivariate eFC-the-*cb*-factor markers. As we mentioned above, these edge-centric node was vectored to be the eFC-sepcific patterns (*n* x 4,949, *n* = the number of participants), and the inter-subject correlations were estimated to generate 4,949 neural RDMs with *n* x *n* scale. By iterating each one to correlate with behavioral RDM, we obtained representation similarity (RS, positive r values) and representation dissimilarity (RDS, negative r values), with statistical significance at $p < .05$, with Benjamini-Hochberg correction **(Fig. S13)**. Results showed that 1,158 edge-centric nodes with eFC-the-*cb*-factor RS and 1,180 edge-centric nodes with eFC-the-*cb*-factor RDS have been captured. Given no prominently biological interpretations in RDS, we integrated these RS eFCs into the Scheafer-100 atlas, with averaged RS values for each parcel **(Tab. S17)**.

| Nodes | RS |
|---|---|
| 7Networks_LH_Vis_1 | 0.0271719200000000 |
| 7Networks_LH_Vis_2 | 0.0148789990000000 |
| 7Networks_LH_Vis_3 | 0.0233085890000000 |
| 7Networks_LH_Vis_4 | 0.0244879620000000 |
| 7Networks_LH_Vis_5 | 0.0188743130000000 |
| 7Networks_LH_Vis_6 | 0.0266775690000000 |
| 7Networks_LH_Vis_7 | 0.0196614270000000 |
| 7Networks_LH_Vis_8 | 0.0236687430000000 |
| 7Networks_LH_Vis_9 | 0.0214331770000000 |
| 7Networks_LH_SomMot_1 | 0.0223908970000000 |
| 7Networks_LH_SomMot_2 | 0.0257552910000000 |
| 7Networks_LH_SomMot_3 | 0.0206479630000000 |
| 7Networks_LH_SomMot_4 | 0.0238521530000000 |
| 7Networks_LH_SomMot_5 | 0.0231481340000000 |
| 7Networks_LH_SomMot_6 | 0.0166694610000000 |
| 7Networks_LH_DorsAttn_Post_1 | 0.0277598010000000 |
| 7Networks_LH_DorsAttn_Post_2 | 0.0288457620000000 |
| 7Networks_LH_DorsAttn_Post_3 | 0.0291154290000000 |
| 7Networks_LH_DorsAttn_Post_4 | 0.0187413390000000 |
| 7Networks_LH_DorsAttn_Post_5 | 0.0242693850000000 |
| 7Networks_LH_DorsAttn_Post_6 | 0.0246016900000000 |
| 7Networks_LH_DorsAttn_PrCv_1 | 0.0287685250000000 |
| 7Networks_LH_DorsAttn_FEF_1 | 0.0222069170000000 |
| 7Networks_LH_SalVentAttn_ParOper_1 | 0.0220004930000000 |
| 7Networks_LH_SalVentAttn_FrOperIns_1 | 0.0217618710000000 |
| 7Networks_LH_SalVentAttn_FrOperIns_2 | 0.0227569430000000 |
| 7Networks_LH_SalVentAttn_PFCl_1 | 0.0261246620000000 |
| 7Networks_LH_SalVentAttn_Med_1 | 0.0269020550000000 |
| 7Networks_LH_SalVentAttn_Med_2 | 0.0165035340000000 |
| 7Networks_LH_SalVentAttn_Med_3 | 0.0213884080000000 |
| 7Networks_LH_Limbic_OFC_1 | 0.0211717250000000 |
| 7Networks_LH_Limbic_TempPole_1 | 0.0257965370000000 |
| 7Networks_LH_Limbic_TempPole_2 | 0.0220041540000000 |
| 7Networks_LH_Cont_Par_1 | 0.0221143430000000 |
| 7Networks_LH_Cont_PFCl_1 | 0.0208807620000000 |
| 7Networks_LH_Cont_pCun_1 | 0.0242338300000000 |
| 7Networks_LH_Cont_Cing_1 | 0.0176615300000000 |
| 7Networks_LH_Default_Temp_1 | 0.0205227720000000 |
| 7Networks_LH_Default_Temp_2 | 0.0175799240000000 |
| 7Networks_LH_Default_Par_1 | 0.0213613730000000 |
| 7Networks_LH_Default_Par_2 | 0.0191704550000000 |
| 7Networks_LH_Default_PFC_1 | 0.0214162450000000 |

| | |
|---|---|
| 7Networks_LH_Default_PFC_2 | 0.0244810310000000 |
| 7Networks_LH_Default_PFC_3 | 0.0204378900000000 |
| 7Networks_LH_Default_PFC_4 | 0.0203324190000000 |
| 7Networks_LH_Default_PFC_5 | 0.0258590910000000 |
| 7Networks_LH_Default_PFC_6 | 0.0243977550000000 |
| 7Networks_LH_Default_PFC_7 | 0.0247106510000000 |
| 7Networks_LH_Default_pCunPCC_1 | 0.0232824100000000 |
| 7Networks_LH_Default_pCunPCC_2 | 0.0316195030000000 |
| 7Networks_RH_Vis_1 | 0.0243805050000000 |
| 7Networks_RH_Vis_2 | 0.0264672770000000 |
| 7Networks_RH_Vis_3 | 0.0273907120000000 |
| 7Networks_RH_Vis_4 | 0.0166355800000000 |
| 7Networks_RH_Vis_5 | 0.0296444110000000 |
| 7Networks_RH_Vis_6 | 0.0246015190000000 |
| 7Networks_RH_Vis_7 | 0.0229151490000000 |
| 7Networks_RH_Vis_8 | 0.0295023160000000 |
| 7Networks_RH_SomMot_1 | 0.0290477390000000 |
| 7Networks_RH_SomMot_2 | 0.0226799350000000 |
| 7Networks_RH_SomMot_3 | 0.0272502390000000 |
| 7Networks_RH_SomMot_4 | 0.0243843170000000 |
| 7Networks_RH_SomMot_5 | 0.0205110210000000 |
| 7Networks_RH_SomMot_6 | 0.0261751260000000 |
| 7Networks_RH_SomMot_7 | 0.0221083700000000 |
| 7Networks_RH_SomMot_8 | 0.0245935790000000 |
| 7Networks_RH_DorsAttn_Post_1 | 0.0246325540000000 |
| 7Networks_RH_DorsAttn_Post_2 | 0.0213391610000000 |
| 7Networks_RH_DorsAttn_Post_3 | 0.0158658220000000 |
| 7Networks_RH_DorsAttn_Post_4 | 0.0144952260000000 |
| 7Networks_RH_DorsAttn_Post_5 | 0.0218211460000000 |
| 7Networks_RH_DorsAttn_PrCv_1 | 0.0205770480000000 |
| 7Networks_RH_DorsAttn_FEF_1 | 0.0286898370000000 |
| 7Networks_RH_SalVentAttn_TempOccPar_1 | 0.0226947500000000 |
| 7Networks_RH_SalVentAttn_TempOccPar_2 | 0.0236837590000000 |
| 7Networks_RH_SalVentAttn_FrOperIns_1 | 0.0263105190000000 |
| 7Networks_RH_SalVentAttn_Med_1 | 0.0286610760000000 |
| 7Networks_RH_SalVentAttn_Med_2 | 0.0216829630000000 |
| 7Networks_RH_Limbic_OFC_1 | 0.0391947670000000 |
| 7Networks_RH_Limbic_TempPole_1 | 0.0331263840000000 |
| 7Networks_RH_Cont_Par_1 | 0.0286537480000000 |
| 7Networks_RH_Cont_Par_2 | 0.0271849530000000 |
| 7Networks_RH_Cont_PFCl_1 | 0.0233408720000000 |
| 7Networks_RH_Cont_PFCl_2 | 0.0221979880000000 |
| 7Networks_RH_Cont_PFCl_3 | 0.0149296100000000 |
| 7Networks_RH_Cont_PFCl_4 | 0.0201350490000000 |

| | |
|---|---|
| 7Networks_RH_Cont_Cing_1 | 0.0271008620000000 |
| 7Networks_RH_Cont_PFCmp_1 | 0.0179178250000000 |
| 7Networks_RH_Cont_pCun_1 | 0.0220030370000000 |
| 7Networks_RH_Default_Par_1 | 0.0182638760000000 |
| 7Networks_RH_Default_Temp_1 | 0.0210696310000000 |
| 7Networks_RH_Default_Temp_2 | 0.0241553650000000 |
| 7Networks_RH_Default_Temp_3 | 0.0233022450000000 |
| 7Networks_RH_Default_PFCv_1 | 0.0262566630000000 |
| 7Networks_RH_Default_PFCv_2 | 0.0210338760000000 |
| 7Networks_RH_Default_PFCdPFCm_1 | 0.0161017480000000 |
| 7Networks_RH_Default_PFCdPFCm_2 | 0.0188686240000000 |
| 7Networks_RH_Default_PFCdPFCm_3 | 0.0241650740000000 |
| 7Networks_RH_Default_pCunPCC_1 | 0.0259240790000000 |
| 7Networks_RH_Default_pCunPCC_2 | 0.0259240790000000 |

**Tab S17. Regional eFC-the-*cb*-factor representation similarity.**

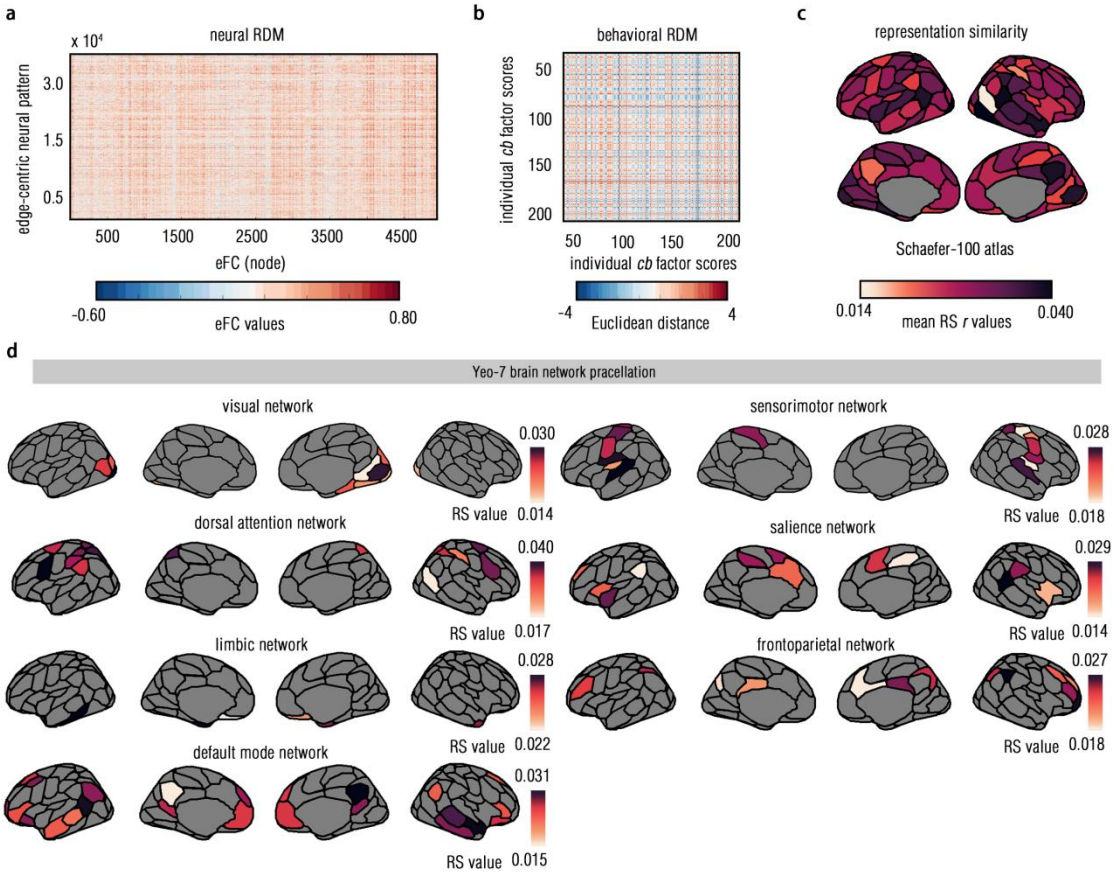


**Fig S13. The eFCs with representation similarity (RS). a,** The eFC-specific neural patterns for each "eFC" node have been illustrated by this 4,950 x 4,949 neural representation dissimilarity matrix (RDM). **b,** We drew the behavioral RDM by showing the Euclidean distance between each pair of the *cb* factor scores. **c,** We rearranged RS *r* values into each parcel from the Schaefer-100 atlas, showing RS of the eFC-specific neural patterns to the *cb* factor. The *r* values were calculated by

the Spearman correlation test (Two-sided *r* tests, Benjamini-Hochberg correction). **d,** We calculated and illustrated RS values into seven brain system that parceled by the Yeo-7 atlas. Source data are provided as a Source Data file.

We also integrated these edge-centric nodes into brain systems that defined by the Yeo-7 atlas. Full results have been tabulated into **Tab S18-21**.

| | VAN | SMN | DAN | VAN | LIM | FPN | DMN |
|---|---|---|---|---|---|---|---|
| **RS** | 0.0232 | 0.0225 | 0.0284 | 0.0241 | 0.0224 | 0.0216 | 0.0241 |

**Tab S18. Representation similarity (RS) of each brain system that defined by Yeo-7 atlas in the left hemisphere.**

| | VAN | SMN | DAN | VAN | LIM | FPN | DMN |
|---|---|---|---|---|---|---|---|
| **RS** | 0.0261 | 0.0253 | 0.0216 | 0.0289 | 0.0304 | 0.0225 | 0.0227 |

**Tab S19. Representation similarity (RS) of each brain system that defined by Yeo-7 atlas in the right hemisphere.**

| | VAN | SMN | DAN | VAN | LIM | FPN | DMN |
|---|---|---|---|---|---|---|---|
| **RDS** | -0.0237 | -0.0243 | -0.0186 | -0.0219 | -0.0262 | -0.0221 | -0.0235 |

**Tab S20. Representation dissimilarity (RDS) of each brain system that defined by Yeo-7 atlas in the left hemisphere.**

| | VAN | SMN | DAN | VAN | LIM | FPN | DMN |
|---|---|---|---|---|---|---|---|
| **RDS** | -0.0214 | -0.0225 | -0.0223 | -0.0235 | -0.0190 | -0.0180 | -0.0226 |

**Tab S21. Representation dissimilarity (RDS) of each brain system that defined by Yeo-7 atlas in the right hemisphere.**

### 7. Heritability of representation similarity between the eFC and the *cb* factor

By adjusting the potential artifacts of sex and age, the full ACE model was constructed for examining the heritability of eFC patterns that represented by normalized entropy. A total of 17 brain parcels were found heritable by showing > 10% $a^2$ values, especially in the regions of attention network (e.g., RH_DorsAttnB_FEF_1, 22.9%, 95% CI: 7.4 - 37.2). Full list for these results have been sorted into the **Tab S22 and Fig S14**. For the model modifications and statistical estimations, these nested submodels (AE, E, AC submodels) were built to be compared for full ACE models. Results showed the best-fitting model into the AE model, with minimum AIC, BIC and non-significant $X^2$ changes in these comparisons **(Tab S23).**

| Region | 2ll | Lower bound | Upper bound | $a^2$ |
|---|---|---|---|---|

| | | | | |
|---|---|---|---|---|
| RH_VisCent_ExStr_3 | 1353.7676 | 0.087060077 | 0.400910361 | 0.2506 |
| RH_DorsAttnB_FEF_1 | 1313.4688 | 0.074458165 | 0.372331138 | 0.2288 |
| RH_VisPeri_ExStrSup_1 | 1308.8460 | 0.030737871 | 0.349047154 | 0.1941 |
| LH_LimbicA_TempPole_2 | 1346.8072 | 0.044243501 | 0.329464911 | 0.191 |
| RH_SomMotB_Cent_1 | 1383.6913 | 0.037003465 | 0.335071856 | 0.1909 |
| LH_SomMotB_Cent_1 | 1383.4985 | 0.039113013 | 0.328467245 | 0.1886 |
| RH_DorsAttnB_PostC_2 | 1358.1517 | 0.022999333 | 0.32053699 | 0.1766 |
| LH_DefaultC_Rsp_1 | 1384.7959 | 0.017723052 | 0.316756791 | 0.1718 |
| LH_SalVentAttnA_Ins_2 | 1385.3267 | 0.007583115 | 0.301869848 | 0.1585 |
| LH_DefaultB_PFCv_2 | 1364.0519 | 4.48E-27 | 0.302336386 | 0.1514 |
| LH_DorsAttnB_FEF_1 | 1325.9469 | 5.74E-26 | 0.287485866 | 0.1426 |
| LH_SalVentAttnB_PFCl_1 | 1355.6974 | 2.76E-33 | 0.27597075 | 0.132 |
| RH_SalVentAttnA_ParOper_1 | 1344.3772 | 3.93E-32 | 0.28680721 | 0.1319 |
| LH_SalVentAttnA_ParOper_1 | 1358.2814 | 7.24E-30 | 0.278551304 | 0.1227 |
| RH_VisPeri_StriCal_1 | 1334.9884 | 4.01E-31 | 0.2699054 | 0.1171 |
| RH_DorsAttnB_PostC_1 | 1362.6313 | 5.63E-38 | 0.270900757 | 0.116 |
| RH_SomMotA_3 | 1332.0386 | 3.22E-28 | 0.266000182 | 0.1102 |
| LH_VisPeri_ExStrInf_1 | 1388.1227 | NA | 0.271016587 | 0.1054 |

**Tab S22. Model estimates for heritability ($a^2$).** 2ll = twofold log likelihood; lower bound and upper bound illustrated 95% confidence interval (CI) of the $a^2$.

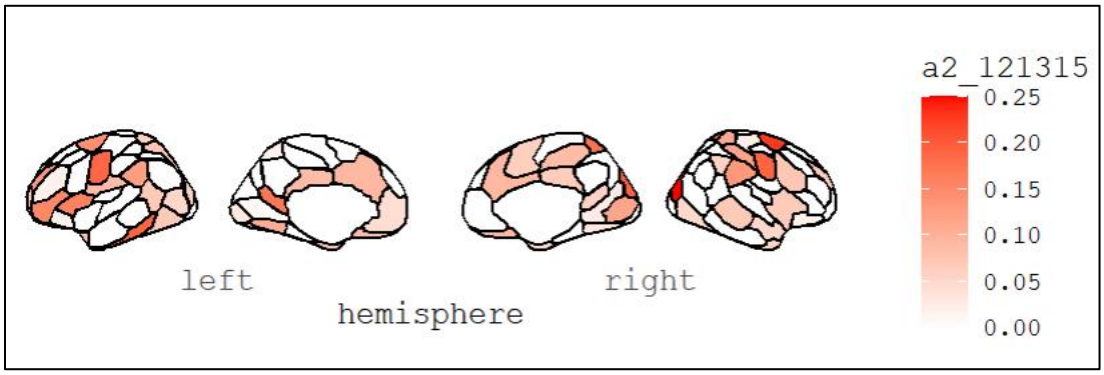


**Fig S14. Brain maps for the heritability of eFC patterns.** Source data are provided as a Source Data file.

| Model | AIC | BIC | p of Δ $X^2$ | $a^2$ (95% CI) | $c^2$ (95% CI) | $e^2$ (95% CI) |
|---|---|---|---|---|---|---|
| ACE | 343.46 | -1354.64 | | 0.22 (.07-.37) | - | 0.77 (.62-.92) |
| AE* | 341.46 | -1360.14 | 1.0 | 0.22 (.07-.37) | - | 0.77 (.62-.92) |
| CE | 343.19 | -1357.67 | 0.11 | - | - | - |
| E | 347.78 | -1357.32 | 0.015 | - | - | - |

**Tab S23. Model comparisons of ACE to nested submodels.** *, best-fitting model with minimum AIC, BIC and non-significant Δ $X^2$. *P* values are estimated by two-sided *z* tests to Δ $X^2$, without multiple comparison correction.

**8. Transcriptomic signatures for RS of the *cb* factor**

By using the PLS model, we reveled that the PLS1 and PLS2 component cumulatively explained 32.4% variances. Further, we used Bootstrapping method (*n* = 10,000) to estimate the weights (z scores) for each gene in these PLS loading. To prevent from over-fitting, we added the 10-fold cross-validation method in this PLS model. Results showed the acceptable mean-square error (MES) in each submodel (averaged MSE = 1.43, IQR: 0.87-1.62), which demonstrated no significant over-fitting issue in establishing this PLS model. For screening associated genes, we re-ranked these genes by descending order, and calculated the *p* value for each weight with statistical threshold at Z >3.0 or Z < -3.0). By using these criterion, a total of 258 genes (27 genes with positive weight, PLS1+; 231 genes with negative weight, PLS1-) in PLS1 component, and 156 genes (44 genes with positive weight, PLS2+; 112 genes with negative weight, PLS2-) have been revealed. We have provided unfolded tables underneaths for reporting both gene lists **(Tab S24-27)**.

| Gene Symbol | Entrez Gene ID | Z scores | P values |
|---|---|---|---|
| *MORC4* | 7370 | 3.74098 | 0.000183304 |
| *EIF4EBP1* | 808 | 3.466012 | 0.00052824 |
| *CMTM3* | 8621 | 3.450845 | 0.000558834 |
| *TMC8* | 8922 | 3.444022 | 0.000573129 |
| *ZNF438* | 9326 | 3.416663 | 0.000633937 |
| *RARRES3* | 2345 | 3.342505 | 0.000830259 |
| *RGS9* | 3356 | 3.297965 | 0.000973883 |
| *MSN* | 1706 | 3.280022 | 0.00103799 |
| *SLC44A2* | 6666 | 3.275871 | 0.001053367 |
| *FAM181A* | 8154 | 3.258772 | 0.001118956 |
| *VAMP8* | 3315 | 3.257163 | 0.001125318 |
| *ZFAND3* | 6968 | 3.251099 | 0.001149598 |
| *DNAJC12* | 6546 | 3.236752 | 0.001208984 |
| *SERPINA1* | 2028 | 3.228923 | 0.001242573 |
| *RHOC* | 170 | 3.219445 | 0.00128439 |
| *PLEKHA4* | 6838 | 3.155858 | 0.001600267 |
| *WDFY4* | 6857 | 3.151061 | 0.001626785 |
| *NPC2* | 4226 | 3.148884 | 0.001638952 |
| *ZFP36L2* | 299 | 3.139448 | 0.001692665 |
| *NPFF* | 3284 | 3.121731 | 0.001797911 |
| *TCF3* | 2774 | 3.070935 | 0.002133896 |
| *TMPRSS5* | 7626 | 3.03011 | 0.002444647 |
| *LEPROT* | 5995 | 3.026626 | 0.002472997 |
| *PRAM1* | 7816 | 3.01776 | 0.002546505 |
| *FYN* | 982 | 3.014155 | 0.002576961 |
| *CASTOR1* | 9963 | 3.011769 | 0.002597302 |
| *SCUBE2* | 6870 | 3.003439 | 0.002669471 |

**Tab S24. Gene list for statistically significant association with RS changes in the PLS1+ component**. *P* values were estimated by using two-sided *Z* sampling distribution test without corrections.

| Gene Symbol | Entrez Gene ID | Z scores | P values |
|---|---|---|---|
| *UGCG* | 2949 | -4.374419 | 1.22E-05 |
| *LDHB* | 1530 | -4.342102 | 1.41E-05 |
| *PPM1A* | 2126 | -4.258463 | 2.06E-05 |
| *JKAMP* | 5769 | -4.193562 | 2.75E-05 |
| *CORO2A* | 2994 | -4.06925 | 4.72E-05 |
| *PIP4P2* | 6314 | -4.060411 | 4.90E-05 |
| *GLRX2* | 5563 | -4.007282 | 6.14E-05 |
| *WDR37* | 4614 | -4.005691 | 6.18E-05 |
| *RNF111* | 6002 | -3.998406 | 6.38E-05 |
| *CTXN2* | 9818 | -3.973974 | 7.07E-05 |
| *EIF2B2* | 3405 | -3.971699 | 7.14E-05 |
| *KCTD1* | 9516 | -3.925714 | 8.65E-05 |
| *VWC2* | 9732 | -3.910422 | 9.21E-05 |
| *ENPP5* | 6918 | -3.872204 | 0.000107856 |
| *IDH3B* | 1333 | -3.86638 | 0.000110463 |
| *USO1* | 3282 | -3.843314 | 0.000121384 |
| *ATP5MC3* | 222 | -3.830336 | 0.000127968 |
| *MDH1* | 1636 | -3.826888 | 0.000129774 |
| *SORL1* | 2653 | -3.818574 | 0.000134225 |
| *FBXO9* | 5204 | -3.816334 | 0.000135449 |
| *UGP2* | 2951 | -3.801465 | 0.000143843 |
| *MTRF1L* | 5945 | -3.786548 | 0.000152755 |
| *TM9SF2* | 3605 | -3.784463 | 0.000154041 |
| *GABRA1* | 993 | -3.776621 | 0.00015897 |
| *PAIP2* | 5663 | -3.770757 | 0.000162753 |
| *QPCT* | 5031 | -3.768445 | 0.000164268 |
| *ARL8B* | 6209 | -3.761164 | 0.000169124 |
| *ITPA* | 1424 | -3.75428 | 0.00017384 |
| *PITPNA* | 2047 | -3.744261 | 0.000180926 |
| *CCDC184* | 9761 | -3.736524 | 0.000186582 |
| *RRP12* | 4774 | -3.723743 | 0.000196291 |
| *PSMD14* | 4040 | -3.716981 | 0.000201618 |
| *GGH* | 3380 | -3.705714 | 0.000210796 |
| *BDH1* | 269 | -3.696279 | 0.000218783 |
| *CDH18* | 446 | -3.694002 | 0.000220752 |
| *ZNF425* | 9057 | -3.691184 | 0.000223213 |
| *NQO2* | 1843 | -3.685399 | 0.000228345 |
| *RNF8* | 3455 | -3.68408 | 0.00022953 |
| *ANAPC7* | 5743 | -3.681812 | 0.000231582 |
| *DPP8* | 6044 | -3.676331 | 0.000236612 |

| | | | |
|---|---|---|---|
| *PTGES2* | 7513 | -3.67603 | 0.000236892 |
| *ATP5F1B* | 220 | -3.674286 | 0.000238515 |
| *KCNC3* | 1449 | -3.661997 | 0.000250257 |
| *CLTC* | 532 | -3.634122 | 0.000278929 |
| *NDUFV2* | 1795 | -3.627964 | 0.000285665 |
| *EPHX4* | 9385 | -3.620014 | 0.000294587 |
| *KCNS3* | 1482 | -3.610481 | 0.00030563 |
| *CCNDBP1* | 4952 | -3.600073 | 0.000318128 |
| *SLC25A3* | 2022 | -3.580662 | 0.000342725 |
| *VDAC2* | 2972 | -3.575839 | 0.000349106 |
| *ATP5F1A* | 218 | -3.572323 | 0.000353829 |
| *NAE1* | 3402 | -3.561756 | 0.000368383 |
| *COX5A* | 3606 | -3.55904 | 0.000372213 |
| *RND2* | 3139 | -3.551454 | 0.000383109 |
| *CLCN4* | 517 | -3.539623 | 0.000400699 |
| *PPP2R2D* | 6463 | -3.53412 | 0.000409135 |
| *GAD2* | 1007 | -3.524979 | 0.000423516 |
| *DHRS7* | 5799 | -3.522751 | 0.000427092 |
| *NABP2* | 7228 | -3.522699 | 0.000427176 |
| *PTPRM* | 2284 | -3.519611 | 0.00043218 |
| *COPA* | 565 | -3.51932 | 0.000432655 |
| *KCNC2* | 1448 | -3.517161 | 0.000436189 |
| *CUL3* | 3210 | -3.517129 | 0.000436242 |
| *EXOC8* | 8964 | -3.516806 | 0.000436773 |
| *ADAT1* | 4933 | -3.515314 | 0.000439234 |
| *UFSP2* | 6270 | -3.507692 | 0.000452012 |
| *CEND1* | 5680 | -3.505916 | 0.000455039 |
| *TNPO3* | 4932 | -3.498935 | 0.00046712 |
| *COQ3* | 5849 | -3.493409 | 0.000476895 |
| *ISCU* | 4908 | -3.493012 | 0.000477605 |
| *ZBTB8OS* | 9624 | -3.49202 | 0.000479382 |
| *EXTL2* | 876 | -3.490667 | 0.000481816 |
| *GHITM* | 5268 | -3.486169 | 0.000489991 |
| *G3BP2* | 3881 | -3.479451 | 0.000502442 |
| *ARL4C* | 3989 | -3.476412 | 0.000508171 |
| *GYG1* | 1189 | -3.47009 | 0.000520284 |
| *WAC* | 5700 | -3.466306 | 0.000527662 |
| *GNB5* | 4281 | -3.459579 | 0.000541021 |
| *TIGAR* | 6647 | -3.456482 | 0.000547276 |
| *GOT1* | 1095 | -3.452368 | 0.000555689 |
| *STEAP2* | 9459 | -3.440563 | 0.000580505 |
| *COX7B* | 574 | -3.434043 | 0.00059465 |
| *SCRN1* | 3826 | -3.430369 | 0.000602761 |
| *UBXN10* | 8688 | -3.428181 | 0.00060764 |

| | | | |
|---|---|---|---|
| *SLU7* | 4220 | -3.4251 | 0.000614573 |
| *THOC5* | 3264 | -3.422172 | 0.00062123 |
| *SAE1* | 3952 | -3.421328 | 0.000623161 |
| *IGBP1* | 1347 | -3.42106 | 0.000623776 |
| *HSPA12A* | 9451 | -3.418073 | 0.000630662 |
| *GCHFR* | 1033 | -3.411299 | 0.000646542 |
| *TTC9* | 4920 | -3.405027 | 0.000661575 |
| *AMIGO1* | 6731 | -3.396939 | 0.000681442 |
| *RIMS3* | 3817 | -3.39468 | 0.000687089 |
| *YIPF5* | 7644 | -3.387794 | 0.000704572 |
| *RMND1* | 6104 | -3.38356 | 0.000715526 |
| *USPL1* | 4036 | -3.378511 | 0.000728795 |
| *GAD1* | 1006 | -3.376563 | 0.000733976 |
| *NDUFB2* | 1785 | -3.374694 | 0.000738978 |
| *CHML* | 491 | -3.373817 | 0.000741336 |
| *BLVRA* | 280 | -3.367157 | 0.000759474 |
| *BNIP3* | 290 | -3.364274 | 0.000767453 |
| *CACNG8* | 6923 | -3.361289 | 0.000775796 |
| *GSTO1* | 3633 | -3.360573 | 0.00077781 |
| *MRPS23* | 5805 | -3.353398 | 0.000798258 |
| *MMADHC* | 5321 | -3.352155 | 0.000801851 |
| *COA1* | 6409 | -3.350881 | 0.000805549 |
| *ZNF385D* | 7388 | -3.34691 | 0.000817177 |
| *CAPRIN2* | 7186 | -3.346117 | 0.000819518 |
| *ZNF57* | 8656 | -3.34474 | 0.000823597 |
| *ZFYVE9* | 3604 | -3.340504 | 0.000836265 |
| *NDUFA8* | 1780 | -3.338334 | 0.000842824 |
| *PNMA2* | 4284 | -3.33781 | 0.000844415 |
| *UCHL5* | 5722 | -3.33756 | 0.000845175 |
| *PGD* | 2015 | -3.335482 | 0.000851517 |
| *MED21* | 3621 | -3.324862 | 0.000884623 |
| *MAP9* | 7443 | -3.324627 | 0.000885369 |
| *CLASP2* | 4722 | -3.321618 | 0.000894971 |
| *DNAJA2* | 4080 | -3.314763 | 0.000917209 |
| *CCDC34* | 8220 | -3.313936 | 0.000919926 |
| *DPH3* | 9558 | -3.312769 | 0.000923772 |
| *AKAP12* | 3715 | -3.301518 | 0.000961632 |
| *GSK3B* | 1163 | -3.298814 | 0.000970942 |
| *MRPL15* | 5409 | -3.294563 | 0.000985748 |
| *CACNG2* | 4112 | -3.290395 | 0.001000468 |
| *AHSA1* | 4237 | -3.289018 | 0.001005376 |
| *POLR2E* | 2099 | -3.287842 | 0.001009585 |
| *C12orf10* | 6939 | -3.286984 | 0.001012666 |
| *KPNA5* | 1500 | -3.28102 | 0.001034324 |

| | | | |
|---|---|---|---|
| *ZNF654* | 6248 | -3.275865 | 0.001053389 |
| *PITPNM1* | 3717 | -3.2752 | 0.001055872 |
| *NAP1L5* | 9463 | -3.272079 | 0.001067597 |
| *COPS5* | 4412 | -3.266612 | 0.001088427 |
| *KRT222* | 8645 | -3.266607 | 0.001088447 |
| *NR1H2* | 2954 | -3.266601 | 0.00108847 |
| *NOMO1* | 4882 | -3.262516 | 0.001104279 |
| *UQCRH* | 2960 | -3.261757 | 0.00110724 |
| *TGFBRAP1* | 3613 | -3.259993 | 0.00111415 |
| *MRPL4* | 5580 | -3.258331 | 0.001120696 |
| *ADPRHL1* | 8410 | -3.24349 | 0.00118075 |
| *ACSL3* | 897 | -3.235863 | 0.001212756 |
| *ATP5PO* | 235 | -3.235137 | 0.001215844 |
| *CKAP2* | 5236 | -3.234646 | 0.001217936 |
| *TCEAL3* | 8082 | -3.231485 | 0.001231488 |
| *AP1S2* | 3412 | -3.223024 | 0.001268449 |
| *ZNF641* | 8586 | -3.215079 | 0.001304086 |
| *SIK2* | 4779 | -3.213516 | 0.001311205 |
| *AARS* | 4 | -3.208954 | 0.001332188 |
| *PIP5K1B* | 3186 | -3.208585 | 0.001333899 |
| *KLC2* | 7120 | -3.202699 | 0.001361462 |
| *HECA* | 5822 | -3.201944 | 0.001365035 |
| *CERK* | 7107 | -3.201615 | 0.001366595 |
| *TMCC1* | 4677 | -3.200408 | 0.001372332 |
| *BCAT1* | 257 | -3.194837 | 0.001399098 |
| *SCN2B* | 2516 | -3.19474 | 0.001399569 |
| *MAFB* | 3895 | -3.194385 | 0.001401291 |
| *LEPROTL1* | 4910 | -3.187697 | 0.001434107 |
| *ANO5* | 9280 | -3.187385 | 0.001435655 |
| *SSX2IP* | 8545 | -3.185191 | 0.001446585 |
| *TRNP1* | 9780 | -3.183847 | 0.001453318 |
| *TCEAL6* | 9088 | -3.183429 | 0.001455418 |
| *PAQR3* | 9027 | -3.178519 | 0.001480295 |
| *RRP15* | 5561 | -3.176427 | 0.001491013 |
| *TSPAN5* | 3978 | -3.174519 | 0.001500851 |
| *MKKS* | 3146 | -3.171126 | 0.001518493 |
| *CAMKK2* | 4266 | -3.168958 | 0.001529865 |
| *NDUFA9* | 1782 | -3.168218 | 0.001533765 |
| *TRMU* | 6379 | -3.167578 | 0.001537145 |
| *TAGLN3* | 5422 | -3.165231 | 0.001549599 |
| *FH* | 934 | -3.155735 | 0.001600942 |
| *TIMM10B* | 5226 | -3.152865 | 0.001616766 |
| *KCNA2* | 1442 | -3.152573 | 0.001618384 |
| *PRIM1* | 2158 | -3.144782 | 0.001662106 |

| | | | |
|---|---|---|---|
| *NXPH2* | 4525 | -3.143476 | 0.001669541 |
| *SLC25A4* | 126 | -3.13969 | 0.001691267 |
| *SNX21* | 8166 | -3.136862 | 0.001707665 |
| *ZBTB16* | 3046 | -3.133367 | 0.001728132 |
| *STAG3L4* | 7144 | -3.132307 | 0.001734384 |
| *CHCHD7* | 7269 | -3.130334 | 0.001746077 |
| *PSMD12* | 2248 | -3.124739 | 0.001779629 |
| *MYADML2* | 9415 | -3.124253 | 0.001782571 |
| *NDUFA12* | 6499 | -3.105597 | 0.001898953 |
| *NDUFAB1* | 1784 | -3.101164 | 0.001927615 |
| *RPS6KB1* | 2458 | -3.10006 | 0.001934814 |
| *KIF9* | 7026 | -3.095515 | 0.001964714 |
| *AKT3* | 3923 | -3.09504 | 0.001967864 |
| *SELENOH* | 9464 | -3.092667 | 0.001983666 |
| *INIP* | 6902 | -3.0884 | 0.002012374 |
| *GLS* | 1065 | -3.086772 | 0.002023427 |
| *SUPV3L1* | 2724 | -3.085675 | 0.002030907 |
| *WDR7* | 4835 | -3.077325 | 0.002088674 |
| *PRPF4* | 3500 | -3.07268 | 0.002121458 |
| *CDKL3* | 5670 | -3.072586 | 0.002122127 |
| *BAG5* | 3682 | -3.070274 | 0.002138625 |
| *H2AFZ* | 1196 | -3.069739 | 0.002142459 |
| *CHAC1* | 7255 | -3.069368 | 0.002145122 |
| *MTO1* | 5044 | -3.068922 | 0.002148327 |
| *NDUFV1* | 1792 | -3.065465 | 0.002173318 |
| *FGF12* | 925 | -3.065231 | 0.002175019 |
| *AGGF1* | 6155 | -3.064725 | 0.002178702 |
| *DNM3* | 5152 | -3.063043 | 0.002190986 |
| *SESN2* | 7739 | -3.058259 | 0.002226271 |
| *ZNF124* | 3039 | -3.054932 | 0.002251116 |
| *SLC25A32* | 7630 | -3.054059 | 0.002257677 |
| *TRAP1* | 3995 | -3.053783 | 0.002259755 |
| *TTC39B* | 9074 | -3.047908 | 0.002304405 |
| *LIN28B* | 9800 | -3.044394 | 0.002331496 |
| *RIMKLA* | 9538 | -3.043426 | 0.00233901 |
| *ENTPD3* | 416 | -3.041348 | 0.002355214 |
| *MOCS3* | 5337 | -3.040958 | 0.002358267 |
| *BECN1* | 3317 | -3.040122 | 0.002364823 |
| *PRDX2* | 2790 | -3.035516 | 0.002401245 |
| *C16orf72* | 5396 | -3.03546 | 0.002401691 |
| *CLSTN3* | 3797 | -3.031986 | 0.002429505 |
| *SRPRB* | 6894 | -3.028063 | 0.002461268 |
| *TUBE1* | 5639 | -3.026681 | 0.002472547 |
| *CYC1* | 647 | -3.025209 | 0.002484614 |

| | | | |
|---|---|---|---|
| *C12orf49* | 7407 | -3.024809 | 0.002487902 |
| *PEX5* | 2301 | -3.023996 | 0.002494597 |
| *MAPK14* | 604 | -3.022477 | 0.002507151 |
| *HTR5A* | 1317 | -3.020219 | 0.00252592 |
| *ABCF2* | 3957 | -3.019418 | 0.002532608 |
| *CEP97* | 7310 | -3.018267 | 0.002542248 |
| *TIMM44* | 4170 | -3.016283 | 0.002558943 |
| *AQP11* | 9465 | -3.014889 | 0.002570733 |
| *DLD* | 704 | -3.012468 | 0.002591328 |
| *FLT3* | 956 | -3.010669 | 0.002606728 |
| *PSMD11* | 2247 | -3.004263 | 0.002662251 |
| *PBX1* | 1941 | -3.003846 | 0.002665902 |
| *AES* | 81 | -3.003392 | 0.002669883 |
| *CLEC2L* | 9052 | -3.002589 | 0.002676937 |
| *GNPDA2* | 8771 | -3.000978 | 0.00269114 |

**Tab S25. Gene list for statistically significant association with RS changes in the PLS1- component.** *P* values were estimated by using two-sided *Z* sampling distribution test without corrections.

| Gene Symbol | Entrez Gene ID | Z scores | P values |
|---|---|---|---|
| *SCRIB* | 4922 | 4.06975 | 2.35E-05 |
| *HDAC7* | 5780 | 3.966845 | 3.64E-05 |
| *ANKS3* | 8628 | 3.948843 | 3.93E-05 |
| *POLN* | 9702 | 3.752042 | 8.77E-05 |
| *CCDC57* | 9506 | 3.70669 | 0.000104993 |
| *FTCD* | 4336 | 3.663562 | 0.000124366 |
| *EMX1* | 826 | 3.56694 | 0.000180587 |
| *NPFF* | 3284 | 3.526771 | 0.00021033 |
| *MIS18BP1* | 6266 | 3.521834 | 0.000214286 |
| *KCNH3* | 4879 | 3.517478 | 0.000217834 |
| *ADAMTS13* | 4450 | 3.489246 | 0.000242193 |
| *MTG1* | 8280 | 3.475323 | 0.000255119 |
| *LINC00999* | 9820 | 3.421223 | 0.000311701 |
| *FAM153A* | 9567 | 3.418396 | 0.000314957 |
| *ADAM8* | 45 | 3.395943 | 0.000341963 |
| *DGKZ* | 3244 | 3.382624 | 0.000358984 |
| *SRRT* | 5788 | 3.332454 | 0.000430418 |
| *TYK2* | 2924 | 3.292106 | 0.000497201 |
| *MEG3* | 6298 | 3.286214 | 0.000507719 |
| *LAMA3* | 1513 | 3.285712 | 0.000508625 |
| *EMILIN3* | 8164 | 3.265639 | 0.000546087 |
| *GRIPAP1* | 6568 | 3.256408 | 0.000564157 |
| *EBF4* | 6804 | 3.254952 | 0.000567058 |
| *GSDMB* | 6476 | 3.246112 | 0.000584964 |

| | | | |
|---|---|---|---|
| *SPACA6* | 8930 | 3.216953 | 0.000647799 |
| *MTMR1* | 3353 | 3.189171 | 0.000713407 |
| *PIDD1* | 6295 | 3.181672 | 0.000732138 |
| *ELMOD3* | 7835 | 3.174372 | 0.000750806 |
| *BCL7A* | 266 | 3.162453 | 0.00078223 |
| *SNAPC4* | 2639 | 3.158381 | 0.00079324 |
| *POLA1* | 2095 | 3.156877 | 0.000797343 |
| *ADAM33* | 7580 | 3.145372 | 0.000829379 |
| *PXN* | 2300 | 3.124419 | 0.000890783 |
| *ACTN1* | 35 | 3.115988 | 0.000916649 |
| *NEIL1* | 7349 | 3.083962 | 0.001021318 |
| *NEK9* | 8265 | 3.083051 | 0.00102445 |
| *RTEL1* | 5838 | 3.077982 | 0.001042038 |
| *COQ10A* | 8326 | 3.073677 | 0.001057191 |
| *EEF2K* | 5458 | 3.059521 | 0.001108456 |
| *KIFC2* | 8217 | 3.052079 | 0.001136311 |
| *DOCK1* | 731 | 3.047793 | 0.001152643 |
| *UIMC1* | 5832 | 3.017027 | 0.001276335 |
| *WNT2B* | 3004 | 3.007014 | 0.001319138 |
| *VIPR1* | 2981 | 3.005881 | 0.001324063 |

**Tab S26. Gene list for statistically significant association with RS changes in the PLS2+ component.** *P* values were estimated by using two-sided *Z* sampling distribution test without corrections.

| Gene Symbol | Entrez Gene ID | Z scores | P values |
|---|---|---|---|
| *INPP4A* | 1387 | -4.415929 | 5.03E-06 |
| *RMND1* | 6104 | -4.113508 | 1.95E-05 |
| *EIF2B2* | 3405 | -4.07667 | 2.28E-05 |
| *SIK2* | 4779 | -3.98645 | 3.35E-05 |
| *CORO2A* | 2994 | -3.910244 | 4.61E-05 |
| *COQ10B* | 7541 | -3.880977 | 5.20E-05 |
| *NME7* | 5465 | -3.863845 | 5.58E-05 |
| *IDH3B* | 1333 | -3.789534 | 7.55E-05 |
| *RAD18* | 6570 | -3.71529 | 0.000101485 |
| *AP2B1* | 79 | -3.711378 | 0.000103067 |
| *RBMX* | 5340 | -3.681139 | 0.000116097 |
| *ZNF654* | 6248 | -3.664551 | 0.000123886 |
| *RAB39B* | 8522 | -3.637822 | 0.000137477 |
| *HSDL1* | 7742 | -3.621528 | 0.000146434 |
| *TIMM8A* | 691 | -3.619141 | 0.000147791 |
| *TM6SF1* | 5858 | -3.615214 | 0.00015005 |
| *ANAPC7* | 5743 | -3.58293 | 0.000169881 |
| *KRAS* | 1502 | -3.543614 | 0.000197341 |
| *OPRM1* | 1905 | -3.543277 | 0.000197594 |

| | | | |
|---|---|---|---|
| *DENND6B* | 9869 | -3.535926 | 0.000203174 |
| *PIGP* | 5656 | -3.525366 | 0.000211449 |
| *RABIF* | 2318 | -3.500896 | 0.000231848 |
| *TM2D2* | 7775 | -3.464677 | 0.000265434 |
| *SCRN1* | 3826 | -3.455056 | 0.000275089 |
| *AHNAK2* | 8396 | -3.439422 | 0.000291479 |
| *CDKL3* | 5670 | -3.436702 | 0.000294422 |
| *CCT4* | 4224 | -3.430182 | 0.000301588 |
| *TOMM20* | 3825 | -3.408291 | 0.000326856 |
| *TRUB2* | 5251 | -3.402544 | 0.000333808 |
| *IGBP1* | 1347 | -3.374541 | 0.000369695 |
| *AGAP3* | 8539 | -3.372698 | 0.000372178 |
| *TMEM182* | 8748 | -3.370629 | 0.000374984 |
| *MBD5* | 6424 | -3.353209 | 0.000399402 |
| *TMEM260* | 6059 | -3.350832 | 0.000402846 |
| *TXNRD3* | 8420 | -3.346089 | 0.0004098 |
| *CLTA* | 530 | -3.343036 | 0.000414336 |
| *DYNLL1* | 3305 | -3.339935 | 0.00041899 |
| *FAM49A* | 7642 | -3.330551 | 0.000433371 |
| *NXPH2* | 4525 | -3.329425 | 0.000435127 |
| *STK17B* | 3554 | -3.319462 | 0.000450955 |
| *LDHB* | 1530 | -3.31711 | 0.000454769 |
| *SLC41A2* | 7814 | -3.315748 | 0.000456991 |
| *CPSF4* | 4362 | -3.2983 | 0.000486361 |
| *TOMM5* | 9846 | -3.288636 | 0.000503371 |
| *NDUFA9* | 1782 | -3.258758 | 0.000559505 |
| *ARHGEF3* | 5532 | -3.258406 | 0.0005602 |
| *NCAM1* | 1773 | -3.251459 | 0.000574072 |
| *NT5DC2* | 7145 | -3.251152 | 0.000574692 |
| *PRKAA2* | 2160 | -3.248411 | 0.000580258 |
| *MMGT1* | 8338 | -3.236998 | 0.000603971 |
| *PTS* | 2290 | -3.231767 | 0.000615137 |
| *DCX* | 677 | -3.227754 | 0.000623831 |
| *CTXN2* | 9818 | -3.222994 | 0.000634291 |
| *TSPAN17* | 5202 | -3.217145 | 0.000647366 |
| *BECN1* | 3317 | -3.216409 | 0.000649028 |
| *NAE1* | 3402 | -3.214989 | 0.000652248 |
| *LSAMP* | 1570 | -3.214294 | 0.000653829 |
| *CC2D2B* | 9756 | -3.213381 | 0.000655911 |
| *SERP1* | 5312 | -3.20879 | 0.000666474 |
| *IRAK4* | 5619 | -3.207856 | 0.000668642 |
| *ZFAND2A* | 8194 | -3.206189 | 0.000672528 |
| *G3BP2* | 3881 | -3.203754 | 0.000678242 |
| *PBX1* | 1941 | -3.19897 | 0.000689598 |

| | | | |
|---|---|---|---|
| *SV2B* | 3876 | -3.193078 | 0.000703825 |
| *FBXL2* | 5048 | -3.192423 | 0.000705423 |
| *P4HA2* | 3437 | -3.16829 | 0.000766692 |
| *JKAMP* | 5769 | -3.164349 | 0.000777151 |
| *NABP2* | 7228 | -3.163138 | 0.000780392 |
| *SUV39H1* | 2728 | -3.16088 | 0.000786466 |
| *AKT3* | 3923 | -3.160804 | 0.000786672 |
| *GDPGP1* | 9813 | -3.156932 | 0.000797193 |
| *UFSP2* | 6270 | -3.155518 | 0.000801067 |
| *RNF175* | 9565 | -3.154965 | 0.000802587 |
| *LPIN2* | 3754 | -3.154629 | 0.000803512 |
| *CCDC34* | 8220 | -3.153322 | 0.000807118 |
| *AGMAT* | 7413 | -3.121955 | 0.000898272 |
| *PSMD7* | 2245 | -3.1213 | 0.000900273 |
| *RIMS3* | 3817 | -3.119764 | 0.00090498 |
| *NCOA7* | 8798 | -3.115006 | 0.000919706 |
| *PSMF1* | 3660 | -3.112098 | 0.000928814 |
| *CDH13* | 445 | -3.108095 | 0.000941488 |
| *NXPH1* | 5502 | -3.105903 | 0.000948495 |
| *DHX36* | 9174 | -3.104277 | 0.000953723 |
| *RLIM* | 5616 | -3.100923 | 0.000964592 |
| *CORO1B* | 6675 | -3.09909 | 0.00097058 |
| *KCNS3* | 1482 | -3.095278 | 0.000983143 |
| *POLR2E* | 2099 | -3.090028 | 0.001000688 |
| *DRG1* | 1796 | -3.085784 | 0.001015081 |
| *FGGY* | 6246 | -3.082589 | 0.001026042 |
| *TPM3* | 2882 | -3.077099 | 0.001045129 |
| *COX11* | 576 | -3.071542 | 0.001064781 |
| *CAPNS1* | 365 | -3.070586 | 0.001068196 |
| *NOP10* | 6306 | -3.070476 | 0.001068589 |
| *XYLT1* | 7022 | -3.068092 | 0.001077151 |
| *ENOX1* | 6134 | -3.056434 | 0.001119934 |
| *RFC3* | 2374 | -3.054366 | 0.001127684 |
| *WDR31* | 8469 | -3.038555 | 0.001188579 |
| *USO1* | 3282 | -3.03556 | 0.001200447 |
| *MRPL4* | 5580 | -3.034682 | 0.001203947 |
| *CLPB* | 7653 | -3.034288 | 0.001205521 |
| *GLRX2* | 5563 | -3.034031 | 0.001206548 |
| *CIB2* | 4192 | -3.029335 | 0.001225464 |
| *SH3GLB1* | 5599 | -3.024199 | 0.001246462 |
| *SGCB* | 2547 | -3.023167 | 0.001250721 |
| *MMP16* | 1683 | -3.013723 | 0.001290317 |
| *MOCS3* | 5337 | -3.011181 | 0.001301168 |
| *GGH* | 3380 | -3.010684 | 0.0013033 |

| | | | |
|---|---|---|---|
| *RAB15* | 9739 | -3.008356 | 0.001313326 |
| *KCTD1* | 9516 | -3.005994 | 0.001323571 |
| *RBM8A* | 3898 | -3.005741 | 0.001324673 |
| *PAK3* | 1932 | -3.000161 | 0.001349185 |
| *RAB3C* | 8493 | -3.000095 | 0.001349477 |

**Tab S27. Gene list for statistically significant association with RS changes in the PLS2- component.** *P* values were estimated by using two-sided *Z* sampling distribution test without corrections.

**9. Association of single-gene expression level to RS values**

Rather gene lists in PLS components, we estimated the univariate correlation between each gene that survived from Z > 3 or Z < -3) and RS values. Results revealed the statistically significant correlations of single-gene expression levels **(Tab S28-29)**.

| Gene Symbol | Entrez Gene ID | Z scores | P values |
|---|---|---|---|
| *SCRIB* | 4922 | 2.85E-01 | 0.004104 |
| *FTCD* | 4336 | 2.73E-01 | 0.005966 |
| *ZNF438* | 9326 | 2.65E-01 | 0.007705 |
| *NPFF* | 3284 | 2.42E-01 | 0.015128 |
| *EBF4* | 6804 | 2.35E-01 | 0.018532 |
| *TMC8* | 8922 | 2.31E-01 | 0.02097 |
| *POLN* | 9702 | 2.23E-01 | 0.025571 |
| *TLR3* | 2846 | 2.20E-01 | 0.027625 |
| *ACTN1* | 35 | 2.16E-01 | 0.030868 |
| *ZFAND3* | 6968 | 2.16E-01 | 0.031227 |
| *DENND2A* | 5298 | 2.15E-01 | 0.03202 |
| *SLC2A5* | 2584 | 2.14E-01 | 0.032205 |
| *LIMK2* | 1544 | 2.14E-01 | 0.032557 |
| *EIF4EBP1* | 808 | 2.11E-01 | 0.03501 |
| *HLA-DOA* | 1234 | 2.11E-01 | 0.035096 |
| *TMEM106A* | 8402 | 2.09E-01 | 0.036728 |
| *DNAJC12* | 6546 | 2.08E-01 | 0.037381 |
| *CMTM3* | 8621 | 2.08E-01 | 0.037491 |
| *FYN* | 982 | 2.07E-01 | 0.038627 |
| *LEPROT* | 5995 | 2.06E-01 | 0.039903 |
| *TYK2* | 2924 | 2.04E-01 | 0.041698 |
| *DOCK1* | 731 | 2.03E-01 | 0.042742 |
| *POLA1* | 2095 | 2.03E-01 | 0.043154 |
| *HCLS1* | 1211 | 2.02E-01 | 0.043448 |
| *SERPINA1* | 2028 | 2.01E-01 | 0.045078 |
| *MORC4* | 7370 | 2.01E-01 | 0.045335 |
| *TCF3* | 2774 | 1.99E-01 | 0.046997 |
| *GRIA3* | 1132 | 1.98E-01 | 0.047798 |
| *ITIH4* | 1423 | 1.97E-01 | 0.049393 |

**Tab S28. Associations between single-gene expression level and RS values in the PLS1+ component.** The order of these genes have been descended by correlation strength. Results were shown only if this correlation reached statistical significance (Two-sided *r* test, $p < .05$, uncorrected).

| Gene Symbol | Entrez Gene ID | Z scores | P values |
|---|---|---|---|
| *RMND1* | 6104 | -3.32E-01 | 0.000745 |
| *CORO2A* | 2994 | -2.99E-01 | 0.002544 |
| *TNPO3* | 4932 | -2.96E-01 | 0.002792 |
| *ANAPC7* | 5743 | -2.96E-01 | 0.002825 |
| *IDH3B* | 1333 | -2.90E-01 | 0.003456 |
| *IGBP1* | 1347 | -2.89E-01 | 0.003557 |
| *CTXN2* | 9818 | -2.84E-01 | 0.004245 |
| *INPP4A* | 1387 | -2.83E-01 | 0.004272 |
| *SIK2* | 4779 | -2.82E-01 | 0.004423 |
| *EIF2B2* | 3405 | -2.74E-01 | 0.005741 |
| *CDKL3* | 5670 | -2.73E-01 | 0.005901 |
| *MRPL4* | 5580 | -2.72E-01 | 0.006196 |
| *SCRN1* | 3826 | -2.69E-01 | 0.006766 |
| *TMEM260* | 6059 | -2.66E-01 | 0.007538 |
| *JKAMP* | 5769 | -2.65E-01 | 0.007738 |
| *MTRF1L* | 5945 | -2.65E-01 | 0.007761 |
| *DCX* | 677 | -2.64E-01 | 0.007888 |
| *LDHB* | 1530 | -2.64E-01 | 0.008021 |
| *USO1* | 3282 | -2.62E-01 | 0.008435 |
| *KCTD1* | 9516 | -2.61E-01 | 0.008842 |
| *PIP4P2* | 6314 | -2.60E-01 | 0.009087 |
| *ZFAND2A* | 8194 | -2.60E-01 | 0.009122 |
| *UFSP2* | 6270 | -2.58E-01 | 0.009464 |
| *GGH* | 3380 | -2.56E-01 | 0.010105 |
| *CLCN4* | 517 | -2.55E-01 | 0.010366 |
| *ARHGEF3* | 5532 | -2.55E-01 | 0.010461 |
| *RIMS3* | 3817 | -2.55E-01 | 0.010467 |
| *NXPH2* | 4525 | -2.55E-01 | 0.010468 |
| *ZNF654* | 6248 | -2.54E-01 | 0.010627 |
| *RRP12* | 4774 | -2.53E-01 | 0.011106 |
| *NQO2* | 1843 | -2.53E-01 | 0.011229 |
| *G3BP2* | 3881 | -2.52E-01 | 0.011299 |
| *NAE1* | 3402 | -2.52E-01 | 0.011348 |
| *TIMM8A* | 691 | -2.52E-01 | 0.011451 |
| *AMIGO1* | 6731 | -2.51E-01 | 0.011662 |
| *GYG1* | 1189 | -2.51E-01 | 0.011756 |
| *CCT4* | 4224 | -2.51E-01 | 0.011765 |
| *KRAS* | 1502 | -2.50E-01 | 0.01212 |
| *VDAC2* | 2972 | -2.50E-01 | 0.012186 |

| | | | |
|---|---|---|---|
| *RNF8* | 3455 | -2.49E-01 | 0.012665 |
| *MRPL46* | 5237 | -2.47E-01 | 0.013317 |
| *WDR37* | 4614 | -2.47E-01 | 0.013343 |
| *PPM1A* | 2126 | -2.46E-01 | 0.013563 |
| *PHOSPHO2* | 9907 | -2.46E-01 | 0.013631 |
| *TM9SF2* | 3605 | -2.46E-01 | 0.013636 |
| *SAE1* | 3952 | -2.44E-01 | 0.014521 |
| *PTPRM* | 2284 | -2.44E-01 | 0.014564 |
| *AKT3* | 3923 | -2.43E-01 | 0.014986 |
| *NDUFB2* | 1785 | -2.43E-01 | 0.015043 |
| *GLRX2* | 5563 | -2.42E-01 | 0.015219 |
| *CCDC184* | 9761 | -2.42E-01 | 0.015407 |
| *YIPF5* | 7644 | -2.41E-01 | 0.015499 |
| *RBMX* | 5340 | -2.41E-01 | 0.015662 |
| *CLTC* | 532 | -2.41E-01 | 0.015867 |
| *NABP2* | 7228 | -2.40E-01 | 0.016289 |
| *MOCS3* | 5337 | -2.40E-01 | 0.016292 |
| *GHITM* | 5268 | -2.39E-01 | 0.016429 |
| *TXNL1* | 3594 | -2.39E-01 | 0.01668 |
| *NDUFB9* | 1788 | -2.39E-01 | 0.016729 |
| *FAM219B* | 6681 | -2.38E-01 | 0.016945 |
| *PAIP2* | 5663 | -2.38E-01 | 0.017172 |
| *MRPS23* | 5805 | -2.37E-01 | 0.017468 |
| *ZNF425* | 9057 | -2.37E-01 | 0.017519 |
| *SLC25A3* | 2022 | -2.37E-01 | 0.017836 |
| *KCNS3* | 1482 | -2.36E-01 | 0.017861 |
| *TERF2* | 2799 | -2.36E-01 | 0.01792 |
| *ATP5F1B* | 220 | -2.35E-01 | 0.018642 |
| *PSMD14* | 4040 | -2.35E-01 | 0.018716 |
| *CEP97* | 7310 | -2.34E-01 | 0.019224 |
| *ATP5PO* | 235 | -2.33E-01 | 0.019766 |
| *RNASEL* | 2401 | -2.32E-01 | 0.019979 |
| *BECN1* | 3317 | -2.32E-01 | 0.020006 |
| *UBXN10* | 8688 | -2.32E-01 | 0.020144 |
| *NDUFAB1* | 1784 | -2.32E-01 | 0.020264 |
| *VWC2* | 9732 | -2.31E-01 | 0.020717 |
| *NDUFA9* | 1782 | -2.31E-01 | 0.020732 |
| *SLU7* | 4220 | -2.30E-01 | 0.021415 |
| *NME7* | 5465 | -2.30E-01 | 0.0216 |
| *GSTO1* | 3633 | -2.29E-01 | 0.021658 |
| *CCDC34* | 8220 | -2.29E-01 | 0.021946 |
| *PSMF1* | 3660 | -2.29E-01 | 0.022027 |
| *BDH1* | 269 | -2.28E-01 | 0.022372 |
| *COQ10B* | 7541 | -2.28E-01 | 0.022553 |

| | | | |
|---|---|---|---|
| *PEX5* | 2301 | -2.27E-01 | 0.023046 |
| *MRPL33* | 3698 | -2.26E-01 | 0.02384 |
| *COX5A* | 3606 | -2.26E-01 | 0.0239 |
| *ITPA* | 1424 | -2.26E-01 | 0.023989 |
| *DHRS7* | 5799 | -2.25E-01 | 0.024137 |
| *UGCG* | 2949 | -2.24E-01 | 0.024922 |
| *UBL4A* | 3160 | -2.24E-01 | 0.02539 |
| *TCEAL3* | 8082 | -2.23E-01 | 0.025431 |
| *NXPH1* | 5502 | -2.23E-01 | 0.025723 |
| *ISCU* | 4908 | -2.22E-01 | 0.026147 |
| *KCNC2* | 1448 | -2.22E-01 | 0.026149 |
| *ATP5MC3* | 222 | -2.22E-01 | 0.026207 |
| *CAPRIN2* | 7186 | -2.22E-01 | 0.026705 |
| *ODF2* | 1896 | -2.21E-01 | 0.027065 |
| *PRKAA2* | 2160 | -2.21E-01 | 0.027282 |
| *UQCRH* | 2960 | -2.21E-01 | 0.027348 |
| *IFIT1* | 1342 | -2.21E-01 | 0.027355 |
| *TCEAL6* | 9088 | -2.20E-01 | 0.027683 |
| *AKAP12* | 3715 | -2.20E-01 | 0.027823 |
| *TOMM20* | 3825 | -2.19E-01 | 0.028225 |
| *RAD18* | 6570 | -2.19E-01 | 0.028415 |
| *COA1* | 6409 | -2.19E-01 | 0.028759 |
| *COPA* | 565 | -2.18E-01 | 0.029062 |
| *GFPT1* | 1042 | -2.18E-01 | 0.029427 |
| *TOMM5* | 9846 | -2.18E-01 | 0.029444 |
| *TM2D2* | 7775 | -2.18E-01 | 0.02955 |
| *NDUFV2* | 1795 | -2.18E-01 | 0.029572 |
| *PBX1* | 1941 | -2.18E-01 | 0.02961 |
| *PMS1* | 2086 | -2.17E-01 | 0.029916 |
| *DNAJA2* | 4080 | -2.17E-01 | 0.029993 |
| *MED21* | 3621 | -2.17E-01 | 0.030236 |
| *NDUFS4* | 1793 | -2.17E-01 | 0.030323 |
| *TRAPPC1* | 6897 | -2.16E-01 | 0.030549 |
| *AHSA1* | 4237 | -2.16E-01 | 0.030745 |
| *WDR7* | 4835 | -2.16E-01 | 0.030989 |
| *RND2* | 3139 | -2.15E-01 | 0.031318 |
| *NFU1* | 5320 | -2.15E-01 | 0.031393 |
| *DRG1* | 1796 | -2.15E-01 | 0.031412 |
| *ARL8B* | 6209 | -2.15E-01 | 0.031474 |
| *TAX1BP1* | 3404 | -2.15E-01 | 0.03159 |
| *FBXO9* | 5204 | -2.15E-01 | 0.03197 |
| *PITPNM1* | 3717 | -2.15E-01 | 0.032109 |
| *GAD2* | 1007 | -2.14E-01 | 0.032437 |
| *ZNF248* | 6691 | -2.14E-01 | 0.032614 |

| | | | |
|---|---|---|---|
| *GCHFR* | 1033 | -2.14E-01 | 0.032634 |
| *POLR2E* | 2099 | -2.14E-01 | 0.032904 |
| *RNF111* | 6002 | -2.13E-01 | 0.033119 |
| *PSMD13* | 2249 | -2.13E-01 | 0.033148 |
| *PSMD7* | 2245 | -2.13E-01 | 0.033176 |
| *BAG5* | 3682 | -2.13E-01 | 0.033223 |
| *MAP2K6* | 2196 | -2.13E-01 | 0.033353 |
| *TAGLN3* | 5422 | -2.13E-01 | 0.033451 |
| *DHX36* | 9174 | -2.13E-01 | 0.033607 |
| *TMEM126A* | 7853 | -2.13E-01 | 0.0337 |
| *RPL9* | 2421 | -2.13E-01 | 0.033758 |
| *COX11* | 576 | -2.12E-01 | 0.034 |
| *CLASP2* | 4722 | -2.12E-01 | 0.034324 |
| *GS1-124K5.11* | 9904 | -2.12E-01 | 0.034503 |
| *TIMM44* | 4170 | -2.11E-01 | 0.034727 |
| *COX7B* | 574 | -2.11E-01 | 0.03478 |
| *CEND1* | 5680 | -2.11E-01 | 0.034787 |
| *RAB15* | 9739 | -2.11E-01 | 0.035009 |
| *PPARG* | 2117 | -2.11E-01 | 0.035084 |
| *SUPV3L1* | 2724 | -2.11E-01 | 0.035348 |
| *RAB39B* | 8522 | -2.11E-01 | 0.035407 |
| *MBD5* | 6424 | -2.10E-01 | 0.035544 |
| *PNMA2* | 4284 | -2.10E-01 | 0.035947 |
| *MMADHC* | 5321 | -2.10E-01 | 0.036004 |
| *JOSD1* | 3892 | -2.10E-01 | 0.036248 |
| *USPL1* | 4036 | -2.09E-01 | 0.036732 |
| *IARS2* | 6386 | -2.09E-01 | 0.036857 |
| *ADPRHL1* | 8410 | -2.09E-01 | 0.03726 |
| *AKTIP* | 7062 | -2.08E-01 | 0.037582 |
| *STEAP2* | 9459 | -2.08E-01 | 0.038117 |
| *MDH1* | 1636 | -2.07E-01 | 0.038529 |
| *ZNF385D* | 7388 | -2.07E-01 | 0.038669 |
| *CPSF4* | 4362 | -2.07E-01 | 0.038748 |
| *PRKAB1* | 2161 | -2.07E-01 | 0.038911 |
| *GON7* | 7937 | -2.07E-01 | 0.039005 |
| *SESN2* | 7739 | -2.07E-01 | 0.039025 |
| *WAC* | 5700 | -2.07E-01 | 0.039219 |
| *PITPNA* | 2047 | -2.06E-01 | 0.039362 |
| *CLTA* | 530 | -2.06E-01 | 0.039558 |
| *HSPA12A* | 9451 | -2.06E-01 | 0.039707 |
| *EXOC8* | 8964 | -2.06E-01 | 0.040102 |
| *CCNDBP1* | 4952 | -2.06E-01 | 0.040138 |
| *AKAP11* | 4509 | -2.06E-01 | 0.040161 |
| *SELENOH* | 9464 | -2.05E-01 | 0.040288 |

| | | | |
|---|---|---|---|
| *NCOA7* | 8798 | -2.05E-01 | 0.040709 |
| *PSMD2* | 2242 | -2.05E-01 | 0.040719 |
| *ALG14* | 9221 | -2.05E-01 | 0.040727 |
| *NRG1* | 1220 | -2.05E-01 | 0.040761 |
| *PPP2R2D* | 6463 | -2.05E-01 | 0.040776 |
| *PPP2R3C* | 6110 | -2.05E-01 | 0.0408 |
| *ITSN1* | 2555 | -2.05E-01 | 0.041215 |
| *NDUFA12* | 6499 | -2.04E-01 | 0.04138 |
| *TRAF3* | 2890 | -2.04E-01 | 0.041507 |
| *AQP11* | 9465 | -2.04E-01 | 0.041569 |
| *CRNKL1* | 5710 | -2.04E-01 | 0.041732 |
| *CDC37L1* | 6367 | -2.04E-01 | 0.041978 |
| *RRP15* | 5561 | -2.03E-01 | 0.042399 |
| *BLVRA* | 280 | -2.03E-01 | 0.042466 |
| *HDAC8* | 6475 | -2.03E-01 | 0.042517 |
| *TMCC1* | 4677 | -2.02E-01 | 0.043383 |
| *HINT1* | 1224 | -2.02E-01 | 0.043579 |
| *SORL1* | 2653 | -2.02E-01 | 0.0437 |
| *VPS33A* | 7165 | -2.02E-01 | 0.043877 |
| *PTGES2* | 7513 | -2.02E-01 | 0.044251 |
| *NDUFV1* | 1792 | -2.02E-01 | 0.044351 |
| *CGRRF1* | 4274 | -2.01E-01 | 0.044579 |
| *CYC1* | 647 | -2.01E-01 | 0.044724 |
| *NR1H2* | 2954 | -2.01E-01 | 0.044962 |
| *ZFP82* | 9525 | -2.01E-01 | 0.045033 |
| *TM6SF1* | 5858 | -2.01E-01 | 0.045039 |
| *GORAB* | 8295 | -2.01E-01 | 0.045151 |
| *PAQR3* | 9027 | -2.01E-01 | 0.045168 |
| *ZNF76* | 3036 | -2.01E-01 | 0.045169 |
| *ENPP5* | 6918 | -2.01E-01 | 0.045246 |
| *ZNF253* | 6530 | -2.00E-01 | 0.045538 |
| *ATP5F1A* | 218 | -2.00E-01 | 0.045873 |
| *ZFYVE9* | 3604 | -2.00E-01 | 0.045909 |
| *TTC9* | 4920 | -2.00E-01 | 0.046194 |
| *H2AFZ* | 1196 | -2.00E-01 | 0.046408 |
| *HECA* | 5822 | -2.00E-01 | 0.046439 |
| *TRNP1* | 9780 | -1.99E-01 | 0.046637 |
| *ZNF780A* | 9519 | -1.99E-01 | 0.046755 |
| *AES* | 81 | -1.99E-01 | 0.046929 |
| *TAF11* | 2750 | -1.99E-01 | 0.04698 |
| *LINC01963* | 8990 | -1.99E-01 | 0.047198 |
| *BNIP3* | 290 | -1.99E-01 | 0.047202 |
| *BUD31* | 3409 | -1.99E-01 | 0.04762 |
| *NDUFA8* | 1780 | -1.99E-01 | 0.047705 |

| | | | |
|---|---|---|---|
| *MID2* | 4432 | -1.98E-01 | 0.047747 |
| *TRUB2* | 5251 | -1.98E-01 | 0.047762 |
| *KBTBD11* | 3888 | -1.98E-01 | 0.047769 |
| *TUBA1B* | 4115 | -1.98E-01 | 0.04792 |
| *PRPF4* | 3500 | -1.98E-01 | 0.047966 |
| *RLIM* | 5616 | -1.98E-01 | 0.04819 |
| *KIF9* | 7026 | -1.98E-01 | 0.048453 |
| *GABRA1* | 993 | -1.98E-01 | 0.048495 |
| *MANSC1* | 5987 | -1.98E-01 | 0.048522 |
| *KCNC3* | 1449 | -1.98E-01 | 0.04861 |
| *GOT1* | 1095 | -1.98E-01 | 0.048707 |
| *AHNAK2* | 8396 | -1.97E-01 | 0.049121 |
| *CHST10* | 3658 | -1.97E-01 | 0.049356 |

**Tab S29. Associations between single-gene expression level and RS values in the PLS1- component.** The order of these genes have been descended by correlation strength. Results were shown only if this correlation reached statistical significance (Two-sided *r* test, $p < .05$, uncorrected).

**10. Enrichment analysis for PLS1 component**

To reveal the biological process and enrichment pathways, we used the Metascape tool by meta-analyzing PLS1 gene list. All the annotations and datasets were updated recently, with plus from the ChatGPT resources (30-04-2023). All genes in the genome have been used as the enrichment background. *P* values for all the GO terms and pathways were corrected by Benjamini-Hochberg FDR method. Full results for enrichment analysis for PLS1 have been structured into the **Tab S30** and **Fig S15**. For each given gene list, protein-protein interaction enrichment analysis has been carried out with the following databases: STRING, BioGrid, OmniPath, InWeb_IM. Only physical interactions in STRING (physical score > 0.132) and BioGrid are used). The resultant network (PPI) contains the subset of proteins that form physical interactions with at least one other member in the list. If the network contains between 3 and 500 proteins, the Molecular Complex Detection (MCODE) algorithm10 has been applied to identify densely connected network components. The results of PPI have been sorted into the **Tab S31** and **Fig S16**. No table was provided to show MCODE results in the PLS2 because only one module was detected from MCODE.

| GO | Category | Description | Count | % | Log10(P) | Log10(q) |
|---|---|---|---|---|---|---|
| GO:0045859 | GO Biological Processes | regulation of protein kinase activity | 26 | 11.50 | -11.78 | -7.43 |
| GO:0001568 | GO Biological Processes | blood vessel development | 22 | 9.73 | -10.19 | -6.32 |
| GO:0006066 | GO Biological Processes | alcohol metabolic | 15 | 6.64 | -7.59 | -4.28 |

| | | | | | | |
|---|---|---|---|---|---|---|
| | | process | | | | |
| GO:0007548 | GO Biological Processes | sex differentiation | 14 | 6.19 | -7.47 | -4.20 |
| R-HSA-109582 | Reactome Gene Sets | Hemostasis | 20 | 8.85 | -7.27 | -4.04 |
| hsa05200 | KEGG Pathway | Pathways in cancer | 18 | 7.96 | -6.92 | -3.80 |
| GO:0009725 | GO Biological Processes | response to hormone | 21 | 9.29 | -6.25 | -3.28 |
| GO:1903522 | GO Biological Processes | regulation of blood circulation | 12 | 5.31 | -6.22 | -3.27 |
| WP3888 | WikiPathways | VEGFA-VEGFR2 signaling | 15 | 6.64 | -5.98 | -3.08 |
| GO:1902074 | GO Biological Processes | response to salt | 14 | 6.19 | -5.91 | -3.03 |
| R-HSA-1280215 | Reactome Gene Sets | Cytokine Signaling in Immune system | 19 | 8.41 | -5.55 | -2.73 |
| GO:0050730 | GO Biological Processes | regulation of peptidyl-tyrosine phosphorylation | 11 | 4.87 | -5.48 | -2.69 |
| GO:0010942 | GO Biological Processes | positive regulation of cell death | 17 | 7.52 | -5.42 | -2.64 |
| hsa00350 | KEGG Pathway | Tyrosine metabolism | 5 | 2.21 | -5.16 | -2.43 |
| GO:0007423 | GO Biological Processes | sensory organ development | 16 | 7.08 | -5.12 | -2.41 |
| GO:0007420 | GO Biological Processes | brain development | 19 | 8.41 | -5.08 | -2.38 |

| | | | | | | |
|---|---|---|---|---|---|---|
| GO:0060977 | GO Biological Processes | coronary vasculature morphogenesis | 4 | 1.77 | -4.97 | -2.27 |
| GO:0032147 | GO Biological Processes | activation of protein kinase activity | 7 | 3.10 | -4.95 | -2.27 |
| GO:0007169 | GO Biological Processes | transmembrane receptor protein tyrosine kinase signaling pathway | 13 | 5.75 | -4.75 | -2.15 |
| GO:0030855 | GO Biological Processes | epithelial cell differentiation | 16 | 7.08 | -4.71 | -2.12 |

**Tab S30 Top 20 clusters with their representative enriched terms (one per cluster) for PLS1 component.** "Count" is the number of genes in the user-provided lists with membership in the given ontology term. "%" is the percentage of all of the user-provided genes that are found in the given ontology term (only input genes with at least one ontology term annotation are included in the calculation). *P* values are estimated by two-sided cumulative hypergeometric distribution test, with Benjamini-Hochberg FDR correction. "Log10(P)" is the p-value in log base 10. "Log10(q)" is the multi-test adjusted p-value in log base 10.

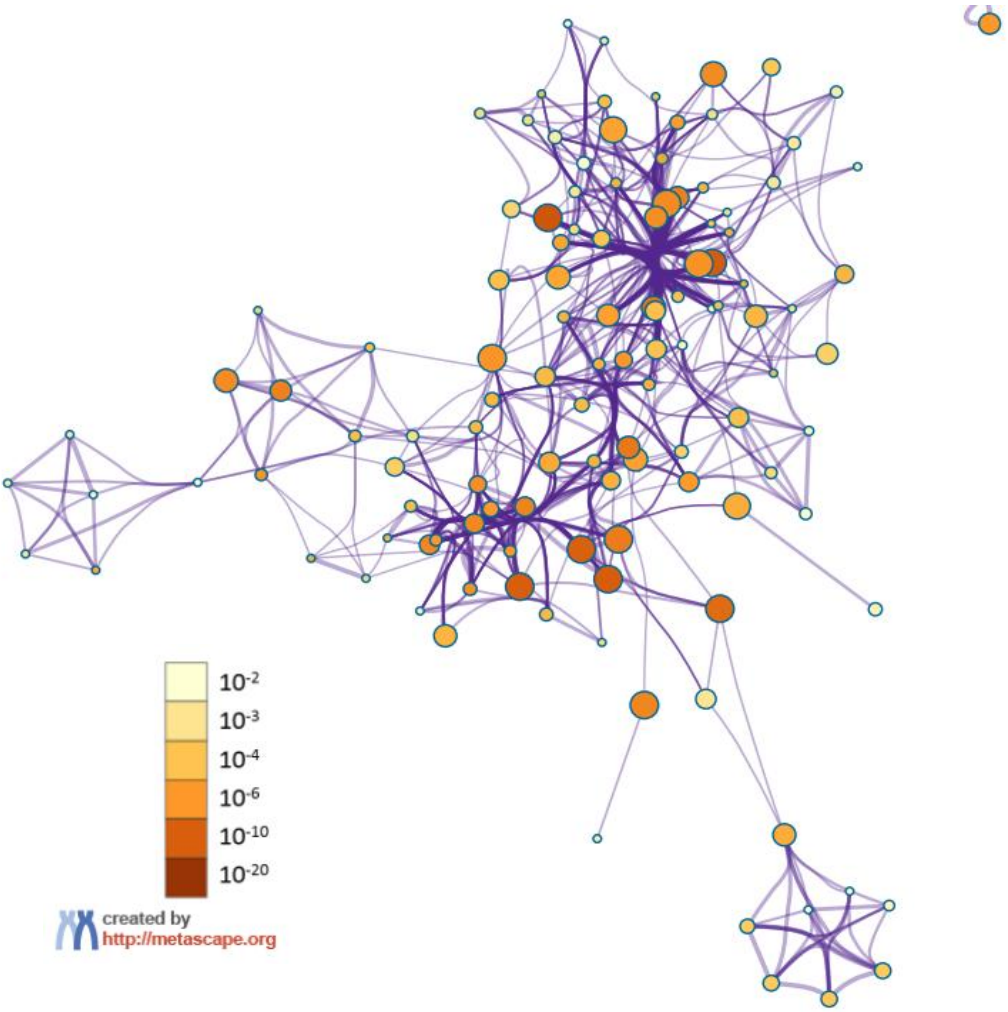

**Fig S15. Network of enriched terms that colored by *p* values.** The network is visualized using Cytoscape. *P* values are estimated by two-sided cumulative hypergeometric distribution test, with Benjamini-Hochberg FDR correction. This colorbar indicated corrected *p* values. Source data are provided as a Source Data file.

| MCODE | GO | Description | Log10(P) |
|---|---|---|---|
| MCODE_1 | hsa00010 | Glycolysis / Gluconeogenesis | -7.3 |
| MCODE_1 | hsa00982 | Drug metabolism - cytochrome P450 | -7.2 |
| MCODE_1 | hsa00980 | Metabolism of xenobiotics by cytochrome P450 | -7.0 |
| MCODE_2 | GO:0019934 | cGMP-mediated signaling | -7.1 |
| MCODE_2 | GO:0019935 | cyclic-nucleotide-mediated signaling | -6.2 |
| MCODE_2 | hsa05012 | Parkinson disease | -5.9 |
| MCODE_4 | R-HSA-1799339 | SRP-dependent cotranslational protein targeting to membrane | -7.3 |
| MCODE_4 | R-HSA-72766 | Translation | -6.1 |
| MCODE_5 | GO:0000079 | regulation of cyclin-dependent protein serine/threonine kinase activity | -7.3 |
| MCODE_5 | GO:1904029 | regulation of cyclin-dependent protein kinase activity | -7.3 |
| MCODE_5 | GO:0044772 | mitotic cell cycle phase transition | -6.8 |

**Tab S31. Protein-Protein Interaction (PPI) networks based on the Molecular Complex Detection (MCODE) algorithm.** *P* values are estimated by two-sided cumulative hypergeometric distribution test, with Benjamini-Hochberg FDR correction. "Log10(P)" is the p-value in log base 10. "Log10(q)" is the multi-test adjusted p-value in log base 10.

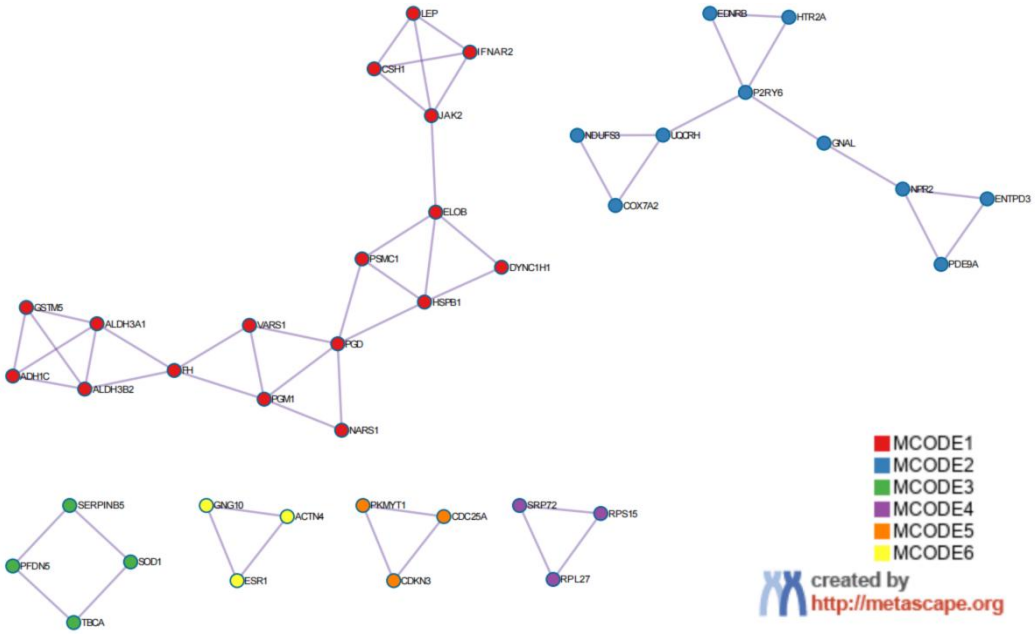


**Fig S16. Protein-Protein Interaction (PPI) networks colored by independent modules that identified by Molecular Complex Detection (MCODE) algorithm.** The network is visualized using Cytoscape. Source data are provided as a Source Data file.

### 11. Enrichment analysis for PLS2 component

To enrich our understanding of the functional processes of these gene sets, we replicated these enrichment-related analyses by inputting PLS2 gene set. Full results have been documented into the **Tab. S32** and **Fig. S17-18**.

| GO | Category | Description | Count | % | Log10(P) | Log10(q) |
|---|---|---|---|---|---|---|
| GO:0009725 | GO Biological Processes | response to hormone | 18 | 13.53 | -7.91 | -3.57 |
| GO:0071396 | GO Biological Processes | cellular response to lipid | 14 | 10.53 | -6.94 | -2.89 |
| GO:1904035 | GO Biological Processes | regulation of epithelial cell apoptotic process | 7 | 5.26 | -6.20 | -2.45 |
| GO:0009991 | GO Biological Processes | response to extracellular stimulus | 12 | 9.02 | -5.63 | -1.98 |
| GO:0050727 | GO Biological Processes | regulation of inflammatory response | 11 | 8.27 | -5.48 | -1.91 |
| GO:0007494 | GO Biological Processes | midgut development | 3 | 2.26 | -4.87 | -1.51 |

| | | | | | | |
|---|---|---|---|---|---|---|
| hsa04380 | KEGG Pathway | Osteoclast differentiation | 6 | 4.51 | -4.65 | -1.38 |
| GO:0070166 | GO Biological Processes | enamel mineralization | 3 | 2.26 | -4.53 | -1.30 |
| GO:1900180 | GO Biological Processes | regulation of protein localization to nucleus | 6 | 4.51 | -4.41 | -1.24 |
| GO:0002673 | GO Biological Processes | regulation of acute inflammatory response | 4 | 3.01 | -4.22 | -1.15 |
| GO:0071383 | GO Biological Processes | cellular response to steroid hormone stimulus | 6 | 4.51 | -4.20 | -1.15 |
| GO:0008283 | GO Biological Processes | cell population proliferation | 12 | 9.02 | -4.16 | -1.15 |
| WP272 | WikiPathways | Blood clotting cascade | 3 | 2.26 | -3.92 | -1.03 |
| hsa00310 | KEGG Pathway | Lysine degradation | 4 | 3.01 | -3.76 | -0.97 |
| M10 | Canonical Pathways | PID BCR 5PATHWAY | 4 | 3.01 | -3.76 | -0.97 |
| GO:0032355 | GO Biological Processes | response to estradiol | 5 | 3.76 | -3.71 | -0.95 |
| R-HSA-2262752 | Reactome Gene Sets | Cellular responses to stress | 12 | 9.02 | -3.71 | -0.95 |
| WP4754 | WikiPathways | IL-18 signaling pathway | 7 | 5.26 | -3.67 | -0.95 |
| GO:0019934 | GO Biological Processes | cGMP-mediated signaling | 3 | 2.26 | -3.65 | -0.95 |
| R-HSA-8963743 | Reactome Gene Sets | Digestion and absorption | 3 | 2.26 | -3.65 | -0.95 |

**Tab S32. Top 20 clusters with their representative enriched terms (one per cluster) for PLS2 component.** "Count" is the number of genes in the user-provided lists with membership in the given ontology term. "%" is the percentage of all of the user-provided genes that are found in the given ontology term (only input genes with at least one ontology term annotation are included in the calculation). *P* values are estimated by two-sided cumulative hypergeometric distribution test, with Benjamini-Hochberg FDR correction. "Log10(P)" is the p-value in log base 10. "Log10(q)" is the multi-test adjusted p-value in log base 10.

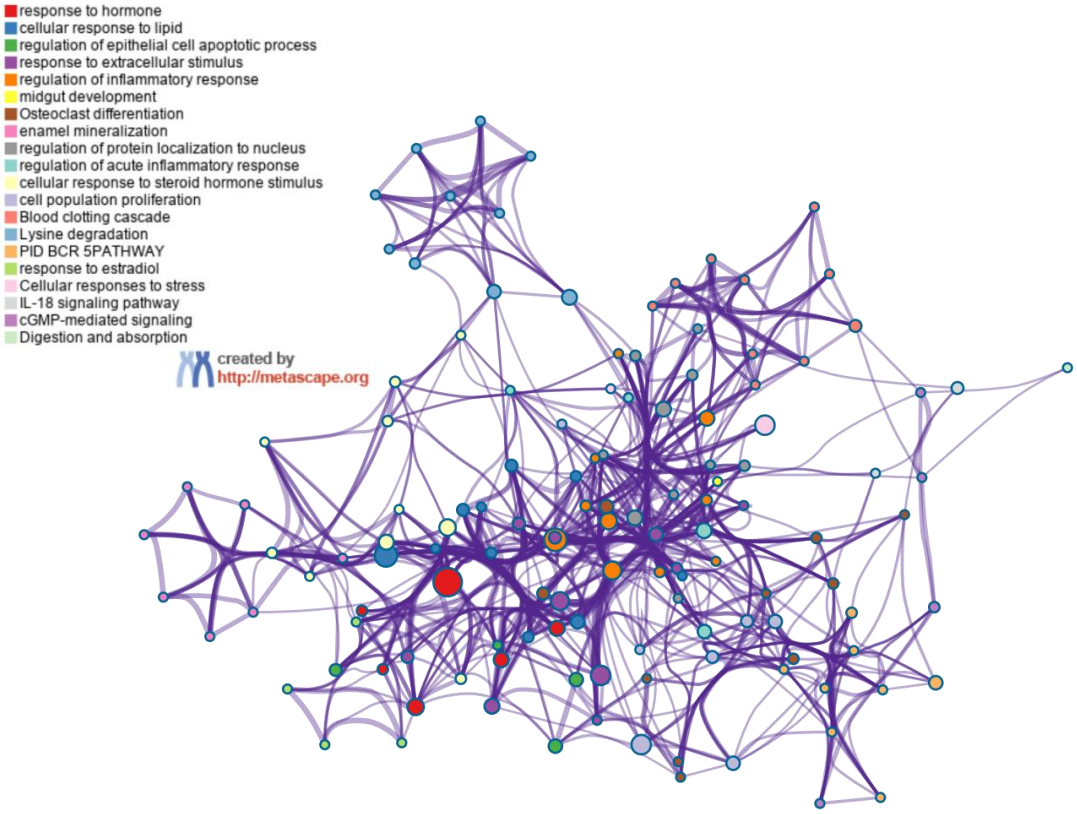


**Fig S17. Network of enriched terms that colored by cluster ID in the PLS2.** The network is visualized using Cytoscape. Source data are provided as a Source Data file.

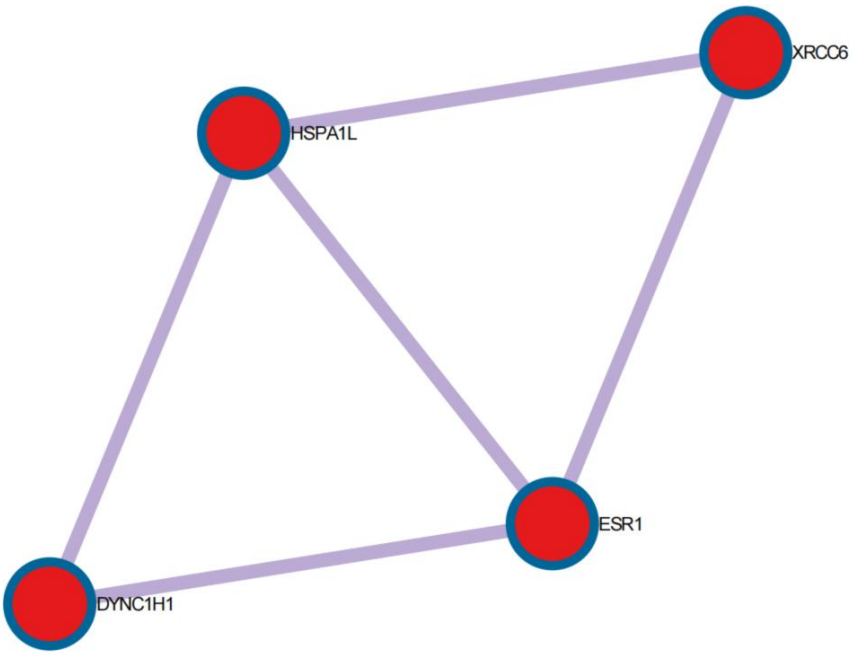


**Fig S18. Protein-Protein Interaction (PPI) networks colored by independent modules that identified by Molecular Complex Detection (MCODE) algorithm.** The network is visualized using Cytoscape.

Source data are provided as a Source Data file.

### 12. Tissue-specific, cell type-specific and disease-specific enrichment in the PLS1

We have analyzed PLS1 gene-set enrichment by capitalizing on both Metascape and Specific Expression Analysis (SEA). Statistical threshold was set to be $p < .05$ with Benjamini-Hochberg FDR corrections. All genes in the genome have been used as the enrichment background. Terms with a p-value < 0.01, a minimum count of 3, and an enrichment factor > 1.5 (the enrichment factor is the ratio between the observed counts and the counts expected by chance) are collected and grouped into clusters based on their membership similarities. Full results could be found in the **Tab S33-35**.

| GO | Description | Count | % | Log10(P) |
|---|---|---|---|---|
| PGB:00004 | Tissue-specific: kidney | 14 | 6.20 | -4.70 |
| PGB:00014 | Cell-specific: DRG | 13 | 5.80 | -4.40 |
| PGB:00022 | Tissue-specific: adrenal gland | 8 | 3.50 | -3.80 |
| PGB:00048 | Tissue-specific: bone marrow | 8 | 3.50 | -3.50 |
| PGB:00020 | Tissue-specific: retina | 5 | 2.20 | -2.50 |
| PGB:00045 | Tissue-specific: placenta | 7 | 3.10 | -2.10 |

**Tab S33. Tissue-specific enrichment in the PLS1 gene set.** *P* values are estimated by two-sided cumulative hypergeometric distribution test, with Benjamini-Hochberg FDR correction. "Log10(P)" is the p-value in log base 10.

| GO | Description | Count | % | Log10(P) |
|---|---|---|---|---|
| M41746 | RUBENSTEIN SKELETAL MUSCLE SMOOTH MUSCLE CELLS | 14 | 6.20 | -5.10 |
| M39070 | MANNO MIDBRAIN NEUROTYPES HNBGABA | 17 | 7.50 | -4.60 |
| M40010 | BUSSLINGER GASTRIC ISTHMUS CELLS | 13 | 5.80 | -4.30 |
| M39055 | MANNO MIDBRAIN NEUROTYPES HRGL2A | 15 | 6.60 | -4.30 |
| M39125 | AIZARANI LIVER C24 EPCAM POS BILE DUCT CELLS 3 | 8 | 3.50 | -4.10 |
| M39122 | AIZARANI LIVER C21 STELLATE CELLS 1 | 8 | 3.50 | -3.90 |
| M40026 | BUSSLINGER DUODENAL TRANSIT AMPLIFYING CELLS | 8 | 3.50 | -3.90 |
| M39054 | MANNO MIDBRAIN NEUROTYPES HRGL2B | 12 | 5.30 | -3.90 |
| M41710 | FAN OVARY CL8 MATURE CUMULUS GRANULOSA CELL 2 | 14 | 6.20 | -3.40 |
| M39174 | MURARO PANCREAS ACINAR CELL | 15 | 6.60 | -3.40 |
| M40025 | BUSSLINGER DUODENAL DIFFERENTIATING STEM CELLS | 9 | 4.00 | -3.30 |
| M40261 | DESCARTES FETAL PANCREAS ERYTHROBLASTS | 6 | 2.70 | -3.30 |

| | | | | |
|---|---|---|---|---|
| M39072 | MANNO MIDBRAIN NEUROTYPES HSERT | 11 | 4.90 | -3.20 |
| M39231 | LAKE ADULT KIDNEY C12 THICK ASCENDING LIMB | 10 | 4.40 | -3.20 |
| M39264 | HU FETAL RETINA FIBROBLAST | 10 | 4.40 | -3.20 |
| M39209 | HAY BONE MARROW STROMAL | 15 | 6.60 | -3.20 |
| M41659 | TRAVAGLINI LUNG ALVEOLAR EPITHELIAL TYPE 1 CELL | 10 | 4.40 | -3.10 |
| M39238 | LAKE ADULT KIDNEY C19 COLLECTING DUCT INTERCALATED CELLS TYPE A MEDULLA | 9 | 4.00 | -3.10 |
| M39050 | MANNO MIDBRAIN NEUROTYPES HPERIC | 15 | 6.60 | -3.00 |
| M39034 | FAN EMBRYONIC CTX ASTROCYTE 2 | 6 | 2.70 | -3.00 |

**Tab S34. Cell type-specific enrichment in the PLS1 gene set.** *P* values are estimated by two-sided cumulative hypergeometric distribution test, with Benjamini-Hochberg FDR correction. "Log10(P)" is the p-value in log base 10.

| GO | Description | Count | % | Log10(P) |
|---|---|---|---|---|
| C0013080 | Down Syndrome | 28 | 12.00 | -11.00 |
| C0001339 | Acute pancreatitis | 21 | 9.30 | -11.00 |
| C0008626 | Congenital chromosomal disease | 27 | 12.00 | -11.00 |
| C4521042 | Complete Trisomy 21 Syndrome | 25 | 11.00 | -10.00 |
| C0740391 | Middle Cerebral Artery Occlusion | 24 | 11.00 | -10.00 |
| C0520679 | Sleep Apnea, Obstructive | 21 | 9.30 | -10.00 |
| C0015672 | Fatigue | 26 | 12.00 | -9.90 |
| C0003872 | Arthritis, Psoriatic | 20 | 8.80 | -9.60 |
| C0085605 | Liver Failure | 16 | 7.10 | -9.10 |
| C1449563 | Cardiomyopathy, Familial | 25 | 11.00 | -9.00 |
| C0002726 | Idiopathic Amyloidosis | 23 | 10.00 | -8.50 |
| C0011884 | Diabetic Retinopathy | 22 | 9.70 | -8.40 |
| C0856169 | Endothelial dysfunction | 23 | 10.00 | -8.30 |
| C0007787 | Transient | 16 | 7.10 | -8.10 |

| | | | | |
|---|---|---|---|---|
| C0038525 | Ischemic Attack Subarachnoid Hemorrhage | 19 | 8.40 | -8.00 |
| C0003811 | Cardiac Arrhythmia | 20 | 8.80 | -8.00 |
| C4529962 | Fatty Liver Disease | 23 | 10.00 | -8.00 |
| C1868683 | B-CELL MALIGNANCY, LOW-GRADE | 16 | 7.10 | -8.00 |
| C0024530 | Malaria | 22 | 9.70 | -7.90 |
| C0007785 | Cerebral Infarction | 22 | 9.70 | -7.90 |

**Tab S35. Disease-specific enrichment in the PLS1 gene set.** *P* values are estimated by two-sided cumulative hypergeometric distribution test, with Benjamini-Hochberg FDR correction. "Log10(P)" is the p-value in log base 10.

**13. Decoding the macroscale brain network associations with PLS gene sets**

On the basis of GAMBA tool, we decoded PLS gene sets for eFC-the-*cb*-factor RS values into brain networks that defined by Yeo-7 atlas, including visual network (VIS), sensory/motor network (SMN), dorsal attention network (DAN), ventral attention network (VAN), limbic network (LIB), frontoparital network (FPN) and default model network (DMN). The general linear regression models were used to fit the PLS gene sets to brain network properties, respectively. To control the inflation of false-positive error, the Bonferroni-Holm FDR corrections have been performed. The standardized beta values indicated the slope of corresponding models. Full results have been sorted into **Tab S36-37**.

| Components | Network | Standardized Beta | Significance |
|---|---|---|---|
| PLS1+ | Visual | -0.348970433 | * |
| PLS1+ | Somatomotor | -0.068245765 | - |
| PLS1+ | Dorsal_attention | -0.193886534 | - |
| PLS1+ | Ventral_attention | 0.183763953 | - |
| PLS1+ | Limbic | 0.462173532 | * |
| PLS1+ | Frontal_parietal | -0.104238378 | - |
| PLS1+ | Default_mode | 0.099242359 | - |
| PLS1- | Visual | 0.220736296 | - |
| PLS1- | Somatomotor | 0.273855053 | - |
| PLS1- | Dorsal_attention | 0.28601827 | - |
| PLS1- | Ventral_attention | -0.141005989 | - |
| PLS1- | Limbic | -0.492881165 | * |
| PLS1- | Frontal_parietal | -0.050425016 | - |
| PLS1- | Default_mode | -0.165696456 | - |

**Tab S36.** Association of gene set in the PLS1 component for brain network properties in healthy brain. Statistical significance was set as two-sided $p < .05$ with Bonferroni-Holm FDR correction from *z* test to linear regression model. * $p < .05$ after correction; - not reach significant level after correction.

| Components | Network | Standardized Beta | Significance |
|---|---|---|---|
| PLS2+ | Visual | 0.592813035 | * |
| PLS2+ | Somatomotor | 0.06800721 | - |
| PLS2+ | Dorsal_attention | 0.0335436 | - |
| PLS2+ | Ventral_attention | -0.2516267 | - |
| PLS2+ | Limbic | -0.197339257 | - |
| PLS2+ | Frontal_parietal | -0.342684233 | - |
| PLS2+ | Default_mode | -0.245343157 | - |
| PLS2- | Visual | -0.522499534 | * |
| PLS2- | Somatomotor | -0.103394804 | - |
| PLS2- | Dorsal_attention | -0.206554892 | - |
| PLS2- | Ventral_attention | 0.341218657 | - |
| PLS2- | Limbic | 0.111579815 | - |
| PLS2- | Frontal_parietal | 0.262378052 | - |
| PLS2- | Default_mode | 0.367425603 | - |

**Tab S37.** Association of gene set in the PLS2 component for brain network properties in healthy brain. Statistical significance was set as two-sided $p < .05$ with Bonferroni-Holm FDR correction from *z* test to linear regression model. * $p < .05$ after correction; - not reach significant level after correction.

**14. Decoding the brain cognitive ontology associations with PLS gene sets**

Yeo et al. (2015)[23] have provided an ontology system to annotate brain cognitive functions into 12 components. We labeled the ontology for corresponding cognitive component by using most probability of corresponding task. More details can be found in the original paper. Ontology in the current study included as followed: Component 1, Vibrotactile Mon/Discrim; Component 2, Recitation/Repetition; Component 3, Pitch Mon/Discrim; Component 4, Visual Pursuit/Tracking; Component 5, Naming; Component 6, Saccades; Component 7, Micturition; Component 8, Flanker; Component 9, WCST; Component 10, Theory of Mind; Component 11, Face Mon/Discrim; Component 12, Reward Task. Full results have been tabulated into **Tab S38-39** for both PLS1 and PLS2 gene sets.

| PLS | Components | Standardized Beta | Significance |
|---|---|---|---|
| PLS1+ | Comp01 | -0.112157066 | - |
| PLS1+ | Comp02 | -0.012928104 | - |
| PLS1+ | Comp03 | -0.105038412 | - |
| PLS1+ | Comp04 | -0.269337787 | - |
| PLS1+ | Comp05 | -0.219292511 | - |
| PLS1+ | Comp06 | -0.33533867 | - |
| PLS1+ | Comp07 | 0.238815117 | - |

| | | | |
|---|---|---|---|
| PLS1+ | Comp08 | 0.145543505 | - |
| PLS1+ | Comp09 | -0.253079794 | - |
| PLS1+ | Comp10 | -0.054714602 | - |
| PLS1+ | Comp11 | 0.375323252 | - |
| PLS1+ | Comp12 | 0.162080235 | - |
| PLS1- | Comp01 | 0.411721924 | * |
| PLS1- | Comp02 | 0.161070745 | - |
| PLS1- | Comp03 | -0.107058522 | - |
| PLS1- | Comp04 | 0.300926413 | - |
| PLS1- | Comp05 | 0.175759571 | - |
| PLS1- | Comp06 | 0.50229855 | * |
| PLS1- | Comp07 | -0.244003981 | - |
| PLS1- | Comp08 | -0.155763237 | - |
| PLS1- | Comp09 | 0.272553053 | - |
| PLS1- | Comp10 | -0.086197421 | - |
| PLS1- | Comp11 | -0.456965337 | * |
| PLS1- | Comp12 | -0.373807075 | * |

**Tab S38** Association of gene set in the PLS1 set for brain cognitive ontology (component). Statistical significance was set as two-sided $p < .05$ with Bonferroni-Holm FDR correction from $z$ test to linear regression model. * $p < .05$ after correction; - not reach significant level after correction.

| PLS | Components | Standardized Beta | Significance |
|---|---|---|---|
| PLS2+ | Comp01 | -0.02879248 | - |
| PLS2+ | Comp02 | 0.005807242 | - |
| PLS2+ | Comp03 | -0.003672292 | - |
| PLS2+ | Comp04 | 0.512062777 | * |
| PLS2+ | Comp05 | -0.164728478 | - |
| PLS2+ | Comp06 | 0.070092962 | - |
| PLS2+ | Comp07 | -0.123980789 | - |
| PLS2+ | Comp08 | -0.390845432 | * |
| PLS2+ | Comp09 | -0.151376057 | - |
| PLS2+ | Comp10 | 0.313807963 | - |
| PLS2+ | Comp11 | -0.185341371 | - |
| PLS2+ | Comp12 | -0.297846314 | - |
| PLS2- | Comp01 | 0.079659003 | - |
| PLS2- | Comp02 | 0.135710957 | - |
| PLS2- | Comp03 | -0.089923852 | - |
| PLS2- | Comp04 | -0.192065611 | - |
| PLS2- | Comp05 | 0.226577557 | - |
| PLS2- | Comp06 | 0.114419489 | - |
| PLS2- | Comp07 | -0.00075858 | - |
| PLS2- | Comp08 | 0.286413492 | - |
| PLS2- | Comp09 | 0.202929483 | - |

| | | | |
|---|---|---|---|
| PLS2- | Comp10 | -0.115680798 | - |
| PLS2- | Comp11 | 0.196093112 | - |
| PLS2- | Comp12 | 0.058543554 | - |

**Tab S39.** Association of gene set in the PLS2 set for brain cognitive ontology (component). Statistical significance was set as two-sided $p < .05$ with Bonferroni-Holm FDR correction from $z$ test to linear regression model. * $p < .05$ after correction; - not reach significant level after correction.

**15. Decoding the cognitive terms of these gene sets**

By using the online meta-analytic decoding at the NeuroSynth, we found these gene sets have been implicated to cognitive functions relating to fears, emotions, and visual processing. Full lists to these cognitive terms have been provided in the **Tab S40-41**.

| Cognitive terms | Standardized Beta (PLS1+) | Standardized Beta (PLS1-) |
|---|---|---|
| Acoustic | 0.00865019 | -0.115795294 |
| Action_observation | -0.240959353 | 0.255430384 |
| Action | -0.217749428 | 0.333017476 |
| Actions | -0.20713669 | 0.30176066 |
| Affect | 0.408356251 | -0.111509974 |
| Age_controls | 0.006564886 | 0.149449687 |
| Alzheimer_disease | 0.368735698 | -0.33541442 |
| Alzheimer | 0.367867813 | -0.351768271 |
| Anger | 0.062139167 | -0.244588462 |
| Angry | 0.243667845 | -0.079955934 |
| Anticipation | 0.401834118 | -0.276402692 |
| Anxiety | 0.516775044 | -0.3225892 |
| Aphasia | -0.0354192 | 0.111247623 |
| Arithmetic | -0.132607497 | 0.258909455 |
| Attention_network | -0.144056109 | 0.303661185 |
| Attention_task | -0.198811919 | 0.233377535 |
| Attentional | -0.204685017 | 0.323456281 |
| Audio | -0.141411355 | -0.068527364 |
| Audiovisual | -0.086727644 | -0.081955197 |
| Auditory | -0.022138665 | -0.117801105 |
| Auditory_stimuli | 0.028156831 | -0.132406854 |
| Auditory_visual | -0.126781638 | -0.068674607 |
| Autism | 0.146664722 | -0.123580846 |
| Autism_spectrum | 0.172250455 | -0.210726775 |
| Autobiographical_memory | 0.140803725 | -0.206243688 |
| Autobiographical | 0.180108113 | -0.2661731 |
| Behavioral_responses | 0.119328281 | -0.23726965 |
| Belief | 0.055502921 | 0.076691001 |
| Beliefs | 0.057710565 | -0.012206258 |

| | | |
|---|---|---|
| Bilinguals | -0.106015625 | 0.133580895 |
| Brainstem | 0.454128456 | -0.293650681 |
| Broca | -0.139636339 | 0.102206019 |
| Calculation | -0.20504795 | 0.290322012 |
| Chronic_pain | 0.381255038 | -0.30205703 |
| Comprehension | -0.085853603 | 0.085765602 |
| Comprehensive | -0.068936576 | 0.108410595 |
| Concepts | 0.150392711 | -0.214479525 |
| Conceptual | 0.070060899 | -0.075240541 |
| Consciousness | -0.225143684 | -0.017716885 |
| Contexts | 0.079666947 | -0.168120585 |
| Contextual | -0.101041098 | 0.084374601 |
| Control_network | -0.064147706 | 0.243475973 |
| Control_processes | -0.122580589 | -0.051311303 |
| Craving | 0.140962415 | -0.256845032 |
| Decision_making | 0.223421493 | -0.300994507 |
| Decision | 0.141859752 | -0.239328245 |
| Decision_task | 0.009364216 | -0.017306161 |
| Default_mode | 0.065107855 | 0.00247743 |
| Default_network | 0.155110591 | -0.075614753 |
| Default | 0.102954862 | -0.039484177 |
| Demand | -0.015564642 | 0.190185767 |
| Demands | -0.220354694 | 0.10962497 |
| Dementia | 0.310476433 | -0.322070124 |
| Deprivation | -0.064043085 | 0.148669072 |
| Detection_task | -0.333212925 | 0.304969142 |
| Diagnosed | 0.330890242 | -0.300155658 |
| Diagnostic | 0.393448102 | -0.149395032 |
| Discriminating | -0.015518292 | 0.009564913 |
| Discriminative | 0.191032265 | -0.124612767 |
| Disease_ad | 0.198274039 | -0.266391304 |
| Disease_pd | -0.010279998 | 0.329283404 |
| Disorder_mdd | 0.216737377 | -0.268571007 |
| Dmn | 0.069748625 | 0.039266623 |
| Dopaminergic | 0.309687608 | -0.289657652 |
| Dyslexia | 0.173251659 | -0.039925701 |
| Early_visual | -0.330166793 | 0.236480514 |
| Emotion_regulation | 0.019734722 | 0.009653893 |
| Emotional_faces | 0.153435781 | -0.141525978 |
| Emotional_information | 0.23196515 | -0.298379322 |
| Emotional_neutral | 0.240375692 | -0.345659572 |
| Emotional | 0.337979995 | -0.395352553 |
| Emotional_responses | -0.038898826 | -0.171325772 |
| Emotional_stimuli | 0.372087134 | -0.103194809 |

| | | |
|---|---|---|
| Emotional_valence | 0.273415446 | -0.221321427 |
| Emotionally | 0.469591904 | -0.217090003 |
| Emotions | 0.49023263 | -0.261389454 |
| Empathic | 0.304252215 | -0.375060725 |
| Empathy | 0.222711343 | -0.249668781 |
| Encoding_retrieval | 0.253379274 | -0.202178712 |
| Epilepsy | 0.267057337 | -0.218235757 |
| Episodic_memory | 0.243299607 | -0.233294901 |
| Expectancy | -0.117033361 | 0.022514944 |
| Experiences | 0.194989415 | -0.362436128 |
| Experiencing | 0.289291039 | -0.170258463 |
| Extrastriate | -0.122773627 | 0.19767137 |
| Extrastriate_visual | -0.394629782 | 0.302620819 |
| Eye_field | -0.186982704 | 0.336117837 |
| Eye_movement | -0.136895985 | 0.287774678 |
| Eye_movements | -0.296486473 | 0.425888147 |
| Eyes | -0.270563518 | 0.230832466 |
| Face_ffa | 0.003994765 | 0.090600987 |
| Face | 0.05073677 | 0.05811669 |
| Face_stimuli | 0.091241999 | -0.007096303 |
| Faces | 0.11213202 | 0.020293341 |
| Facial_expressions | 0.396071748 | -0.107943265 |
| Facial | 0.423698748 | -0.140422335 |
| Familiar | 0.098578626 | -0.052769835 |
| Familiarity | 0.036399566 | -0.067586224 |
| Fear | 0.581635974 | -0.294038209 |
| Fearful_faces | 0.341309222 | -0.251854131 |
| Fearful | 0.426909068 | -0.28031828 |
| Female | 0.591243791 | -0.325756939 |
| Finger_movements | -0.149991759 | 0.432985159 |
| Finger | -0.109016322 | 0.392756908 |
| Finger_tapping | -0.085051863 | 0.368813215 |
| Food | 0.08746096 | -0.320993976 |
| Gain | 0.233893216 | -0.269460763 |
| Gains | 0.098271076 | -0.251683279 |
| Globus | 0.323055334 | -0.172900668 |
| Goal_directed | -0.091428709 | 0.257537014 |
| Hand_movements | -0.121765405 | 0.436449327 |
| Hand | -0.160821451 | 0.408398908 |
| Handed | -0.092920649 | 0.387887541 |
| Happy_faces | 0.236724858 | -0.327583717 |
| Happy | 0.369906078 | -0.457741675 |
| Hearing | 0.068142555 | -0.133854922 |
| Heschl | 0.062966526 | -0.128418616 |

| | | |
|---|---|---|
| Hyperactivation | -0.16571859 | 0.219453719 |
| Hypoactivation | 0.180455466 | -0.042097817 |
| Index_finger | -0.063262635 | 0.380010158 |
| Injury | -0.089042252 | -0.025116109 |
| Integrate | -0.241986124 | -0.028858843 |
| Integration | -0.099839332 | -0.026899004 |
| Integrative | 0.119382443 | -0.021645523 |
| Interoceptive | 0.20605653 | -0.174504321 |
| Interpersonal | 0.072945112 | -0.17602119 |
| Judgment | -0.164134774 | 0.106097203 |
| Judgment_task | -0.090245216 | 0.100212189 |
| Judgments | -0.087631115 | 0.021939868 |
| Knowledge | 0.009936466 | 0.13948825 |
| Language_comprehension | -0.109063907 | 0.087009364 |
| Language_network | -0.127161194 | 0.098829101 |
| Language | -0.132961658 | 0.09422713 |
| Languages | -0.148193696 | 0.115598574 |
| Lateralization | 0.021982495 | -0.047739845 |
| Lexical_decision | -0.044587795 | -0.044279255 |
| Lexical | -0.140531202 | 0.061724186 |
| Limbic | 0.456019472 | -0.345977207 |
| Lingual | -0.265210198 | 0.175567306 |
| Linguistic | -0.094961965 | 0.086584581 |
| Major_depression | 0.177127345 | -0.368486577 |
| Matching | -0.11803044 | 0.103225644 |
| Matching_task | -0.049525951 | 0.099133255 |
| Mci | 0.231399992 | -0.416220469 |
| Memories | 0.241558711 | -0.234336178 |
| Memory_encoding | 0.2323167 | -0.273554019 |
| Memory_load | -0.168338624 | 0.176911259 |
| Memory | 0.078597203 | -0.13743443 |
| Memory_performance | 0.094010464 | -0.135020285 |
| Memory_processes | 0.242672823 | -0.06514846 |
| Memory_retrieval | 0.062089693 | -0.101179342 |
| Memory_tasks | -0.196087376 | -0.001478976 |
| Memory_wm | -0.215488799 | 0.097599768 |
| Men_women | -0.115548962 | 0.001428367 |
| Mental_imagery | -0.305485825 | 0.254603136 |
| Mental_states | 0.111395332 | 0.038498458 |
| Mentalizing | 0.083871736 | -0.025479643 |
| Mesolimbic | 0.146234279 | -0.217086692 |
| Metabolism | 0.23885356 | -0.282458255 |
| Mirror_neuron | -0.159613467 | 0.154995704 |
| Moral | -0.006468679 | 0.062104834 |

| | | |
|---|---|---|
| Motion | -0.174228791 | 0.225590962 |
| Motivation | 0.048327029 | -0.328957793 |
| Motivational | 0.426512962 | -0.432469185 |
| Motor_control | -0.110609865 | 0.319289717 |
| Motor_imagery | -0.22410041 | 0.36900965 |
| Motor_network | -0.124547052 | 0.343201655 |
| Motor | -0.161960825 | 0.420404632 |
| Motor_performance | -0.13928884 | 0.413962666 |
| Motor_premotor | -0.096695399 | 0.386829239 |
| Motor_sma | -0.156532096 | 0.319867953 |
| Motor_task | -0.09391717 | 0.39690499 |
| Movement | -0.159120767 | 0.426671961 |
| Movements | -0.195514757 | 0.453158964 |
| Moving | -0.189684559 | 0.306442583 |
| Multisensory | -0.121804824 | -0.079737703 |
| Music | 0.067570338 | -0.127246738 |
| Musical | 0.030050307 | -0.130700114 |
| Musicians | 0.067120677 | 0.075843424 |
| Naturalistic | 0.016154231 | -0.048252757 |
| Navigation | 0.054202946 | -0.064026036 |
| Negative_affect | 0.528856773 | -0.247304088 |
| Negative_neutral | 0.096312607 | -0.149299711 |
| Negative_positive | 0.25592263 | -0.337687381 |
| Network_dmn | 0.085087422 | 0.018051877 |
| Neurodegenerative | 0.198172496 | -0.296091388 |
| Neurodevelopmental | 0.050358554 | -0.162089273 |
| Neutral_faces | 0.379150731 | -0.162942262 |
| Neutral_pictures | 0.258616601 | -0.208635169 |
| Neutral_stimuli | 0.089156664 | -0.339798248 |
| Noun | -0.173814359 | 0.061636235 |
| Nouns | -0.11836165 | -0.028305854 |
| Object | -0.057203399 | 0.121952003 |
| Pain | 0.35790643 | -0.258326643 |
| Painful | 0.322424408 | -0.252456879 |
| Paralimbic | 0.383571973 | -0.300891053 |
| Parieto | -0.178415993 | 0.294927688 |
| Parkinson_disease | -0.036120434 | 0.393536538 |
| Parkinson | -0.040798753 | 0.39620689 |
| Pathophysiological | 0.247152321 | -0.282196236 |
| Personal | 0.139913276 | -0.204708057 |
| Personality | 0.136992071 | -0.15221235 |
| Personality_traits | 0.129756851 | -0.137473764 |
| Pleasant | 0.313890909 | -0.337142908 |
| Pre_sma | -0.091182838 | 0.213388075 |

| | | |
|---|---|---|
| Pre_supplementary | -0.100008121 | 0.146711486 |
| Premotor | -0.175796795 | 0.403588599 |
| Preparation | -0.183471686 | 0.411618458 |
| Preparatory | -0.183562676 | 0.293230925 |
| Primary_auditory | 0.024160616 | -0.136165694 |
| Primary_motor | -0.131835644 | 0.432321507 |
| Primary | -0.077758196 | 0.322174632 |
| Primary_secondary | 0.157403267 | -0.05220327 |
| Primary_sensorimotor | -0.101284624 | 0.389257036 |
| Primary_sensory | -0.159889504 | 0.088859412 |
| Primary_somatosensory | -0.074845527 | 0.21934533 |
| Primary_visual | -0.332237374 | 0.180087302 |
| Retrosplenial | 0.102563655 | -0.183466809 |
| Reward_anticipation | 0.054268269 | -0.307053497 |
| Reward | 0.217999633 | -0.305104113 |
| Rewarding | -0.027580036 | -0.308666956 |
| Rewards | 0.277346693 | -0.287310243 |
| Rhythm | -0.136747569 | 0.348314666 |
| Rotation | -0.30518247 | 0.273404894 |
| Salience_network | 0.005433702 | 0.011939582 |
| Secondary_somatosensory | 0.06333394 | -0.039291272 |
| Selective_attention | -0.197179306 | 0.294643484 |
| Self_referential | 0.123245348 | -0.148967168 |
| Self_reported | -0.069237898 | -0.110994572 |
| Semantic_information | -0.116871248 | 0.039115761 |
| Semantic_knowledge | 0.081434993 | -0.242870155 |
| Semantic_memory | 0.244000728 | -0.323834266 |
| Sensorimotor | -0.117788574 | 0.392570583 |
| Sensory_modalities | -0.241402243 | 0.089971281 |
| Sensory_motor | -0.130773525 | 0.284161307 |
| Sensory | -0.039717729 | -0.043735162 |
| Sentence_comprehension | -0.122079823 | 0.088904136 |
| Sentence | -0.10503101 | 0.087884311 |
| Social_interactions | 0.206568505 | -0.135887844 |
| Socially | 0.125408208 | -0.1780352 |
| Somatosensory | 0.006218428 | 0.182000749 |
| Spatial_attention | -0.25557747 | 0.309609389 |
| Spatial_information | -0.17398885 | 0.229986526 |
| Strategic | -0.082253911 | 0.165167466 |
| Strategy | -0.094208255 | 0.269299491 |
| Striatal | 0.120315855 | -0.228837896 |
| Subsequent_memory | 0.321980365 | -0.249398408 |
| Supplementary_motor | -0.108475798 | 0.393505098 |
| Switch | -0.188193917 | 0.017340966 |

| | | |
|---|---|---|
| Switching | -0.123052388 | 0.253818116 |
| Syntactic | -0.123131213 | 0.075181285 |
| Tactile | -0.077961114 | 0.085136703 |
| Thought | 0.121759036 | -0.178786514 |
| Thoughts | -0.035399073 | 0.019212068 |
| Ventrolateral | -0.224385578 | -0.033478975 |
| Verb | -0.15732941 | 0.096014043 |
| Verbal_fluency | -0.068084071 | 0.080920847 |
| Verbal | -0.169445198 | 0.13560718 |
| Verbal_working | -0.150889807 | 0.10285777 |
| Verbs | -0.15674101 | 0.099759977 |
| Video | -0.173030895 | 0.190390007 |
| Videos | -0.228038519 | 0.240740096 |
| Viewed | -0.094613442 | 0.15524636 |
| Viewing | -0.018067332 | 0.120458078 |
| Vision | -0.209412203 | 0.318188461 |
| Visual_attention | -0.266697607 | 0.35793797 |
| Visual_auditory | -0.082690356 | -0.083332894 |
| Visual_field | -0.167402896 | 0.198134947 |
| Visual_motion | -0.211330654 | 0.239763509 |
| Visual | -0.300803099 | 0.322394792 |
| Visual_perception | -0.108153061 | 0.150318309 |
| Visual_spatial | -0.178448781 | 0.257820891 |
| Visual_stimulus | -0.365994578 | 0.151358259 |
| Visual_stream | -0.039064267 | 0.067776498 |
| Visual_word | -0.021525709 | 0.044076225 |
| Visually | -0.208280611 | 0.477796325 |
| Visually_presented | -0.163882747 | 0.170634435 |
| Visuo | -0.278374557 | 0.41505569 |
| Visuomotor | -0.173426756 | 0.426021639 |
| Visuospatial | -0.223784201 | 0.306828537 |
| Watched | -0.23109372 | 0.157791059 |
| Wm_task | -0.212477635 | 0.021072054 |
| Women | 0.148512659 | -0.290157036 |
| Word_form | -0.01540145 | 0.037876346 |
| Word | -0.164376243 | 0.103716442 |
| Word_pairs | -0.182267962 | 0.120582615 |
| Words | -0.152064196 | 0.096139402 |
| Working_memory | -0.250169257 | 0.183107097 |
| Young_adults | 0.212285437 | -0.272762489 |
| Young_healthy | 0.276774099 | -0.391788022 |
| Younger_adults | 0.071899717 | -0.199307408 |
| Younger | -0.199873665 | 0.015112206 |

**Tab S40.** Association of gene set in the PLS1 set for brain cognitive term. Statistical significance was set as two-sided $p < .05$ with Bonferroni-Holm FDR correction from $z$ test to linear regression model. * $p < .05$ after correction; - not reach significant level after correction.

| Cognitive terms | Standardized Beta (PLS1+) | Standardized Beta (PLS1-) |
|---|---|---|
| Acoustic | 0.11330114 | -0.100229185 |
| Action_observation | -0.059711189 | -0.004900673 |
| Action | -0.135341034 | 0.093909685 |
| Actions | -0.131032324 | 0.073189047 |
| Affect | 0.040890742 | 0.254815815 |
| Age_controls | -0.026156608 | 0.138674083 |
| Alzheimer_disease | 0.055122084 | 0.078139031 |
| Alzheimer | 0.038054248 | 0.070602706 |
| Anger | -0.177806839 | -0.014520607 |
| Angry | 0.067852293 | 0.000787847 |
| Anticipation | -0.13088269 | 0.136172865 |
| Anxiety | 0.168324651 | 0.112679394 |
| Aphasia | 0.020681428 | 0.077387298 |
| Arithmetic | 0.035720784 | 0.207836573 |
| Attention_network | 0.183886729 | 0.145103921 |
| Attention_task | 0.295915375 | -0.002013182 |
| Attentional | 0.050069709 | 0.125731998 |
| Audio | 0.029613402 | -0.109635313 |
| Audiovisual | 0.10255777 | -0.130717198 |
| Auditory | 0.100383656 | -0.125840099 |
| Auditory_stimuli | 0.10906764 | -0.093774345 |
| Auditory_visual | 0.064740965 | -0.131420091 |
| Autism | 0.152241649 | -0.001393325 |
| Autism_spectrum | 0.002031322 | -0.036048062 |
| Autobiographical_memory | 0.034795015 | 0.018636724 |
| Autobiographical | -0.015951051 | -0.002826667 |
| Behavioral_responses | -0.242749083 | -0.157748245 |
| Belief | 0.117227483 | 0.206672225 |
| Beliefs | -0.046932875 | 0.124376247 |
| Bilinguals | -0.082618705 | 0.162477736 |
| Brainstem | 0.150929939 | 0.015430673 |
| Broca | -0.15072168 | 0.130201544 |
| Calculation | 0.004022781 | 0.189718703 |
| Chronic_pain | -0.014019706 | 0.005449545 |
| Comprehension | -0.062364325 | 0.17358494 |
| Comprehensive | -0.082215968 | 0.186291875 |
| Concepts | -0.017842059 | 0.135214587 |
| Conceptual | 0.023858869 | 0.16562061 |

| | | |
|---|---|---|
| Consciousness | 0.155626437 | -0.396630202 |
| Contexts | -0.197995194 | 0.135768278 |
| Contextual | -0.185057056 | 0.233440897 |
| Control_network | 0.110716468 | 0.213315405 |
| Control_processes | -0.353713685 | 0.01571676 |
| Craving | -0.053453882 | -0.014693863 |
| Decision_making | -0.246557067 | 0.104704533 |
| Decision | -0.232368381 | 0.129508142 |
| Decision_task | 0.053027637 | 0.05513904 |
| Default_mode | 0.160647072 | 0.12051618 |
| Default_network | 0.075663097 | 0.150043075 |
| Default | 0.13096999 | 0.129313341 |
| Demand | 0.089476686 | 0.20426214 |
| Demands | -0.346490342 | 0.199193304 |
| Dementia | -0.054369515 | 0.10290625 |
| Deprivation | 0.414765672 | -0.074053763 |
| Detection_task | 0.289408078 | -0.280787427 |
| Diagnosed | -0.062416997 | 0.115257734 |
| Diagnostic | 0.036352208 | 0.246712096 |
| Discriminating | -0.126300156 | 0.092077012 |
| Discriminative | 0.16603408 | -0.117899907 |
| Disease_ad | 0.045535868 | 0.02019023 |
| Disease_pd | -0.058552701 | 0.092315214 |
| Disorder_mdd | -0.119909119 | 0.077379637 |
| Dmn | 0.19583645 | 0.124632063 |
| Dopaminergic | -0.151455678 | 0.103844026 |
| Dyslexia | 0.160110725 | 0.135886076 |
| Early_visual | 0.501838944 | -0.378206915 |
| Emotion_regulation | -0.259373999 | 0.199831733 |
| Emotional_faces | -0.15204592 | 0.064780652 |
| Emotional_information | -0.17185086 | 0.152483071 |
| Emotional_neutral | -0.173535492 | -0.057166557 |
| Emotional | -0.163378117 | 0.131299778 |
| Emotional_responses | -0.23538132 | 0.041939619 |
| Emotional_stimuli | 0.053627633 | 0.330075433 |
| Emotional_valence | -0.121080874 | 0.1071507 |
| Emotionally | 0.055622269 | 0.225926178 |
| Emotions | 0.066516073 | 0.226985207 |
| Empathic | -0.282967376 | -0.153231129 |
| Empathy | -0.03231548 | -0.05226949 |
| Encoding_retrieval | 0.128732549 | 0.028347751 |
| Epilepsy | -0.093760573 | 0.045092143 |
| Episodic_memory | 0.0410954 | 0.059694312 |
| Expectancy | -0.11381445 | -0.036281568 |

| | | |
|---|---|---|
| Experiences | -0.093380262 | 0.051715551 |
| Experiencing | -0.108621441 | 0.136432227 |
| Extrastriate | 0.385211201 | -0.095052537 |
| Extrastriate_visual | 0.516982012 | -0.387757489 |
| Eye_field | -0.045170826 | 0.166755636 |
| Eye_movement | 0.13578021 | 0.008383947 |
| Eye_movements | 0.156824308 | 0.022228649 |
| Eyes | 0.376116082 | -0.285287048 |
| Face_ffa | 0.289949063 | -0.009921545 |
| Face | 0.276766785 | 0.010791886 |
| Face_stimuli | 0.216960035 | 0.027077022 |
| Faces | 0.25743796 | 0.03512569 |
| Facial_expressions | 0.126751063 | 0.207822902 |
| Facial | 0.131987208 | 0.192580348 |
| Familiar | 0.193072469 | 0.000413401 |
| Familiarity | 0.141745103 | 0.045293541 |
| Fear | -0.015348284 | 0.237837664 |
| Fearful_faces | -0.002553291 | 0.145090536 |
| Fearful | -0.071198841 | 0.098010977 |
| Female | -0.059666434 | 0.165262568 |
| Finger_movements | -0.063759795 | 0.116974459 |
| Finger | -0.03810469 | 0.070225045 |
| Finger_tapping | -0.061986428 | 0.103717384 |
| Food | -0.173771744 | -0.118356923 |
| Gain | 0.055544727 | -0.045397152 |
| Gains | -0.235623264 | 0.053259738 |
| Globus | 0.021845592 | 0.086098317 |
| Goal_directed | 0.156960409 | 0.180207338 |
| Hand_movements | -0.010823018 | 0.051318148 |
| Hand | -0.059379709 | 0.011960317 |
| Handed | -0.058814613 | 0.093803053 |
| Happy_faces | -0.213911893 | -0.148211754 |
| Happy | -0.286908886 | -0.004606491 |
| Hearing | 0.125877029 | -0.095152814 |
| Heschl | 0.130407993 | -0.095527954 |
| Hyperactivation | 0.013782386 | -0.010641213 |
| Hypoactivation | -0.051663959 | 0.214127587 |
| Index_finger | 0.030659067 | 0.044189837 |
| Injury | -0.083129951 | -0.323908328 |
| Integrate | 0.232466999 | -0.484384439 |
| Integration | 0.042736718 | -0.085652277 |
| Integrative | 0.127438741 | 0.022041329 |
| Interoceptive | 0.016675671 | -0.104788574 |
| Interpersonal | -0.061516181 | 0.03893715 |

| | | |
|---|---|---|
| Judgment | -0.093674823 | 0.103855261 |
| Judgment_task | 0.075631181 | 0.084443102 |
| Judgments | -0.215603651 | 0.292268313 |
| Knowledge | -0.028250705 | 0.267074871 |
| Language_comprehension | -0.092791913 | 0.181964502 |
| Language_network | -0.021693443 | 0.102810709 |
| Language | -0.094746962 | 0.159354672 |
| Languages | -0.03150099 | 0.102681586 |
| Lateralization | 0.084508792 | -0.008489992 |
| Lexical_decision | -0.039432689 | 0.045305297 |
| Lexical | -0.08682291 | 0.108870011 |
| Limbic | -0.114500263 | 0.169963966 |
| Lingual | 0.463782451 | -0.317175527 |
| Linguistic | -0.039842836 | 0.140020231 |
| Major_depression | -0.306786378 | -0.089118231 |
| Matching | 0.242646287 | -0.092927849 |
| Matching_task | 0.217423369 | -0.01726842 |
| Mci | -0.174689745 | -0.140083506 |
| Memories | 0.002530592 | 0.109896055 |
| Memory_encoding | -0.048672996 | 0.014899539 |
| Memory_load | -0.208031315 | 0.184749954 |
| Memory | -0.097814902 | 0.100590002 |
| Memory_performance | 0.143994418 | -0.04347802 |
| Memory_processes | 0.203166393 | 0.174664022 |
| Memory_retrieval | -0.000684883 | 0.077450419 |
| Memory_tasks | -0.185370096 | 0.009537602 |
| Memory_wm | -0.359485435 | 0.136422427 |
| Men_women | -0.180511287 | -0.001888263 |
| Mental_imagery | 0.360653469 | -0.230675339 |
| Mental_states | 0.053249302 | 0.25158325 |
| Mentalizing | -0.046271795 | 0.273555701 |
| Mesolimbic | -0.119178271 | 0.07398341 |
| Metabolism | -0.158990011 | -0.176045192 |
| Mirror_neuron | -0.099924117 | 0.066501645 |
| Moral | -0.00352891 | 0.218711776 |
| Motion | 0.250841328 | -0.045401312 |
| Motivation | -0.294069239 | -0.019062668 |
| Motivational | -0.235706545 | -0.037195236 |
| Motor_control | -0.151746771 | 0.102313291 |
| Motor_imagery | -0.20521922 | 0.062033536 |
| Motor_network | -0.131613323 | 0.018284027 |
| Motor | -0.111924154 | 0.064537077 |
| Motor_performance | -0.072450031 | 0.100051716 |
| Motor_premotor | -0.054237922 | 0.011805236 |

| | | |
|---|---|---|
| Motor_sma | -0.179903334 | 0.138926192 |
| Motor_task | -0.020356365 | 0.0876134 |
| Movement | -0.094437883 | 0.054694067 |
| Movements | -0.087644642 | 0.078632335 |
| Moving | 0.186221084 | 0.011669327 |
| Multisensory | 0.121496872 | -0.243821851 |
| Music | 0.121013988 | -0.076498305 |
| Musical | 0.103987717 | -0.107179286 |
| Musicians | 0.129872145 | 0.031740893 |
| Naturalistic | 0.228271256 | -0.098893196 |
| Navigation | 0.277607544 | -0.145804566 |
| Negative_affect | 0.007885432 | 0.18446317 |
| Negative_neutral | -0.108204149 | 0.086784246 |
| Negative_positive | -0.203391565 | -0.126412008 |
| Network_dmn | 0.193487373 | 0.111679432 |
| Neurodegenerative | -0.15914644 | 0.061711391 |
| Neurodevelopmental | -0.041306666 | -0.104358291 |
| Neutral_faces | 0.017509185 | 0.202460906 |
| Neutral_pictures | -0.051272449 | 0.181040281 |
| Neutral_stimuli | -0.174859381 | -0.079105496 |
| Noun | -0.145915167 | 0.133916412 |
| Nouns | -0.152791276 | 0.105025512 |
| Object | 0.283238263 | -0.007887737 |
| Pain | -0.076787921 | -0.009733862 |
| Painful | -0.096698236 | -0.002393202 |
| Paralimbic | -0.139677019 | 0.095737952 |
| Parieto | 0.143240809 | -0.013671587 |
| Parkinson_disease | -0.007115613 | 0.096376531 |
| Parkinson | -0.004636206 | 0.077301383 |
| Pathophysiological | -0.065060303 | 0.06834271 |
| Personal | -0.057918327 | 0.153272583 |
| Personality | -0.129161867 | 0.115708692 |
| Personality_traits | -0.174116749 | 0.15796618 |
| Pleasant | -0.060013963 | 0.047944214 |
| Pre_sma | -0.135617971 | 0.258491753 |
| Pre_supplementary | -0.116285931 | 0.216688227 |
| Premotor | -0.143324632 | 0.107130281 |
| Preparation | -0.169710962 | 0.221110176 |
| Preparatory | 0.025341866 | 0.079698864 |
| Primary_auditory | 0.108940786 | -0.119086328 |
| Primary_motor | -0.072059637 | 0.056986327 |
| Primary | 0.007278581 | -0.041519714 |
| Primary_secondary | 0.036892092 | -0.096194154 |
| Primary_sensorimotor | -0.03488664 | 0.093288043 |

| | | |
|---|---|---|
| Primary_sensory | 0.027505453 | -0.266279535 |
| Primary_somatosensory | 0.016066433 | -0.107237926 |
| Primary_visual | 0.405085941 | -0.403757633 |
| Retrosplenial | 0.161010692 | -0.117546228 |
| Reward_anticipation | -0.290160136 | -0.022476586 |
| Reward | -0.155138844 | 0.042604297 |
| Rewarding | -0.274577566 | -0.044916989 |
| Rewards | -0.163379992 | 0.092405692 |
| Rhythm | -0.065802364 | -0.027622724 |
| Rotation | 0.081507476 | -0.111816008 |
| Salience_network | 0.025938244 | 0.196460248 |
| Secondary_somatosensory | -0.042078345 | -0.171737196 |
| Selective_attention | 0.195127565 | 0.082260295 |
| Self_referential | -0.051410636 | 0.177322431 |
| Self_reported | -0.129292284 | -0.013240082 |
| Semantic_information | -0.12507032 | 0.093500063 |
| Semantic_knowledge | -0.170992943 | 0.009337269 |
| Semantic_memory | -0.02347425 | 0.050775469 |
| Sensorimotor | -0.069829216 | 0.02828558 |
| Sensory_modalities | 0.228450839 | -0.167902186 |
| Sensory_motor | -0.098108486 | -0.025193962 |
| Sensory | 0.045793203 | -0.223461017 |
| Sentence_comprehension | -0.063493307 | 0.09352173 |
| Sentence | -0.060349112 | 0.132802851 |
| Social_interactions | -0.032629915 | 0.180757397 |
| Socially | -0.093883094 | 0.074587768 |
| Somatosensory | -0.005856813 | -0.10341692 |
| Spatial_attention | -0.016927195 | 0.034793152 |
| Spatial_information | 0.278062265 | -0.036905393 |
| Strategic | 0.03413716 | 0.197494863 |
| Strategy | 0.059976888 | 0.297096138 |
| Striatal | -0.154580097 | 0.087942111 |
| Subsequent_memory | 0.018943511 | 0.092573164 |
| Supplementary_motor | -0.147293609 | 0.170525315 |
| Switch | -0.177495727 | -0.087136728 |
| Switching | 0.077076339 | 0.145370151 |
| Syntactic | -0.064465504 | 0.079198836 |
| Tactile | -0.015167138 | -0.166820364 |
| Thought | -0.051292428 | 0.046616876 |
| Thoughts | 0.154631359 | 0.019343746 |
| Ventrolateral | -0.40693592 | 0.101633276 |
| Verb | -0.159625285 | 0.145452101 |
| Verbal_fluency | -0.098929724 | 0.10624954 |
| Verbal | -0.223034206 | 0.213622251 |

| | | |
|---|---|---|
| Verbal_working | -0.325207509 | 0.1974232 |
| Verbs | -0.093429526 | 0.137565141 |
| Video | 0.132866717 | -0.06615857 |
| Videos | 0.243509529 | -0.118473321 |
| Viewed | 0.232135515 | -0.009598321 |
| Viewing | 0.312068458 | -0.015912914 |
| Vision | 0.237234915 | -0.006299766 |
| Visual_attention | 0.268135065 | 0.012174036 |
| Visual_auditory | 0.176741713 | -0.203266832 |
| Visual_field | 0.414391992 | -0.186862688 |
| Visual_motion | 0.260615332 | -0.074304927 |
| Visual | 0.526824307 | -0.229759522 |
| Visual_perception | 0.205745201 | -0.05744981 |
| Visual_spatial | 0.191441409 | 0.053300484 |
| Visual_stimulus | 0.391359185 | -0.458832965 |
| Visual_stream | 0.375469145 | -0.12122967 |
| Visual_word | 0.175074035 | 0.022771056 |
| Visually | 0.143914959 | 0.080523467 |
| Visually_presented | 0.2094235 | 0.011205236 |
| Visuo | 0.188420777 | 0.017489634 |
| Visuomotor | -0.070834167 | 0.030348169 |
| Visuospatial | 0.125387064 | 0.057355427 |
| Watched | 0.178810959 | -0.179427926 |
| Wm_task | -0.255596165 | -0.06628936 |
| Women | -0.229209886 | 0.037715821 |
| Word_form | 0.176019424 | 0.021904996 |
| Word | -0.069798801 | 0.13178351 |
| Word_pairs | -0.010785033 | 0.033386581 |
| Words | -0.044185262 | 0.151925131 |
| Working_memory | -0.284189184 | 0.162159841 |
| Young_adults | -0.015232571 | -0.05234766 |
| Young_healthy | -0.272856044 | 0.012139533 |
| Younger_adults | -0.1749336 | -0.10399904 |
| Younger | -0.036627134 | -0.215155201 |

**Tab S41.** Association of gene set in the PLS2 set for brain cognitive term. Statistical significance was set as two-sided $p < .05$ with Bonferroni-Holm FDR correction from $z$ test to linear regression model. * $p < .05$ after correction; - not reach significant level after correction.

**16. Decoding the cortical metabolisms of PLS gene sets**

Vaishnavi and colleagues (2010) have revealed the regional aerobic glycolysis in the cortical areas and provided an atlas to quantify cortical metabolisms, including glycolytic index (GI), oxygen-glucose index (OGI), cerebral metabolic rate of oxygen/glucose ($CMRO_2/GMR_{Glu}$) and cerebral blood flow (CBF). Thus, to uncover whether these gene sets in PLS1 and PLS2 were

associated with cortical metabolisms, the general linear models were built as well. Full results have been sorted into **Tab S42** as underneath.

| PLS | Cortical metabolism | Standardized Beta | Significance |
|---|---|---|---|
| PLS1 | GI | 0.117650644 | - |
| PLS1 | OGI | -0.106936359 | - |
| PLS1 | $CMRO_2$ | 0.362871759 | * |
| PLS1 | $CMR_{Glu}$ | 0.300024051 | - |
| PLS1 | CBF | 0.117884575 | - |
| PLS2 | GI | 0.163868527 | - |
| PLS2 | OGI | -0.15633465 | - |
| PLS2 | $CMRO_2$ | 0.227157674 | - |
| PLS2 | $CMR_{Glu}$ | 0.235166918 | - |
| PLS2 | CBF | 0.094561213 | - |

**Tab S42** Association of gene sets (PLS1 and PLS2) for cortical metabolism. Statistical significance was set as two-sided $p < .05$ with Bonferroni-Holm FDR correction from $z$ test to linear regression model. * $p < .05$ after correction; - not reach significant level; - not reach significant level after correction.

**17. Decoding neurological and neuropsychiatric diseases from gene sets at BrainMap**

We decoded gene sets with PLS1 and PLS2 components at BrainMap to reveal the associations between gene expression patterns and structural/functional abnormalities of 19 diseases in BrainMap dataset. BrainMap provided a outlet to do an online meta-analytic decoding in both VBM and functional MRI dataset. Full results have been documented into following **Tab S43-44**.

| Modality | Diseases | Standardized Beta | Significance |
|---|---|---|---|
| VBM | ADHD | 0.06960949 | - |
| VBM | ALS | 0.000902659 | *** |
| VBM | ASD | 0.052397551 | *** |
| VBM | FTD | -0.428989653 | - |
| VBM | MCI | -0.411329722 | - |
| VBM | MS | -0.043255713 | - |
| VBM | OCD | -0.284539855 | - |
| VBM | PTSD | -0.239418873 | - |
| VBM | Alzheimers | -0.324579979 | - |
| VBM | Anxiety | -0.265799678 | - |
| VBM | Asperger | 0.042849784 | *** |
| VBM | Bipolar | -0.247791271 | - |
| VBM | Dementia | -0.292036869 | - |
| VBM | Depression | -0.016085068 | - |
| VBM | Dyslexia | -0.183235928 | - |
| VBM | Huntington | -0.019801802 | - |
| VBM | Obesity | -0.163868376 | - |

| | | | |
|---|---|---|---|
| VBM | Parkinson | -0.260021271 | - |
| VBM | Psychosis | -0.140236316 | - |
| VBM | Schizophrenia | -0.478664946 | - |
| VBM | SementicDementia | -0.353671241 | - |
| VBM | Stroke | -0.216975952 | - |
| fMRI | ADHD | 0.041031435 | *** |
| fMRI | ASD | 0.194530377 | *** |
| fMRI | MCI | -0.062487733 | - |
| fMRI | MDD | -0.038271047 | - |
| fMRI | OCD | -0.172346708 | - |
| fMRI | PTSD | -0.358653313 | - |
| fMRI | Alzheimers | 0.154703485 | *** |
| fMRI | Anxiety | -0.274582402 | - |
| fMRI | Asperger | 0.338388834 | - |
| fMRI | Bipolar | -0.078530937 | - |
| fMRI | Depression | -0.180505782 | - |
| fMRI | Dyslexia | 0.184685165 | *** |
| fMRI | Obesity | -0.006207422 | - |
| fMRI | Parkinson | 0.358561064 | - |
| fMRI | Schizophrenia | 0.181453636 | - |
| fMRI | Stroke | 0.291994311 | *** |

**Tab S43** Association of gene set in the PLS1 set for neurological and psychiatric diseases.Statistical significance was set as two-sided $p < .05$ with Bonferroni-Holm FDR correction from $z$ test to linear regression model. Each * represents that this $p$ value reached statistical significance in one test. A total of five tests were used here: linear regression model test, null-spatial permutation, null-random-gene permutation, null-brain-gene permutation and null-coexpressed-gene permutation. *** represents to reach statistical significance at least across three of these permutation tests.

| Modality | Diseases | Standardized Beta | Significance |
|---|---|---|---|
| VBM | ADHD | 0.081410261 | - |
| VBM | ALS | 0.015533783 | *** |
| VBM | ASD | 0.054700977 | *** |
| VBM | FTD | -0.301051176 | - |
| VBM | MCI | -0.332810675 | - |
| VBM | MS | -0.055091427 | - |
| VBM | OCD | -0.189167077 | - |
| VBM | PTSD | -0.191315054 | - |
| VBM | Alzheimers | -0.202126348 | - |
| VBM | Anxiety | -0.229628501 | - |
| VBM | Asperger | 0.035532945 | *** |
| VBM | Bipolar | -0.103346651 | - |
| VBM | Dementia | -0.148937602 | - |
| VBM | Depression | 0.037468338 | *** |

| | | | |
|---|---|---|---|
| VBM | Dyslexia | -0.160893327 | - |
| VBM | Huntington | -0.021683156 | - |
| VBM | Obesity | -0.102402886 | - |
| VBM | Parkinson | -0.185468651 | - |
| VBM | Psychosis | -0.174107843 | - |
| VBM | Schizophrenia | -0.369432397 | - |
| VBM | SementicDementia | -0.25001841 | - |
| VBM | Stroke | -0.20606552 | - |
| fMRI | ADHD | 0.100682973 | *** |
| fMRI | ASD | 0.195939882 | *** |
| fMRI | MCI | -0.001519181 | - |
| fMRI | MDD | 0.015077912 | - |
| fMRI | OCD | -0.079751648 | - |
| fMRI | PTSD | -0.266138579 | - |
| fMRI | Alzheimers | 0.182913877 | - |
| fMRI | Anxiety | -0.199654707 | - |
| fMRI | Asperger | 0.296477956 | - |
| fMRI | Bipolar | 0.01193622 | - |
| fMRI | Depression | -0.11808725 | - |
| fMRI | Dyslexia | 0.200262739 | *** |
| fMRI | Obesity | 0.026653133 | - |
| fMRI | Parkinson | 0.288564256 | *** |
| fMRI | Schizophrenia | 0.219173937 | *** |
| fMRI | Stroke | 0.301984314 | - |

**Tab S44** Association of gene set in the PLS1 set for neurological and psychiatric diseases. Statistical significance was set as two-sided $p < .05$ with Bonferroni-Holm FDR correction from $z$ test to linear regression model. Each * represents that this $p$ value reached statistical significance in one test. A total of five tests were used here: linear regression model test, null-spatial permutation, null-random-gene permutation, null-brain-gene permutation and null-coexpressed-gene permutation. *** represents to reach statistical significance at least across three of these permutation tests.

**18. Disconnectivity patterns of gene sets**

By using the diffusion tensor imaging technique, the disconnectivity involvement patterns in the brain structures were found to be the cross-disorder biomarkers[24]. In this vein, the gene sets were correlated with such biomarkers from the GAMBA toolkit. We found that these genetically transcriptional expression patterns had been implicated into the specific neurological and neuropsychiatric diseases. Full findings were tabulated into the **Fig S19-20**.

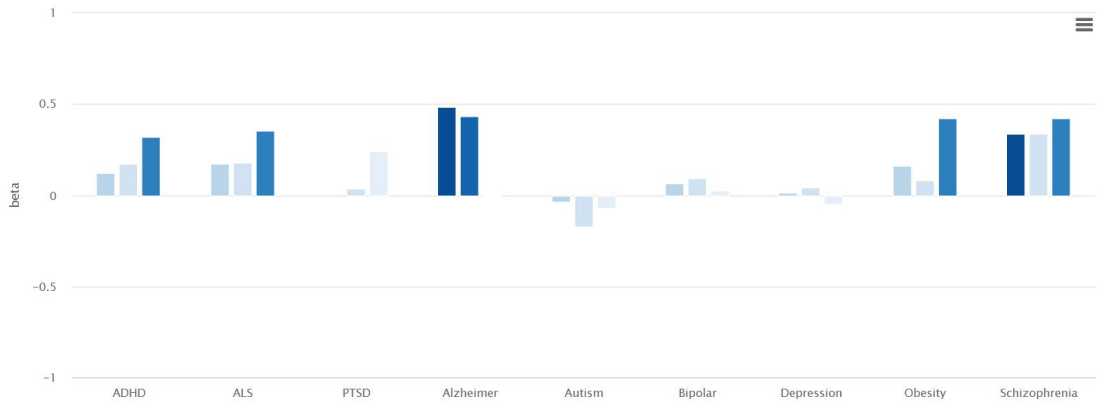


**Fig S19. Disconnectivity in cross-disorder biomarkers in the PLS1.** The bar would be highlighted once this disease was statistically predicted by PLS1 gene set that we captured in the *cb* factor (Two-sided *z* test to linear regression model, Bonferroni-Holm correction). Source data are provided as a Source Data file.

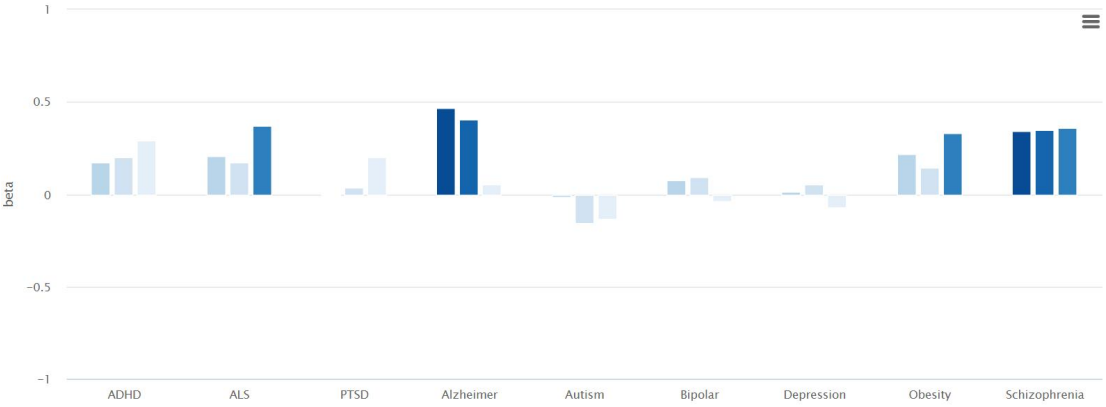


**Fig S20. Disconnectivity in cross-disorder biomarkers in the PLS2.** The bar would be highlighted once this disease was statistically predicted by PLS2 gene set that we captured in the *cb* factor (Two-sided *z* test to linear regression model, Bonferroni-Holm correction). Source data are provided as a Source Data file.

### 19. Tissue-specific, cell type-specific and disease-specific enrichment in the PLS2

The enrichment analysis for the gene set that we captured in the PLS2 have been performed as well. We still found statistically significant enrichment into the specific tissues, cell types and diseases. Given the restrictions to the accesses on the SEA (01-11-2023), no further findings were provided for these analyses in the SEA dataset. Thus, the enrichment on neurodevelopmental periods had not yet to be probed for the gene set in the PLS2. Full results for the PLS2 have been tabulated into the **Tab. S45-47**.

| GO | Description | Count | % | Log10(P) |
|---|---|---|---|---|
| PGB:00022 | Tissue-specific: adrenal gland | 5 | 3.80 | -2.70 |
| PGB:00008 | Tissue-specific: small intestine | 4 | 3.00 | -2.60 |
| PGB:00020 | Tissue-specific: retina | 4 | 3.00 | -2.60 |

**Tab S45. Tissue-specific enrichment in the PLS2 gene set.** *P* values are estimated by two-sided cumulative hypergeometric distribution test, with Benjamini-Hochberg FDR correction. "Log10(P)" is the p-value in log base 10. "Log10(q)" is the multi-test adjusted p-value in log base 10.

| GO | Description | Count | % | Log10(P) |
|---|---|---|---|---|
| M40274 | DESCARTES FETAL PANCREAS LYMPHATIC ENDOTHELIAL CELLS | 4 | 3.00 | -3.70 |
| M41670 | TRAVAGLINI LUNG LYMPHATIC CELL | 6 | 4.50 | -3.50 |
| M39224 | LAKE ADULT KIDNEY C5 PROXIMAL TUBULE EPITHELIAL CELLS STRESS INFLAM | 8 | 6.00 | -3.30 |
| M39175 | MURARO PANCREAS MESENCHYMAL STROMAL CELL | 10 | 7.50 | -3.10 |
| M40234 | DESCARTES FETAL LIVER HEPATOBLASTS | 8 | 6.00 | -2.80 |
| M39159 | GAO LARGE INTESTINE 24W C10 ENTEROCYTE | 3 | 2.30 | -2.70 |
| M40001 | BUSSLINGER ESOPHAGEAL QUIESCENT BASAL CELLS | 3 | 2.30 | -2.30 |
| M41653 | TRAVAGLINI LUNG DIFFERENTIATING BASAL CELL | 4 | 3.00 | -2.30 |
| M41652 | TRAVAGLINI LUNG PROXIMAL BASAL CELL | 8 | 6.00 | -2.20 |
| M40276 | DESCARTES FETAL PLACENTA AFP ALB POSITIVE CELLS | 4 | 3.00 | -2.20 |
| M39305 | CUI DEVELOPING HEART C8 MACROPHAGE | 5 | 3.80 | -2.10 |
| M39102 | ZHONG PFC C3 ASTROCYTE | 6 | 4.50 | -2.10 |
| M39263 | HU FETAL RETINA BLOOD | 5 | 3.80 | -2.10 |
| M39050 | MANNO MIDBRAIN NEUROTYPES HPERIC | 9 | 6.80 | -2.10 |
| M40301 | DESCARTES FETAL STOMACH MUC13 DMBT1 POSITIVE CELLS | 3 | 2.30 | -2.00 |

**Tab S46. Cell type-specific enrichment in the PLS2 gene set.** *P* values are estimated by two-sided cumulative hypergeometric distribution test, with Benjamini-Hochberg FDR correction. "Log10(P)" is the p-value in log base 10. "Log10(q)" is the multi-test adjusted p-value in log base 10.

| GO | Description | Count | % | Log10(P) |
|---|---|---|---|---|
| C0852036 | Pregnancy associated hypertension | 10 | 7.50 | -8.00 |
| C0162871 | Aortic Aneurysm, Abdominal | 15 | 11.00 | -7.30 |
| C0431369 | Dysgenesis of corpus | 5 | 3.80 | -7.10 |

| | | | | |
|---|---|---|---|---|
| | callosum | | | |
| C0149871 | Deep Vein Thrombosis | 10 | 7.50 | -7.10 |
| C0432072 | Dysmorphic features | 12 | 9.00 | -6.20 |
| C0025286 | Meningioma | 14 | 11.00 | -6.10 |
| C4529962 | Fatty Liver Disease | 15 | 11.00 | -6.00 |
| C0025500 | Mesothelioma | 13 | 9.80 | -5.90 |
| C0027831 | Neurofibromatosis 1 | 10 | 7.50 | -5.90 |
| C0032019 | Pituitary Neoplasms | 7 | 5.30 | -5.70 |
| C0009806 | Constipation | 11 | 8.30 | -5.50 |
| C0018800 | Cardiomegaly | 9 | 6.80 | -5.50 |
| C0002895 | Anemia, Sickle Cell | 11 | 8.30 | -5.40 |
| C0333516 | Tumor necrosis | 10 | 7.50 | -5.40 |
| C3241937 | Nonalcoholic Steatohepatitis | 11 | 8.30 | -5.40 |
| C0085413 | Polycystic Kidney, Autosomal Dominant | 9 | 6.80 | -5.40 |
| C1535926 | Neurodevelopmental Disorders | 12 | 9.00 | -5.30 |
| C0221358 | Long narrow head | 7 | 5.30 | -5.20 |
| C0085207 | Gestational Diabetes | 13 | 9.80 | -5.20 |
| C1527390 | Neoplasms, Intracranial | 7 | 5.30 | -5.20 |

**Tab S47. Disease-specific enrichment in the PLS2 gene set.** *P* values are estimated by two-sided cumulative hypergeometric distribution test, with Benjamini-Hochberg FDR correction. "Log10(P)" is the p-value in log base 10. "Log10(q)" is the multi-test adjusted p-value in log base 10.

**SUPPLEMENTAL REFERENCES**


1 Chen, I. H., Lin, C. Y., Zheng, X. & Griffiths, M. D. Assessing Mental Health for China's Police: Psychometric Features of the Self-Rating Depression Scale and Symptom Checklist 90-Revised. *Int J Environ Res Public Health* **17** (2020).

2 Lu, J. *et al.* Prevalence of depressive disorders and treatment in China: a cross-sectional epidemiological study. *The lancet. Psychiatry* **8**, 981-990 (2021).

3 ZUNG, W. W. K., RICHARDS, C. B. & SHORT, M. J. Self-Rating Depression Scale in an Outpatient Clinic: Further Validation of the SDS. *Arch Gen Psychiatry* **13**, 508-515 (1965).

4 Sydeman, S. State-Trait Anxiety Inventory. In: Zeigler-Hill, V., Shackelford, T. (eds) Encyclopedia of Personality and Individual Differences. (Springer, Cham, 2018)

5 Balsamo, M. *et al.* The State-Trait Anxiety Inventory: Shadows and Lights on its Construct Validity. *J Psychopathol Behav Assess* **35**, 475-486, doi:10.1007/s10862-013-9354-5 (2013).

6 Slotta, T., Witthöft, M., Gerlach, A. L. & Pohl, A. The interplay of interoceptive accuracy, facets of interoceptive sensibility, and trait anxiety: A network analysis. *Pers Individ Dif* **183**, 111133 (2021).

7 Heeren, A., Bernstein, E. E. & McNally, R. J. Deconstructing trait anxiety: a network perspective. *Anxiety, stress, and coping* **31**, 262-276 (2018).

8 Constantin, M. A., Schuurman, N. K. & Vermunt, J. K. A general Monte Carlo method for sample size analysis in the context of network models. *Psychol Methods* (2023).

9 Strauss, M. E., & Fritsch, T. Factor structure of the CERAD neuropsychological battery. *Journal of the International Neuropsychological Society : JINS*, **10**, 559–565 (2004).

10 Hayton, J. C., Allen, D. G., & Scarpello, V. Factor retention decisions in exploratory factor analysis: A tutorial on parallel analysis. *Organizational research methods*, **7**, 191-205 (2004). .

11 Faskowitz, J., Esfahlani, F. Z., Jo, Y., Sporns, O. & Betzel, R. F. Edge-centric functional network representations of human cerebral cortex reveal overlapping system-level architecture. *Nat Neurosci* **23**, 1644-1654 (2020).

12 Wang, Y., Luo, Y. L. L., Wu, M. S. & Zhou, Y. Heritability of Justice Sensitivity. *J Individ Differ* **43**, 124-134 (2022).

13 Jiang, N. *et al.* Negative Parenting Affects Adolescent Internalizing Symptoms Through Alterations in Amygdala-Prefrontal Circuitry: A Longitudinal Twin Study. *Biol Psychiatry* **89**, 560-569 (2021).

14 Arnatkeviciute, A., Markello, R. D., Fulcher, B. D., Misic, B. & Fornito, A. Toward Best Practices for Imaging Transcriptomics of the Human Brain. *Biol Psychiatry* **93**, 391-404 (2023).

15 Wei, Y. *et al.* Statistical testing in transcriptomic-neuroimaging studies: A how-to and evaluation of methods assessing spatial and gene specificity. *Hum Brain Mapp* **43**, 885-901 (2022).

16 Shen, E. H., Overly, C. C. & Jones, A. R. The Allen Human Brain Atlas: comprehensive gene expression mapping of the human brain. *Trends Neurosci* **35**, 711-714 (2012).

17 Dougherty, J. D., Schmidt, E. F., Nakajima, M. & Heintz, N. Analytical approaches to RNA profiling data for the identification of genes enriched in specific cells. *Nucleic Acids Res* **38**, 4218-4230 (2010).

18 Bringmann, L. F. *et al.* Psychopathological networks: Theory, methods and practice. *Behav Res*

*Ther* **149**, 104011 (2022).

19 McNally, R. J. Network Analysis of Psychopathology: Controversies and Challenges. *Annu Rev Clin Psychol* **17**, 31-53 (2021).

20 Jo, Y., Faskowitz, J., Esfahlani, F. Z., Sporns, O. & Betzel, R. F. Subject identification using edge-centric functional connectivity. *NeuroImage* **238**, 118204 (2021).

21 Rodriguez, R. X., Noble, S., Tejavibulya, L. & Scheinost, D. Leveraging edge-centric networks complements existing network-level inference for functional connectomes. *NeuroImage* **264**, 119742 (2022).

22 Wang, W. *et al.* Edge-centric functional network reveals new spatiotemporal biomarkers of early mild cognitive impairment. *Brain-X* **1**, e35 (2023).

23 Yeo, B. T. *et al.* Functional Specialization and Flexibility in Human Association Cortex. *Cereb. Cortex* **26**, 465 (2016).

24 de Lange, S. C. *et al.* Shared vulnerability for connectome alterations across psychiatric and neurological brain disorders. *Nat Hum Behav* **3**, 988-998 (2019).